

## **West Coast groundwater dynamics and hydrochemical evolution as inferred from regional water age and chemistry tracer data**

M Moreau

RW van der Raaij

U Morgenstern

J Horrox

**GNS Science Report 2021/16**  
**October 2021**



## **DISCLAIMER**

The Institute of Geological and Nuclear Sciences Limited (GNS Science) and its funders give no warranties of any kind concerning the accuracy, completeness, timeliness or fitness for purpose of the contents of this report. GNS Science accepts no responsibility for any actions taken based on, or reliance placed on the contents of this report and GNS Science and its funders exclude to the full extent permitted by law liability for any loss, damage or expense, direct or indirect, and however caused, whether through negligence or otherwise, resulting from any person's or organisation's use of, or reliance on, the contents of this report.

## **BIBLIOGRAPHIC REFERENCE**

Moreau M, Morgenstern U, van der Raaij RW, Horrox J. 2021. West Coast groundwater dynamics and hydrochemical evolution as inferred from regional water age and chemistry tracer data. Lower Hutt (NZ): GNS Science. 69 p. (GNS Science report; 2021/16). doi:10.21420/60DD-SQ44.

M Moreau, GNS Science, Private Bag 2000, Taupō 3352, New Zealand

U Morgenstern, GNS Science, PO Box 30368, Lower Hutt 5040, New Zealand

RW van der Raaij, Greater Wellington Regional Council, PO Box 41, Masterton 5840, New Zealand

J Horrox, West Coast Regional Council, PO Box 66, Greymouth 7840, New Zealand

## CONTENTS

<b>ABSTRACT .....</b>	<b>IV</b>
<b>KEYWORDS .....</b>	<b>IV</b>
<b>1.0 INTRODUCTION .....</b>	<b>1</b>
1.1 Regional Context .....	1
1.2 Context of the Study .....	2
1.3 Aim of this Project.....	2
<b>2.0 SETTINGS.....</b>	<b>4</b>
2.1 Geology .....	4
2.2 Climate, Hydrology and Surface Water Monitoring .....	6
2.2.1 Climate and Rainfall Monitoring .....	6
2.2.2 Hydrology and Surface Water Monitoring .....	6
2.2.3 Transit Time in Rivers: Recent Insights from the Maimai Catchment .....	10
2.3 Hydrogeology .....	10
2.3.1 Groundwater Resources .....	10
2.4 Groundwater Use .....	11
2.5 Groundwater Monitoring .....	13
<b>3.0 METHODS.....</b>	<b>15</b>
3.1 Environmental Tracing.....	15
3.1.1 Groundwater Dating .....	15
3.1.2 Stable Isotopes of the Water .....	19
3.2 Hydrochemistry.....	19
3.2.1 State and Trend.....	19
3.2.2 Hierarchical Cluster Analysis.....	20
3.3 Recharge Temperature and Excess Air .....	20
3.4 Analytical Techniques.....	20
3.5 Data Processing .....	22
3.5.1 Datasets .....	22
3.5.2 Age Interpretation .....	24
3.5.3 Hydrochemistry Data Processing .....	24
3.5.4 Hierarchical Cluster Analysis.....	25
<b>4.0 RESULTS AND DISCUSSION – GROUNDWATER PROCESSES AND FLOW DYNAMICS.....</b>	<b>26</b>
4.1 Data Outputs .....	26
4.2 Water Levels .....	27
4.3 Water Age .....	28
4.3.1 Long-Term Rainfall Tritium Monitoring .....	28
4.3.2 Groundwater Residence Time.....	28
4.4 Stable Isotopes .....	33
4.5 Hydrochemistry.....	34
4.5.1 Hierarchical Cluster Analysis.....	35
4.5.2 Redox Conditions .....	40

4.5.3	Nutrients .....	43
4.5.4	Hydrochemistry Evolution.....	44
4.5.5	Spatial Distribution of Selected Chemistry Parameters .....	47
4.5.6	Temporal Variability.....	52
4.6	Groundwater Flow Dynamics.....	53
4.6.1	Recharge Source of Groundwater and Connection to Surface Water .....	53
4.6.2	Vertical Flow and Recharge .....	54
4.6.3	Conceptual Groundwater Flow as Indicated by Tracer Concentrations.....	55
<b>5.0</b>	<b>CONCLUSION.....</b>	<b>57</b>
<b>6.0</b>	<b>RECOMMENDATIONS.....</b>	<b>59</b>
<b>7.0</b>	<b>ACKNOWLEDGMENTS .....</b>	<b>60</b>
<b>8.0</b>	<b>REFERENCES .....</b>	<b>60</b>

## FIGURES

Figure 1.1	Changes in consented water takes (1997–2017) .....	1
Figure 2.1	Simplified geology of the West Coast region and major faults.....	5
Figure 2.2	Median rainfall in the West Coast region .....	8
Figure 2.3	West Coast hydrological features .....	9
Figure 2.4	Spatial distribution of soil and bedrock groundwater age and stream water Mean Transit Time across the M8 catchment .....	10
Figure 2.5	Simplified hydrogeology of the West Coast region, caves and spring locations .....	12
Figure 2.6	Location of groundwater monitoring sites, including sites sampled in March 2020 as part of this study.....	14
Figure 3.1	Tritium, CFCs, Halon-1301 and SF <sub>6</sub> input for New Zealand rain .....	15
Figure 3.2	Tritium output for a typical transfer function of 80% exponential flow volume within an exponential piston flow model .....	17
Figure 3.3	Location of sites with groundwater chemistry and age with, where applicable, an indication of the monitoring network in the West Coast region .....	23
Figure 4.1	Spatial distribution of water levels in metres below ground level in the West Coast aquifers, located west of the Alpine Fault.....	27
Figure 4.2	Tritium ratios in rain of Kaitoke and Greymouth, measured in monthly samples.....	28
Figure 4.3	Age tracer measurements for groundwaters in the West Coast .....	29
Figure 4.4	Map of groundwater mean residence time in years.....	30
Figure 4.5	Radon-222 concentrations versus mean residence time.....	31
Figure 4.6	Spatial distribution of Radon-222 concentrations in the March 2020 groundwater samples. ....	32
Figure 4.7	Water stable isotope ratios of West Coast groundwaters and river water. ....	33
Figure 4.8	Spatial distribution of δ <sup>18</sup> O ratios measured in groundwater and rivers in the region, compared to a transect along Arthur's Pass.....	34
Figure 4.9	Dendrogram produced by Hierarchical Cluster Analysis. ....	37
Figure 4.10	Box plots of hydrochemistry parameters organised by second threshold cluster .....	38
Figure 4.11	Geographic distribution of sites assigned to clusters using Hierarchical Cluster Analysis.....	39
Figure 4.12	Piper diagram showing the variation of major ion chemistry by cluster .....	40
Figure 4.13	Dissolved oxygen, Fe, CH <sub>4</sub> and NH <sub>3</sub> -N concentrations versus mean residence time for West Coast groundwater .....	41

Figure 4.14	Map of dissolved oxygen and CH <sub>4</sub> in groundwater.....	42
Figure 4.15	NO <sub>3</sub> -N, SO <sub>4</sub> , DRP and K concentrations versus mean residence time for West Coast groundwater .....	44
Figure 4.16	SiO <sub>2</sub> , Mg, Ca, Na and HCO <sub>3</sub> concentrations versus mean residence time for West Coast groundwater .....	46
Figure 4.17	Spatial distribution of chloride and δ <sup>18</sup> O in West Coast groundwaters .....	48
Figure 4.18	Spatial distribution of nitrate in West Coast groundwater. ....	50
Figure 4.19	Spatial distribution of bicarbonate in West Coast groundwater. ....	51
Figure 4.20	Spatial distribution of sodium and magnesium in West Coast groundwater. ....	52
Figure 4.21	Field conductivity time series at sites with more than 10 data points with a perceptible trend....	53
Figure 4.22	NO <sub>3</sub> -N concentration time series at sites with more than 10 data points exhibiting a perceptible trend. ....	53
Figure 4.23	Groundwater mean residence time versus depth for all wells, separated into the different clusters .....	54
Figure 4.24	Conceptual groundwater flow in the West Coast region inferred from groundwater recharge source and age data.....	56

## TABLES

Table 3.1	Current list of parameters monitored at NGMP sites .....	21
Table 3.2	Dataset summary for hydrochemistry and groundwater age. ....	22
Table 4.1	Hydrochemistry statistics, showing number of wells, minimum and maximum concentrations and the 25 <sup>th</sup> , 50 <sup>th</sup> and 75 <sup>th</sup> percentiles for all hydrochemistry data from wells with groundwater age-tracer data .....	35
Table 4.2	Hierarchical Cluster Analysis clusters, showing water type and a general description of notable hydrochemistry and well depths from each cluster.....	36
Table 4.3	Agricultural indicators for high-intensity land use .....	43

## APPENDICES

<b>APPENDIX 1</b>	<b>MAP OF THE WEST COAST REGION SHOWING THE LOCATIONS OF CHEMISTRY AND AGE SITES.....</b>	<b>67</b>
<b>APPENDIX 2</b>	<b>GROUNDWATER MEAN RESIDENCE TIME.....</b>	<b>69</b>

## APPENDIX FIGURES

Figure A1.1	Map of the West Coast region showing the locations of chemistry and age-tracer sites, north of Hokitika.....	67
Figure A1.2	Map of the West Coast region showing the locations of chemistry and age-tracer sites, south of Hokitika.....	68

## APPENDIX TABLES

Table A2.1	West Coast Regional Council groundwater ages .....	69
------------	--	----

## ATTACHMENTS

GNS SR2021-16\_Data\_Output.xlsx  
GNS SR2021-16\_March2020\_analyses.xlsx

## ABSTRACT

This study aims to holistically describe the flow sources, pathways and lag times of water through the rivers and aquifers of the West Coast catchments. This information is required to ground truth and improve groundwater flow models and management tools. Such improvements will help to prevent degradation of rivers and aquifers from land-use activities that impact on cultural, recreational and economical values, as well as on drinking water supplies and quality. This study is mainly funded through the MBIE Endeavour programme ‘Te Whakaheke o Te Wai’ and complemented by the MBIE Envirolink fund (C05X2005).

Groundwater chemistry and age tracer data were assembled from a range of sources: (i) GNS’s national datasets (National Groundwater Monitoring Programme, National Tracer Survey), (ii) regional datasets (State Of the Environment monitoring and specific site investigations), (iii) existing data from the Water Dating laboratory and (iv) water samples collected in March 2020 as part of this study. The aggregated dataset consists of 100 sites (including 97 bores, two springs and one river) and spans the period November 1998 to March 2020.

The environmental tracer data (age, isotopes, temperature, gas concentration and chemistry) was combined and interpreted using graphical analysis (e.g. Piper diagram) spatial analysis and multivariate statistics. These analyses inform characterisation of groundwater flow and hydrochemical processes in the West Coast aquifers.

Short (less than 10 years) residence times are typical for groundwater resources in the region. Three geographically distinct hydrochemical signatures are consistent with topography and geological distinct areas: pristine, alpine foothills (cluster A); impacted coastal or fluvial (clusters B1 and B2) areas; and a dilute valley with indication of land-use impact (clusters C1, C2 and C3).

West Coast rivers and streams are hydraulically well connected to adjacent Holocene gravel aquifers. These aquifers are mostly oxic in nature. There is does not appear to be a relationship between well depth and groundwater age, indicating absence of confined or disconnected groundwater condition throughout large parts of the region’s aquifers.

In the Grey Valley, groundwaters have tracer signatures indicative of recharge from local rain and rivers. This area has the largest groundwater demand and abstraction for the region (Mourot and White 2020). Time series groundwater age data for the valley was not sensitive enough to identify impact of abstraction on groundwater circulation from increased abstraction between 2012 and 2017 (WCRC 2014). It is expected that significant change in water allocation may be rapidly reflected in future water age monitoring data due to the short residence time of water in this system.

## KEYWORDS

Groundwater, West Coast, age tracers, radon, hydrochemistry

## 1.0 INTRODUCTION

### 1.1 Regional Context

The West Coast Regional Council (WCRC) Regional Land and Water Plan outlines the importance of the groundwater resource and its quantity to serve several recognised uses, including domestic and public water supply, stock drinking water, irrigation and industrial uses. Groundwater is recognised as extensively sustaining surface water flows across the region (WCRC 2014).

Currently, West Coast areas with the largest demand for water are concentrated in the driest parts of the region: the headwater catchments of the northern Grey River (i.e. Mawheraiti, Stony and Rough rivers) and the Inangahua River catchments. In the region, groundwater is used for a range of purposes: south of Hokitika, the main use is hydroelectricity (non-consumptive); in the Inangahua and Upper Grey valleys, irrigation is the main use; and most of Reefton's demand is a combination of both hydro-scheme and irrigation. Groundwater demand has doubled in the region since 2012 and continues to grow. Although the majority of consented takes are sourced from surface water (Figure 1.1), groundwater demand was reported just below  $100 \times 10^6 \text{ m}^3/\text{yr}$  in 2017 (Beaumont et al. 2018; Mourot and White 2020).

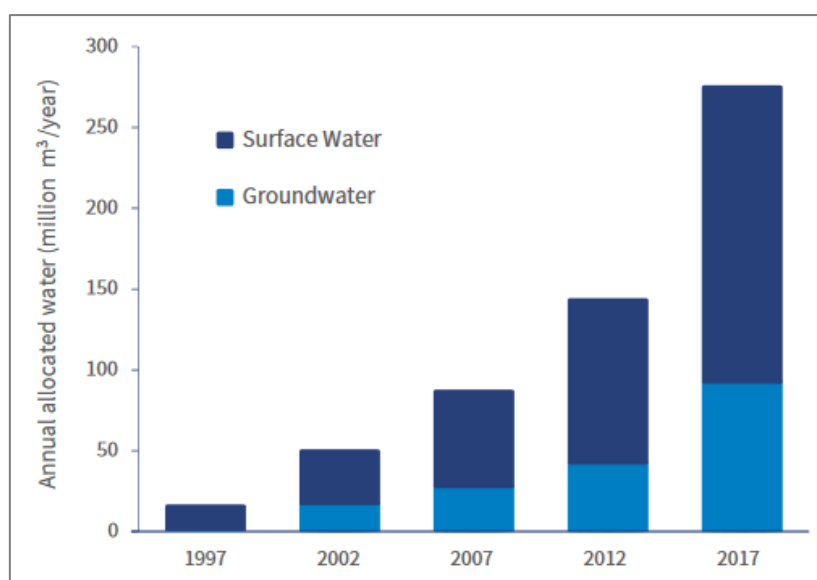


Figure 1.1 Changes in consented water takes (1997–2017) (Beaumont et al. 2018).

To address concerns about the sustainability of the groundwater resource and its contamination from nutrients and pathogens, a better understanding is required of how the water, and dissolved contaminants, moves through the groundwater systems (Beaumont et al. 2018; Moreau 2019).

## **1.2 Context of the Study**

This study was completed by GNS Science (GNS) as part of the MBIE Endeavour programme ‘Te Whakaheke o Te Wai’ (TWOTW) and Envirolink project C05X2005 (2127-WCRC196).

One of the cornerstones of the TWOTW programme is the application of age tracers to inform flow velocities (of water and contaminants) up-gradient from the measurement point. These measurements are interpreted in association with hydrogeological, chemical and isotope data to improve understanding of the origin of recharge, flow pathways, effects of geology, seasonality and stream order. New modelling approaches integrate the tracer and other data across scales for applications that include setting national policies, managing catchment-scale contaminant inflows to groundwater-fed rivers and protecting local potable water supplies.

This report is the first of a series of regional synthesis of environmental tracers planned within the TWOTW programme and aims to holistically describe the flow sources, pathways and time lags of water moving through catchments at the regional scale (Morgenstern et al. 2017; Morgenstern et al. 2019). In addition to previous modelling approaches of water mass balance; hydrochemistry; and evaluation of age tracer, isotope and hydrochemistry data, the programme aims to provide a consistent interpretation of all available data. The resulting improved characterisation of water ages will enhance the understanding of observed hydrochemistry trends and flow rates. It will also inform the assessment of hydraulic parameters and support addressing region-specific water issues. This information is required to ground truth and improve groundwater flow models and management tools. Such improvements will help to prevent degradation of rivers and aquifers from land-use discharges, which impact on cultural, recreational and economical values, as well as on drinking water supplies and quality. At the time of writing of this report, similar work is being undertaken in the Gisborne, Tasman and Auckland regions.

## **1.3 Aim of this Project**

This collaborative project between WCRC and GNS aims to improve the understanding of water dynamics in the West Coast aquifers to enable robust policy development. Environmental tracers (age, isotopes, temperature, gas concentrations and chemistry) are used to characterise: (i) the dynamics of the groundwater from recharge to discharge, (ii) its groundwater interaction with surface water, (iii) source(s) of groundwater recharge and (iv) the processes that control the hydrochemical properties (quality) of the groundwater (including sources of contaminants).

Specifically, this study aims to contribute to answering the following questions:

### **1. Groundwater Recharge, Flow and Discharge Questions**

- How are groundwaters and surface waters connected in the Holocene gravel fans?
- Where does the river-recharged groundwater flow within the aquifer?
- Where is groundwater recharged from local rain?
- What are the time-scales of water flow through the aquifer?

## **2. Groundwater Chemistry Questions**

- What are the drivers of nitrate and phosphorus levels in the groundwater?
- Why do some monitoring wells show a high variability in hydrochemistry parameters, including nitrate?
- Is the source of the water at a well changing over time due to abstraction?
- What characteristics of the water system are being monitored by the existing groundwater monitoring wells?
- Is the groundwater of sufficient age to be sensitive to current land-use changes, or is it diluted by river water?
- What are the flow pathways of surface contaminants, such as agricultural nutrients?

## **3. Groundwater Management Questions**

- Does groundwater age (residence time) vary due to abstraction?

## **2.0 SETTINGS**

This section provides an overview of the geology, climate and hydrology as context for the analysis and interpretation of the environmental tracers.

### **2.1 Geology**

The West Coast region covers a 23,302 km<sup>2</sup> heavily faulted area of the South Island (Figure 2.1). A main geological feature is the Alpine Fault that divides the region along a southwest to northeast direction. The Alpine Fault is a 850-km-long, major strike-slip fault that marks the boundary between the Australian and Pacific tectonic plates. It has accommodated over 460 km of dextral offset since 24 Ma and has a late Quaternary average slip rate of 26 mm/a (Cox et al. 2013 and references therein). This fault fails in large to possibly great earthquakes (moment magnitude greater than 7) at recurrence intervals of  $329 \pm 68$  years and presently poses a substantial seismic hazard, with the most recent rupture recorded in AD 1717 (Cox et al. 2013 and references therein).

West of the Alpine Fault, pre-Cretaceous basement rocks are interluded by plutons and unconformably covered in a sedimentary sequence spanning the Tertiary to Quaternary period. The Quaternary deposits mostly consist of downstream aggradation from moraines and down-valley glacial outwash deposited during cooler periods. During warmer interglacial periods, higher sea levels near the coast enabled marine terrace deposition. These terraces have since been uplifted (Nathan et al. 2002).

East of the Alpine Fault, the predominant outcropping formations are Mesozoic Alpine Schist and Greywacke rocks forming the Southern Alps, exposed due to regional uplift by folding and faulting that started during the late Tertiary (Pliocene) and continues today (Nathan et al. 2002). Steep-sided valleys are infilled with Quaternary deposits, mainly consisting of downstream aggradation from moraines and down-valley glacial outwash.

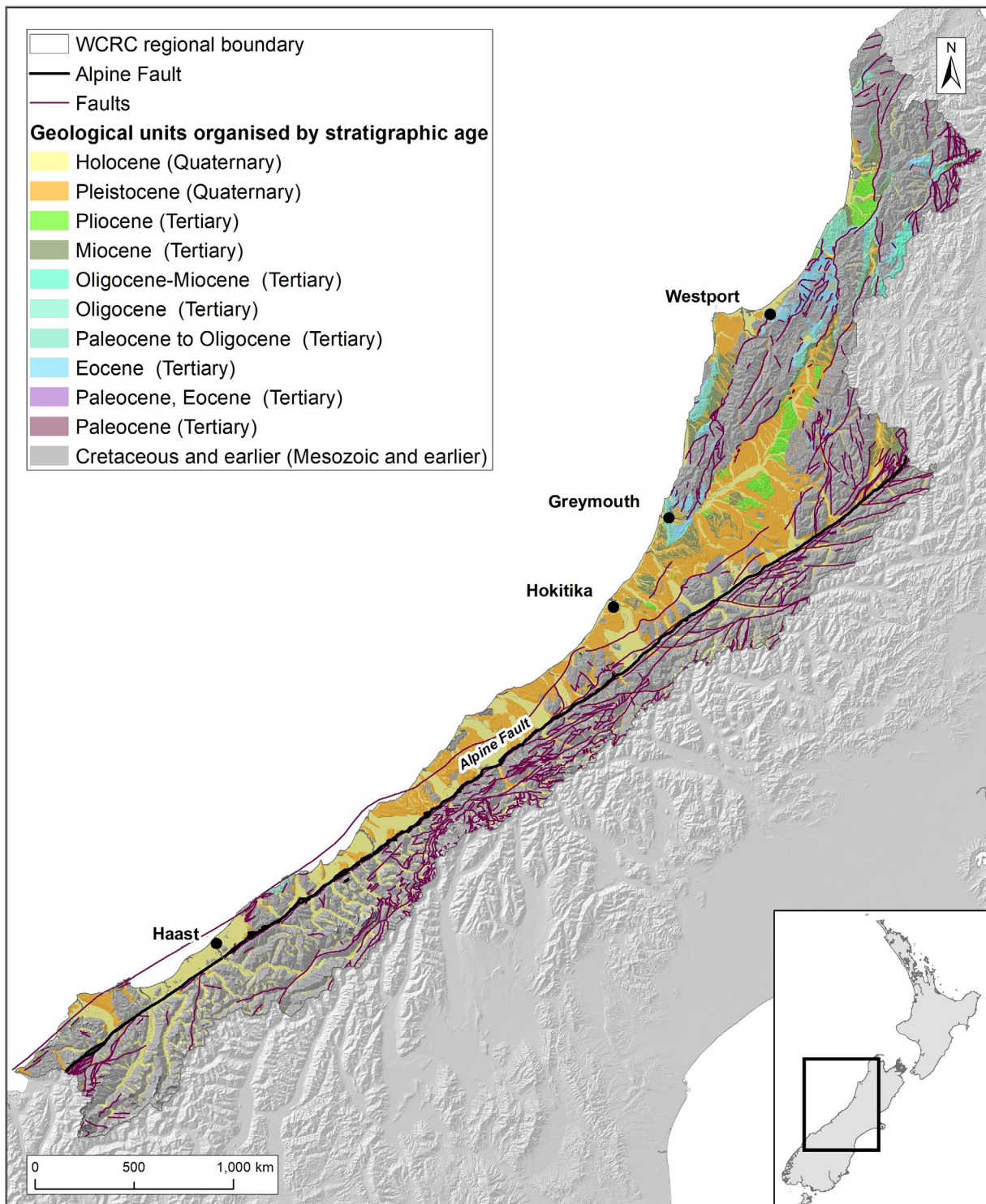


Figure 2.1 Simplified geology of the West Coast region and major faults (modified from Heron 2020).

## **2.2 Climate, Hydrology and Surface Water Monitoring**

### **2.2.1 Climate and Rainfall Monitoring**

The West Coast has a wet, cool climate with occasional dry, hot periods. Rainfall increases southwards, and the region is regarded as the wettest of the country, with median total rainfall in excess of 6000 mm in the Southern Alps for the period 1981–2020 (Figure 2.2). An annual total rainfall of 11228 mm was measured at the Cropp River (waterfall) in 2017 (Beaumont et al. 2018). The Paparoa Range provides a rain shadow for the Reefton area, where the region's lowest rainfall is recorded (annual rainfall of 1943 mm at Reefton for the period 1981–2010); Karamea and Westport, located at the western side of the range, also exhibit lower than regional average rainfall with 1868 mm and 2046 mm, respectively (Figure 2.2; Macara 2016; NIWA [2021]).

Precipitation falls as snow at higher elevations, forming glaciers such as the Fox and Franz Josef glaciers (Figure 2.3). These glaciers, due to their dynamic nature, are regarded as indicators of climate variability (Macara 2016). Temperatures at the coast are mild (median annual temperature between 11°C and 13°C), above zero and decrease inland as elevation increases. Along the Southern Alps, median annual temperatures below 2°C occur. Between 1988 and 2015, the West Coast experienced multiple extreme rainfall events associated with significant flooding (e.g. estimated \$16 million of total flood damage in 1988; Macara 2016).

The concentrations of tritium in rain vary depending on latitude and origin of the meteoric water. Near the coast, with direct input of air masses from the ocean, tritium concentrations are expected to be lower compared to rainfall further inland, due to dilution of tritium-rich high-altitude meteoric water by low-tritium oceanic moisture. Rain in the valleys behind mountain ranges and at higher altitudes is sheltered from direct influence of oceanic air masses and is expected to have a signature similar to that of high-altitude meteoric water with higher tritium concentrations. To establish the scaling factor for the West Coast hydrologic system in comparison to New Zealand's long-term tritium record from Kaitoke at the southern end of the Tararua Ranges, 40 km north of Wellington, a rain collector was installed in Greymouth that provided measurements of tritium in monthly rain samples over the 2.5-year period from April 2009 to October 2011 (Figure 2.3). These data have not been previously reported and are presented in this report (Section 4.3.1).

A transect of river stable-isotope measurements through the Southern Alps demonstrated that the isotope ratios observed in the West Coast rivers decrease with elevation. This survey resulted in the establishment of a local meteoritic line (Kerr et al. 2015).

### **2.2.2 Hydrology and Surface Water Monitoring**

The region is bounded by the coast in the west and by the Southern Alps to the east, with ground elevations of up to 3724 m (Aoraki / Mount Cook; Figure 2.3). The region drains steeply towards the sea, and the rivers are subject to large flow variations in response to rainfall events. River catchments are typically very large and six rivers are currently monitored for flooding: the Karamea, Mokihinui, Buller, Grey, Hokitika and Waiho rivers (Macara 2016; WCRC [2021]).

WCRC monitors surface water quality through its Surface Water Quality Monitoring Programme. This programme assesses surface water quality states and trends at selected sites where human impacts/pressures occur. This network consists of 43 sites, sampled quarterly for

physical, chemical and bacteriological attributes, as well as periphyton and macroinvertebrate communities, since 1996. Lake Brunner water quality has also been monitored since the early 1990s (Horrox et al. 2015).

The world-renowned experimental Maimai headwater catchment (Figure 2.3) has been monitored by the University of Saskatchewan, Canada, since the 1970s as part of an international long-term hillslope joint-research programme aiming to improve understanding of stream flow generation (McGlynn et al. 2002; Ameli et al. 2018; Gabrielli et al. 2018). These programmes include GNS and the National Institute of Water & Atmospheric Research (NIWA) as national collaborators.

Most waterways (88%) come from higher-altitude headwaters that have pristine water quality and that often buffer the impact of contaminants entering downstream. Impacted surface water quality catchments form a small subset of the lowland monitoring sites where agricultural activity has increased. Surface water quality monitoring in these areas indicates decreasing ammonia and phosphorus concentrations, which may reflect improved handling of point source contaminants and better soil nutrient management; however, nitrogen and *Escherichia coli* (*E. coli*) are increasing. Nitrogen levels in rivers are usually high enough to support prolific algal growth but below toxicity thresholds. The high rainfall and low phosphorus concentrations limits the occurrences of such algal blooms. Faecal contamination and pathogen risk are ongoing issues for West Coast water quality (Beaumont et al. 2018). Lake Brunner is an oligotrophic (low-nutrient) lake that is a popular recreational destination for people within and beyond the region. Nutrient increases observed since the 1990s led to improved environmental mitigations among the farming community. Thanks to these efforts, the lake water quality is now classed as a 'low-nutrient' lake (Beaumont et al. 2018).

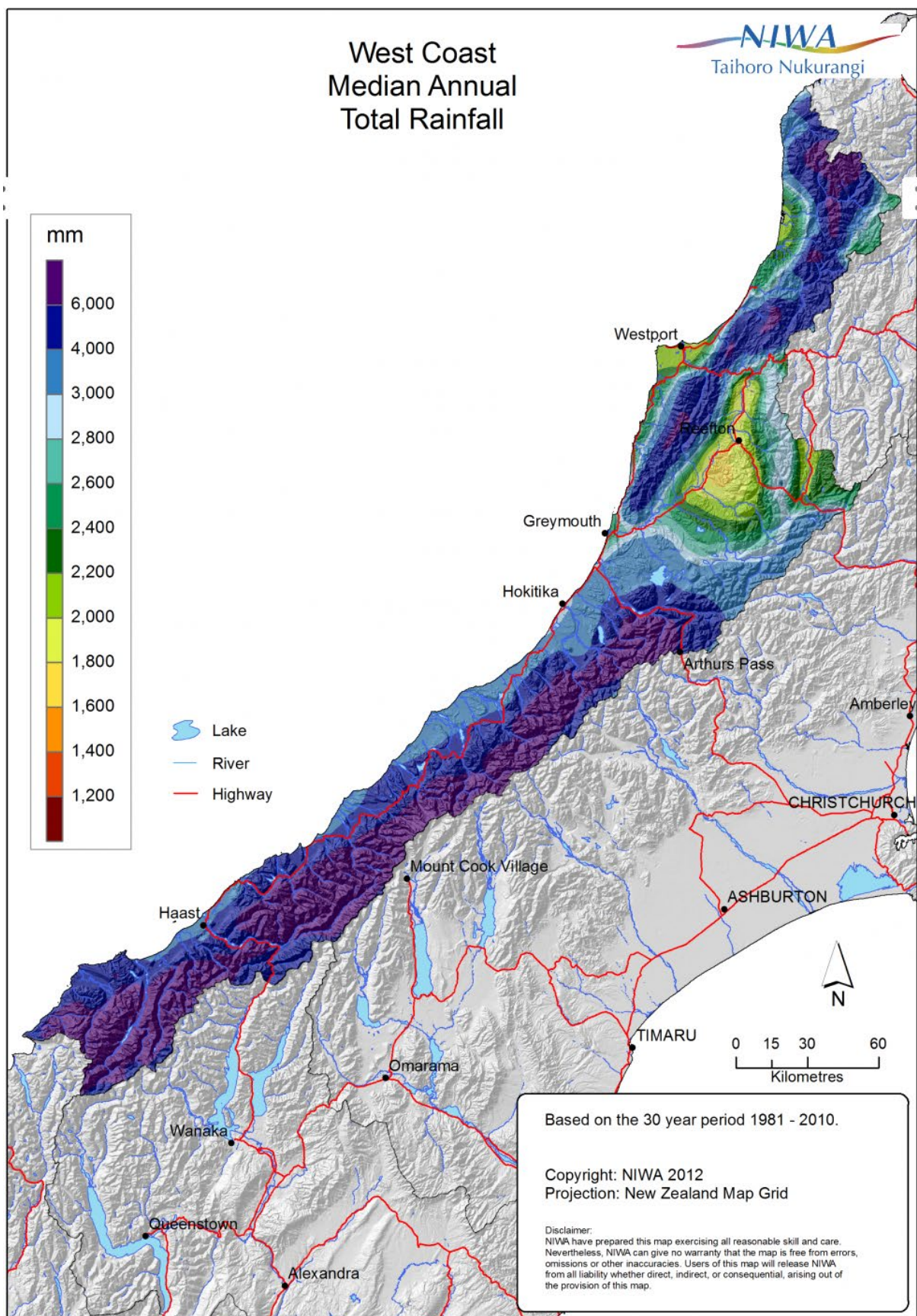


Figure 2.2 Median rainfall in the West Coast region (NIWA [2021]).

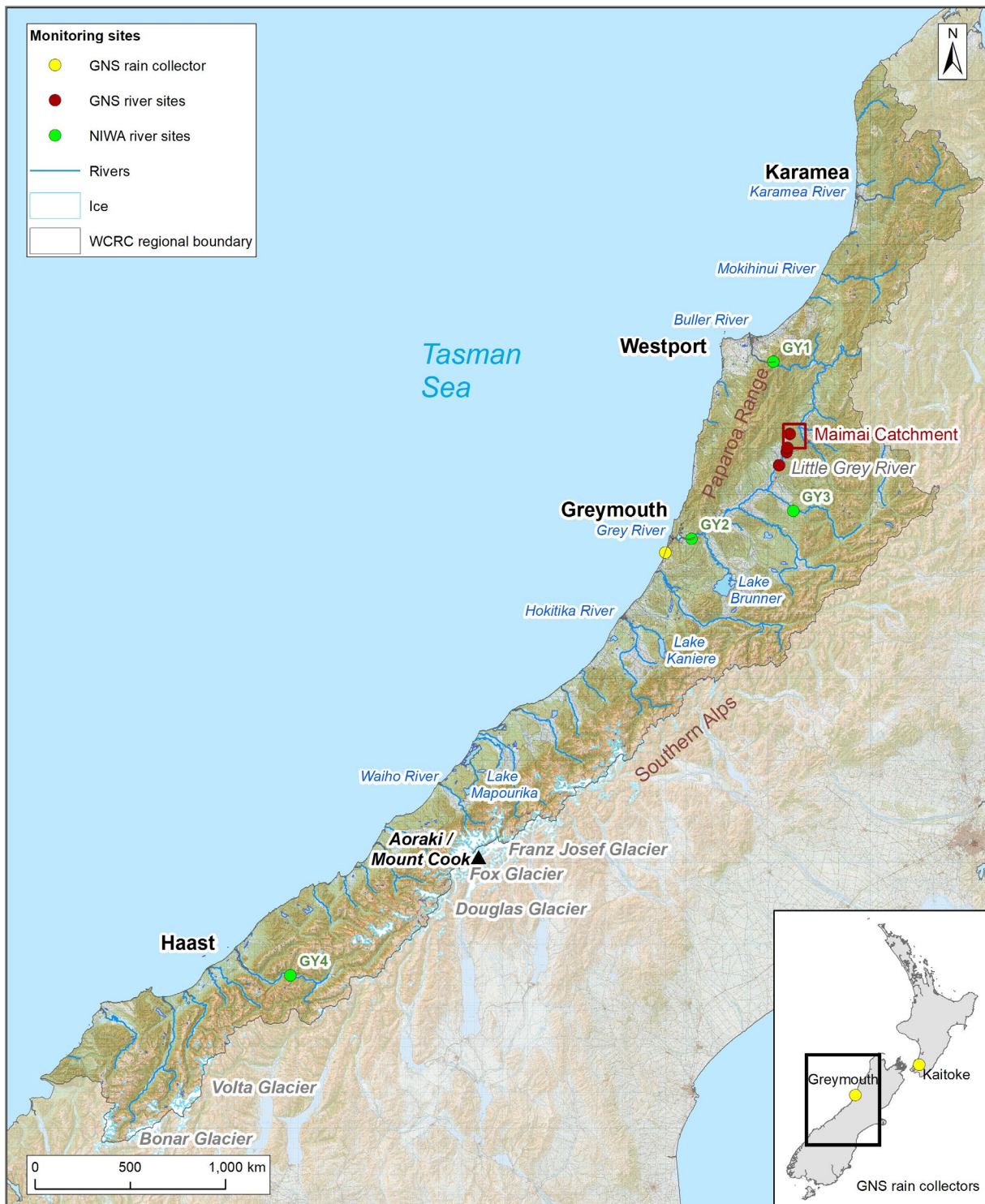


Figure 2.3 West Coast hydrological features. The insert shows the location of the temporary rain collector deployed in the West Coast and the long-term Kaitoke rain collector.

### 2.2.3 Transit Time in Rivers: Recent Insights from the Maimai Catchment

A recent study (Gabrielli et al. 2018) investigated the links between runoff generation processes, groundwater age and their effects on stream water transit time in the Maimai Catchment (Figure 2.3). Tritium dating and hydrogeological characterisation from 40 bedrock wells and headwater streams was utilised to shed light into extent, dynamics and age of the groundwater that contributes to stream flow. Results support the notion that most groundwater is exchanged only slowly with the surface and is therefore relatively old and highlights the need for tracer-calibrated groundwater flow models (Gabrielli et al. 2018).

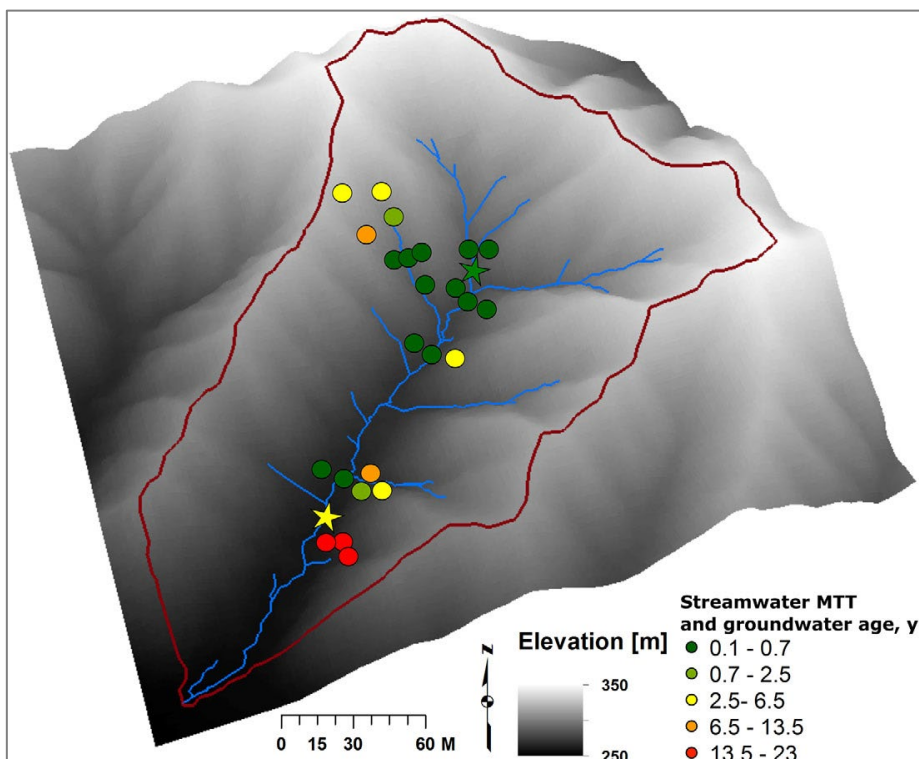


Figure 2.4 Spatial distribution of soil and bedrock groundwater age and stream water Mean Transit Time (MTT) across the M8 catchment. Bedrock and soil samples are indicated by coloured circles, and surface samples are indicated by stars (from Gabrielli et al. 2018).

## 2.3 Hydrogeology

### 2.3.1 Groundwater Resources

The Alpine Fault acts as a hydraulic seal between groundwater held in the schist mountains to the southeast of the fault from the unconfined water table in fan and alluvial gravel deposits northwest of the fault (Cox et al. 2013).

West of the fault, Quaternary alluvial deposits are regarded as the main groundwater source in the region (Figure 2.5). These deposits are typically 20–40 m thick adjacent to streams and rivers (Moreau 2019). Tertiary deposits are generally mudstone or siltstone dominated and therefore regarded as aquitards, with a few notable exceptions. Limestones from the Nile Group (Oligocene to Miocene) outcrop around Karamea and between Charleston and Punakaiki. They host significant karstic features, such as New Zealand's largest limestone arches (Oparara Basin); and the Honeycomb Hill Cave System, with more than 70 entrances (NZSS c2020). In Jackson Bay, the Anataonga Cave occurs within limestone outcrops from the Titirira Formation (Miocene) (Raiber and Daughney 2009; Cox et al. 2007; Rattenbury et al. 1998; Rattenbury et al. 2010; NZSS c2020).

East of the Alpine Fault, multiple warm ( $20^{\circ}\text{C}$ ) to hot ( $82^{\circ}\text{C}$ ) springs have been mapped (Figure 2.5), generally occurring within Quaternary deposits overlying Triassic units (Cox et al. 2007). These springs are the surface expression of active fluid circulation, with a strong hydrothermal gradient associated with rapid uplift of the Alpine Fault hanging walls. These springs are used locally for bathing (Mongillo and Clelland 1984; Nathan et al. 2002; Cox et al. 2007; Rattenbury et al. 2010). One spring ( $20^{\circ}\text{C}$ , discharging in the Cascade River about 1 km northeast of Theta Tarn) issues from the base of an extensive (c.  $100 \text{ m}^2$ ) terraced travertine deposit (Rattenbury et al. 2010). Tertiary and earlier deposits are considered as hydrogeological basement.

## 2.4 Groundwater Use

Groundwater is mainly used by communities for drinking-water, agriculture, processing and bottled water production (Raiber and Daughney 2009; Beaumont et al. 2018). South of Franz Josef, the groundwater resources are only used for communities' drinking-water supplies and are mostly un-utilised, owing to abundant rainfall (Nathan et al. 2002; Cox et al. 2007; Rattenbury et al. 2010). In the Grey Valley, Quaternary alluvial gravel outwash deposits (typically 20–40 m and up to 60–80 m thick) act as unconfined aquifers. The largest allocation volumes are located in the upper Grey Valley and, in this system, baseflow index calculation suggests that just under 50% of the river baseflow is sourced by groundwater (Mourot and White 2020).

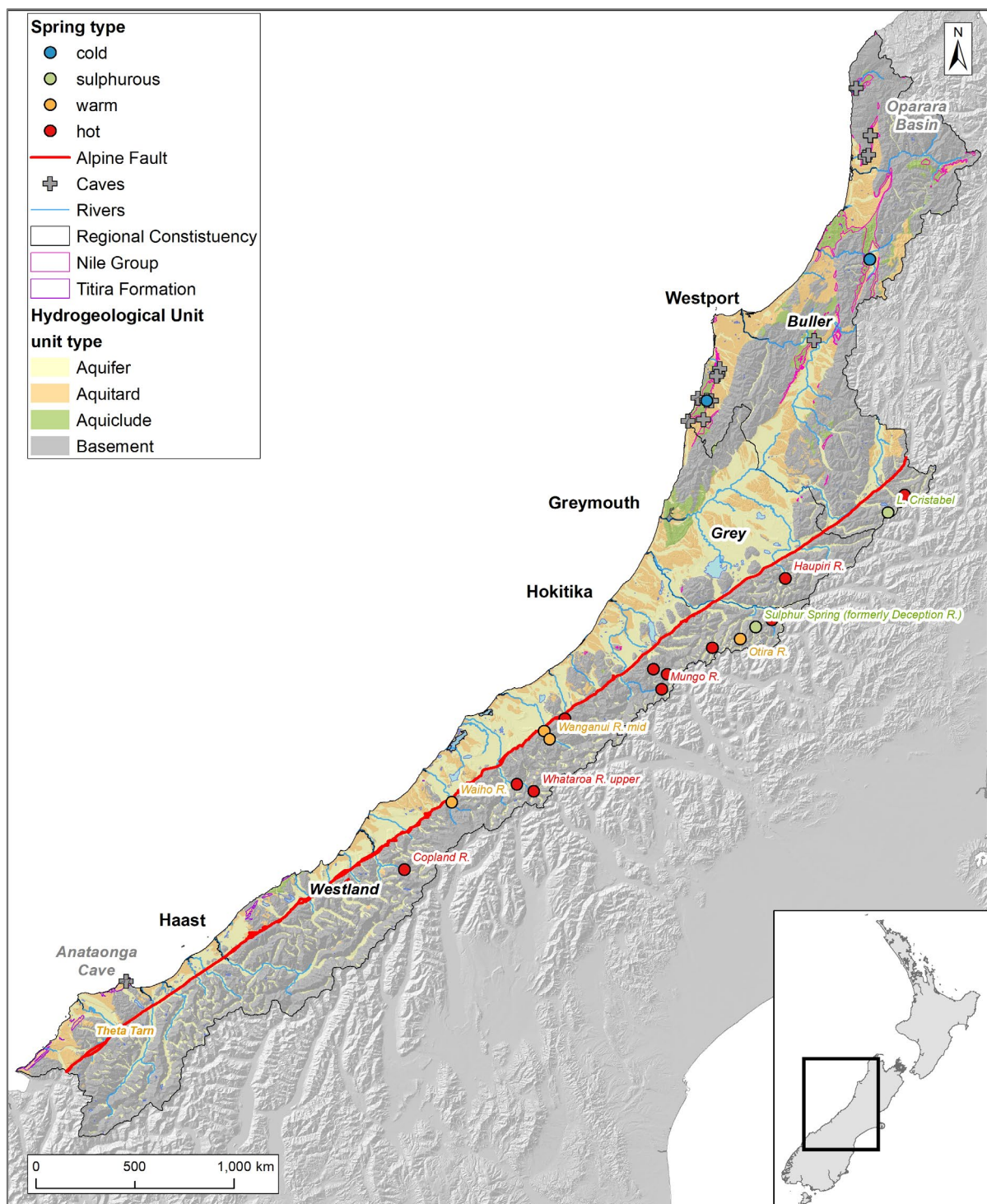


Figure 2.5 Simplified hydrogeology of the West Coast region, caves and spring locations (White et al. 2019; LINZ Data Service 2021).

## 2.5 Groundwater Monitoring

Groundwater quality is currently monitored in the region via three programmes (Figure 2.6):

- WCRC State of the Environment (SOE) groundwater monitoring programme – the West Coast SOE groundwater quality monitoring dataset is a combination of site-specific studies and ongoing monitoring managed by regional authorities to inform environmental reporting and groundwater resource management. In the West Coast, the current network comprises 21 active monitoring wells sampled for 35 parameters annually or bi-annually. Monitoring started in 1998 and the number of SOE monitoring wells significantly increased in 2010 (Moreau 2019).
- National Groundwater Monitoring Programme (NGMP) – the NGMP is a long-term (late 1990s to current) collaborative programme operated between GNS and all regional authorities. It aims to identify spatial patterns and temporal trends in groundwater quality at the national scale and relate them to specific causes. In this programme, groundwater samples are collected quarterly at c. 110 sites nationwide and analysed for over 17 chemical parameters. Water dating at all sites was undertaken in 2009, with irregular ongoing re-sampling. In the West Coast, the NGMP dataset consists of eight active and two retired wells. Monitoring started in 1998, and all sites are shared with the SOE network. This programme is funded by MBIE Strategic Science Investment Fund infrastructure.
- GNS's National Tracer Survey (NTS) – this programme aims to collect age-tracer data in data-sparse regions of New Zealand, which complements age-tracer information collected under the NGMP. This programme was initiated in 2011. Targeted sites are shallow wells where the water is expected to be young enough for the well to have responded already to anthropogenic changes. In the West Coast, the NTS network consists of 21 wells and two springs. This programme is co-funded between MBIE's Strategic Science Investment Fund and TWOTW.

Groundwater levels are monitored by WCRC as part of the SOE programme at 39 wells, all sourced from the Quaternary deposits west from the Alpine Fault, with a monitoring frequency of three times a year to monthly. A detailed description and maps of the SOE monitoring network is available in Moreau (2019).

West of the fault, groundwater in the Quaternary deposits is relatively dilute, with median conductivities close to 100 µS/cm. Both long-term monitoring and local site investigation studies have demonstrated occurrences of high nitrate concentrations. These concentrations are associated with intensive land-use activities and indicate minor changes between the dry and wet seasons, i.e. precipitation-facilitated downward migration of nitrate-nitrogen and sulphate from anthropogenic sources (Zemansky and Horrox 2007a, 2007b). Groundwater age determination at the eight NGMP sites yielded mean residence times (MRT) ranging from 1 to 4 years. Microbial contamination is a recurrent and widespread groundwater quality issue for these aquifers (Moreau 2019). Depth to groundwater in the Quaternary deposits remains relatively stable through time, with medians from 0.77 to 11.98 m below the top of casing. Groundwater level declines have been reported at seven sites for the 2007–2017 and 1997–2017 time periods (Moreau 2019). The groundwater quantity allocation framework is currently being developed to better control groundwater abstraction and will be integrated in the WCRC Regional Land and Water Plan (Mourot and White 2020).

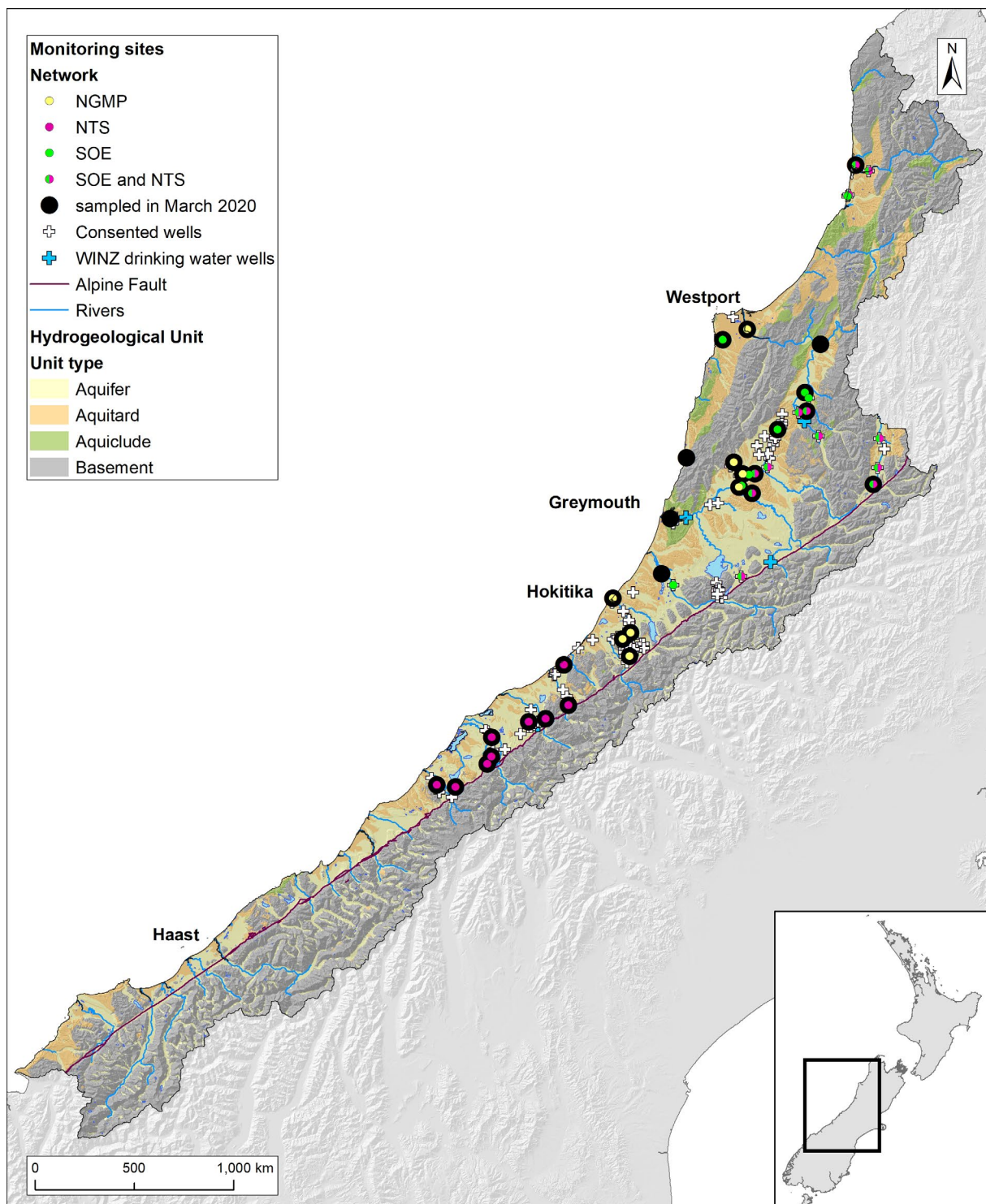


Figure 2.6 Location of groundwater monitoring sites, including sites sampled in March 2020 as part of this study.

## 3.0 METHODS

In this section, a general description of the method and interpretation techniques is presented for the following environmental tracers: water age tracers, radon, stable isotopes, hydrochemistry, temperature, argon and nitrogen gases.

### 3.1 Environmental Tracing

#### 3.1.1 Groundwater Dating

The methods for groundwater dating in the Southern Hemisphere are described in Morgenstern and Daughney (2012). Groundwater dating utilises convolution of a known time-dependent tracer input (via the rain into the groundwater) with a suitable system response function and matching to the tracer concentration measured in groundwater. A range of groundwater age tracers are available (Beyer et al. 2014); they should be applied in a complementary way, as application of a single tracer can result in ambiguous interpretations. Multi-tracer approaches can improve the robustness of the age interpretation and enhance the characterisation of groundwater recharge processes. We routinely use the most robust and cost-effective age tracers in New Zealand, i.e. tritium, sulphur hexafluoride ( $SF_6$ ), chlorofluorocarbons (CFCs) and Halon-1301 (Figure 3.1). Three types of tracers are used to establish residence times: age tracers with long-term time-dependent tracer input concentrations in the atmosphere or that exhibit radioactive decay, allowing groundwater dating in the age range 1–100 years, and radon build-up in groundwater for dating periods of up to several weeks.

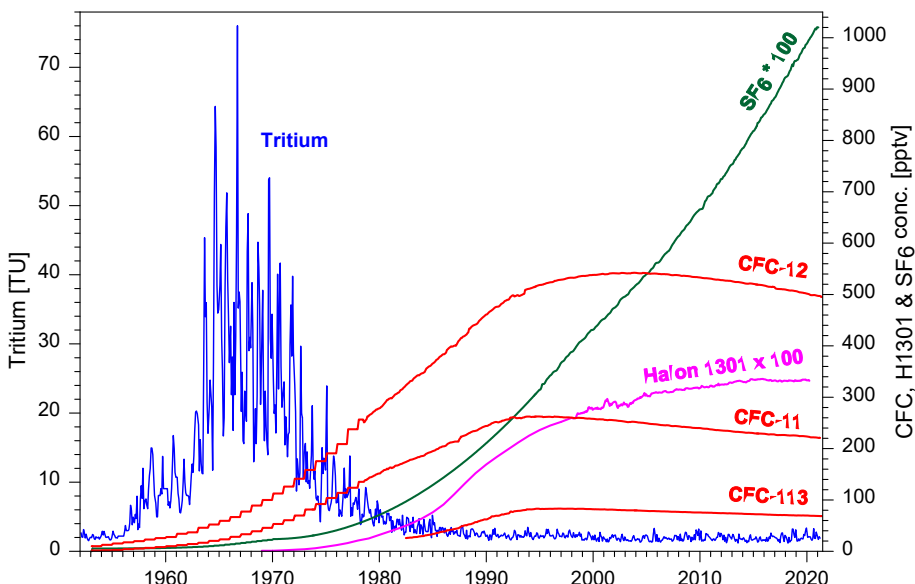


Figure 3.1 Tritium, CFCs, Halon-1301 and  $SF_6$  input for New Zealand rain. Tritium concentrations are in rain at Kaitoke, 40 km north of Wellington (monthly samples), and CFCs, Halon-1301 and  $SF_6$  concentrations are for southern hemispheric air. TU = 1 represents a  $^3H/{}^1H$  ratio of  $10^{-18}$ , and 1 ppt is one part per trillion by volume of CFCs, Halon-1301 or  $SF_6$  in air, or  $10^{-12}$ . Pre-1978 CFC data are reconstructed using methods of Plummer and Busenberg (2000) and scaled to the southern hemisphere by a factor of 0.83 (CFC-11) and of 0.9 (CFC-12). Post-1978 CFC data are from Tasmania. Pre-1970  $SF_6$  data are reconstructed (USGS, Reston), 1970–1995 data are from Maiss and Brenninkmeijer (1998) and post-1995 data were measured in Tasmania. Halon-1301 data are from Beyer et al. 2017.

The measured tracer output concentration in the groundwater ( $C_{out}$ ) is compared to its historical input ( $C_{in}$ ) using the convolution integral:

$$C_{out}(t) = \int_0^{\infty} C_{in}(t - \tau) e^{-\lambda\tau} g(\tau, f) d\tau \quad \text{Equation 3.1}$$

where  $t$  is time of observation;  $\tau$  is transit time (age);  $e^{-\lambda\tau}$  is decay term, with  $\lambda$  being  $\ln(2)/T_{1/2}$  (radioactive decay of tritium with a half-life  $T_{1/2} = 12.32$  years); and  $g(\tau, f)$  is system response function (Maloszewski and Zuber 1982, 1991; Zuber et al. 2005; Cook and Herczeg 2000). The response function describes the distribution of ages within the water sample, for example, arising from mixing of groundwater of different ages within the aquifer or at the well. The two most commonly employed response functions are the dispersion model and the exponential piston flow model (Zuber et al. 2005). The exponential piston flow model is a combination of the piston flow model, which assumes piston flow in a single flow tube with minimal mixing of water from different flow lines at the discharge point (e.g. confined aquifer), and the exponential model, which assumes full mixing of water from different flow paths with exponentially distributed transit times at the groundwater discharge point (e.g. mixing of stratified groundwater at an open well in an unconfined aquifer).

The various response functions are described in Zuber et al. (2005) and Cook and Herczeg (2000). Stewart et al. (2017) showed that the exponential piston flow model covers the age distributions of typical groundwater discharges. The exponential piston flow model response function is given by:

$$g(\tau) = 0 \quad \text{for } \tau < t_t(1-f) \quad \text{Equation 3.2}$$

$$g(\tau) = (f/t_t)^{-1} \exp[-(\tau/f t_t) + (1/f) - 1] \quad \text{for } \tau > t_t(1-f) \quad \text{Equation 3.3}$$

where  $t_t$  is the MRT,  $f$  is the ratio of the volume of exponential flow to the total flow volume at the groundwater discharge point and  $t_t(1-f)$  is the time water takes to flow through the piston flow section of the aquifer (Maloszewski and Zuber [1982] use the variable  $\eta$ ;  $\eta=1/f$ ). The model with  $f = 0$  becomes equivalent to the piston flow model and, with  $f = 1$ , becomes equivalent to the exponential model.

The two parameters of the response functions,  $t_t$  specifying the mean and  $f$  the distribution of transit times, are determined by convoluting the input (tritium concentration in rainfall) to simulate passage through the hydrological system in such a way as to match the output (e.g. tritium concentration in wells or springs).

### 3.1.1.1 Age Tracers

Tritium is produced naturally in the atmosphere by cosmic rays. In addition, large amounts of tritium were released into the atmosphere in the early 1960s during the atmospheric thermonuclear weapons testing, giving rain and surface water high tritium concentrations at that time (Figure 3.1). Surface water becomes separated from the atmospheric tritium source when it infiltrates into the ground; the tritium concentration in the groundwater then decreases over time due to radioactive decay and is therefore a function of time that the water has been underground (age).

Tritium, with its pulse-shaped input, is a particularly sensitive tracer for identifying the two unique age distribution parameters via the delay and dispersion of the bomb-pulse in the groundwater compared to the rain input. This approach is particularly useful for age interpretation of wells

with little other information on mixing of groundwater from varying depths and of different ages. The superimposed bomb-tritium can very sensitively identify water recharged between 1960 and 1975, enabling identification of complicated age distributions in groundwaters, e.g. from multi-screen wells, if tritium time-series and/or multi-tracer data are available.

Tritium has now become the most robust groundwater dating tool in New Zealand. It is part of the water molecule and has no sources or sinks in the groundwater system through chemical processes. The relatively small amount of bomb-tritium that mixed from its northern hemispheric sources into the southern hemisphere (Taylor 1968) has now decayed and, since about 2010, no longer results in ambiguous age interpretations for New Zealand hydrologic systems. Figure 3.2 shows the tritium output of a typical transfer function for New Zealand in comparison to that of Vienna, which is typical for the mid-latitude continental northern hemisphere. Dashed lines show the tritium output 10 years ago, when still-significant levels of bomb-tritium were present in the groundwater systems. In New Zealand, a monotonous decline in tritium output versus MRT was already observed 10 years ago, allowing determination of unique groundwater ages with a single tritium measurement. In the northern hemisphere, there is still a significant amount of bomb-tritium present in the groundwater systems, requiring complementary age tracers ( $\text{SF}_6$ , helium-3) or tritium time-series data to find unique ages. However, from Figure 3.2, it can be derived that, in the coming years, the bomb-tritium will also have declined sufficiently in the northern hemisphere, similar to the situation in New Zealand in 2010, to allow determination of unique ages from single tritium measurements, including surface water dating where no complementary age tracers are available.

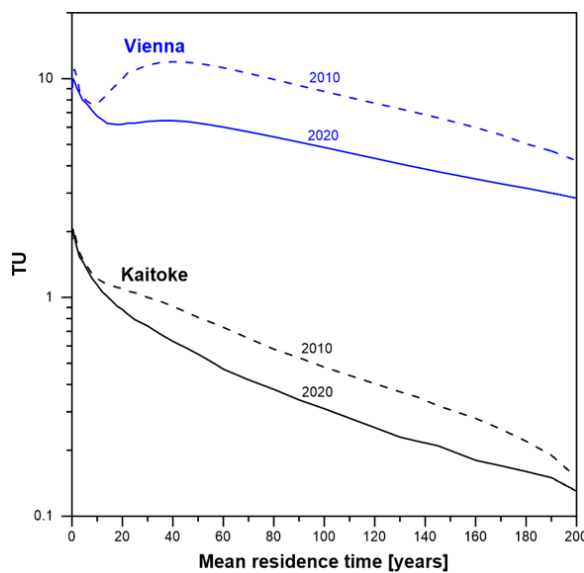


Figure 3.2 Tritium output for a typical transfer function of 80% exponential flow volume within an exponential piston flow model, calculated using the Kaitoke (New Zealand) and Vienna (Europe) tritium input. Solid lines are current tritium output; dashed lines are previous tritium outputs from 10 years ago for comparison to show the decline of the bomb-tritium.

Tritium now also enables dating of river and stream water over time scales of years and decades. No other readily available tracer is able to date surface water, as other tracers are significantly altered when the groundwater is exposed to air. In other parts of the world, the application of accurate and robust groundwater dating for the understanding of hydrological systems on large scales, with respect to groundwater lag times, storage, recharge, hydrochemical evolution and land use versus geologic impact on groundwater quality, is still more complicated as bomb-tritium remains present. Therefore, these new opportunities offered by the tritium method in New Zealand are currently leading to needed improvements in the understanding of hydrologic systems (McDonnell 2017).

To provide the tritium input into New Zealand hydrologic systems, tritium concentrations are measured in rainfall at Kaitoke, 40 km north of Wellington (monthly values, Figure 3.1). This data is used for locations around New Zealand by applying a scale factor to adjust for latitude, altitude and coastal influence. The scale factor is deduced from an additional eight New Zealand rain records at least two years in length.

CFCs are entirely man-made contaminants. They were mainly used for refrigeration and pressurising of aerosol cans, and their concentrations in the atmosphere gradually increased until the mid-1990s (Figure 3.1). CFCs were then phased out of industrial use because of their destructive effects on the ozone layer. Thus, rates of increase of atmospheric CFC concentrations slowed greatly in the 1990s and concentrations are now decreasing, meaning that CFCs are not as effective for dating water recharged after 1990. CFCs are relatively long-lived and slightly soluble in water, therefore entering the groundwater systems with groundwater recharge. Their concentrations in groundwater record the atmospheric concentrations when the water was recharged, allowing determination of the recharge date of the water.

Another chemical compound, Halon-1301 ( $\text{CBrF}_3$ ), holds promise to remain a more efficient age tracer, with still slightly increasing concentrations in the atmosphere (Figure 3.1) and absence of local contamination sources that interfere with the dating (Beyer et al. 2017). Halon-1301 has been used as a refrigerant gas and fire suppressant agent in the mid-1990s but also faces production restriction due to its ozone-depleting effect.

$\text{SF}_6$  is primarily anthropogenic in origin but can also occur in some volcanic and igneous fluids. Significant production of  $\text{SF}_6$  began in the 1960s for use in high-voltage electrical switches, leading to increasing atmospheric concentrations (see Figure 3.1). The residence time of  $\text{SF}_6$  in the atmosphere is extremely long (800–3200 years). It holds considerable promise as a dating tool for post-1990s groundwater because, unlike CFCs, atmospheric concentrations of  $\text{SF}_6$  are expected to continue increasing for some time (Busenberg and Plummer 2000), as evidenced by the recent more-than-linear increase, which makes  $\text{SF}_6$  a very sensitive tool for dating young groundwater.

### **3.1.1.2 Radon**

Radon-222 ( $^{222}\text{Rn}$ ) gas is a radioactive decay product of uranium, which is ubiquitous in almost all rocks and soils. Groundwaters, in a closed system in contact with these rocks, accumulate  $^{222}\text{Rn}$  released from the minerals, resulting in elevated  $^{222}\text{Rn}$  concentrations in the groundwater. These concentrations are a result of equilibrium between  $^{222}\text{Rn}$  delivery and radioactive decay (half-life 3.8 days) and can vary considerably depending on the uranium content and  $^{222}\text{Rn}$  emanation potential of the aquifer material. In surface waters,  $^{222}\text{Rn}$  concentrations are low because of limited contact with its source and because of decay and degassing into the air. This tracer informs on the presence of young (up to weeks) groundwater.

This contrast between high  $^{222}\text{Rn}$  concentrations in groundwater and low concentrations in surface water allows the identification of fresh groundwater discharges into surface water, as indicated by elevated  $^{222}\text{Rn}$  concentrations in the river water (Martindale et al. 2018). Conversely, fresh river water recharge into groundwater systems is indicated by low  $^{222}\text{Rn}$  concentrations in groundwater, as it takes approximately three weeks (5–6 half-lives) for the  $^{222}\text{Rn}$  to equilibrate to the ambient concentration of the groundwater.

### **3.1.2 Stable Isotopes of the Water**

The stable isotope signature of meteoric water depends on the history of the water masses with regard to temperature-dependent kinetic processes, such as evaporation of the water from the sea and re-precipitation. For example, rivers from colder, higher-altitude catchments usually have a more negative isotope signature than local low-altitude rain near the coast, allowing us to distinguish whether groundwater recharge is derived from the river or from local rainfall.

The stable isotope ratios  $^{18}\text{O}/^{16}\text{O}$  and  $^2\text{H}/^1\text{H}$  are expressed as  $\delta$  values and represent the difference in parts per thousand between isotope ratios in water relative to those in Vienna Standard Mean Ocean Water (V-SMOW):  $\delta^{18}\text{O} (\text{\textperthousand}) = [(^{18}\text{O}/^{16}\text{O})_{\text{sample}}/(^{18}\text{O}/^{16}\text{O})_{\text{VSMOW}} - 1] \times 1000$ .  $\delta^2\text{H}$  is expressed in a similar way. The stable isotope analysis was carried out in the Rafter Stable Isotope Lab at GNS using mass spectrometry.

## **3.2 Hydrochemistry**

The hydrochemical composition of groundwater reflects its recharge conditions and evolutionary flow pathways. Various land-use activities or geological formations can result in specific groundwater chemistry signatures that can be traced back to recharge source or area. Increasing ion concentrations of the water due to water-rock interaction with the aquifer material can indicate flow pathways and groundwater processes.

### **3.2.1 State and Trend**

To reflect the natural variability of groundwater chemistry, state and trend of groundwater quality is described using the following statistical metrics, which are consistent with previous SOE and national reporting (Moreau and Daughney 2015; Moreau 2019):

- Median and median absolute deviation (MAD): the median is a measure of central tendency. It is a more robust measure than mean values because it is not affected by outliers. The MAD gives an indication of the data spread around the median; it is likewise more robust than the standard deviation, particularly to long distribution tails (Helsel et al. 2020).
- Percentiles (5<sup>th</sup>, 25<sup>th</sup>, 75<sup>th</sup>, 95<sup>th</sup>): these also inform the data spread around the median (Helsel et al. 2020).
- Trend magnitude: the rate of change in each parameter. In this report, the trend magnitudes are based on Sen's slope estimator, which is commonly used for environmental reporting (Helsel et al. 2020).
- Trend category: this is a descriptive category based on the sign of Sen's slope. A symmetric confidence interval around the trend is calculated. If this interval contains zero, the trend is described as 'uncertain'. If this interval does not contain zero, it is 'established with confidence' and assigned either a 'decreasing' or 'increasing' descriptor. This method was recently developed and applied to river quality state and trend assessments (Larned et al. 2016; McBride 2019).
- Trend type: class is somewhat indicative of the confidence in ability to detect the trend over the natural range of variability in measured concentrations, measured through the MAD (Moreau and Daughney 2021). The trend is classed as 'perceptible' if the change calculated using Sen's slope over the time period is greater than the median plus two MADs and as 'imperceptible' elsewhere.

- Statistical test p-values: in this report, several statistical tests were conducted to assess either the statistical significance of a trend, seasonality or distribution difference. For each test, a hypothesis is formulated and test statistics are calculated. An acceptable error rate is arbitrarily set to reject or accept the hypothesis, based on a data-calculated probability value (p-value). For this report, the significance level was arbitrarily set as  $\alpha = 0.05$  for all tests, which is a common threshold used in environmental statistics reporting. Detailed information about the use of hypothesis tests in general and the tests used in this report can be found in Helsel et al. (2020).

### **3.2.2 Hierarchical Cluster Analysis**

Hierarchical cluster analysis (HCA) is a multivariate statistical method that categorises the chemistry data based on similarities in selected characteristics. We used HCA to assess variations in the hydrochemical composition of the groundwaters within the region and their potential for distinguishing between different recharge sources (e.g. local rain versus river recharge) and identification of flow-evolutionary processes. HCA requires the use of complete cases, i.e. at least one analytical result (below or above detection limit) per parameter per site. The parameter selection represents a compromise between suitable data for processing and interpretation including spatial coverage.

### **3.3 Recharge Temperature and Excess Air**

Recharge temperature and excess air, derived from argon and nitrogen concentrations, can provide insight into the mechanisms controlling recharge. Ingram et al. (2007) found that excess air concentrations are linked to the magnitude of fluctuations in groundwater level and used this relationship to delineate recharge sources and rates. River-recharged groundwaters, in areas where groundwater levels can be expected to show small fluctuations, usually have lower excess air concentrations than rainfall-recharged groundwater in areas with large groundwater level fluctuations.

Recharge temperature and dissolved excess air have been derived from dissolved argon and nitrogen concentrations using the total dissolution model of Heaton and Vogel (1981). In this model, small bubbles of air entrapped in soil pores are completely dissolved into the groundwater under favourable recharge conditions, thus forming an excess air component. In other areas of New Zealand, this method enabled assessment of recharge sources and identification of paleo-groundwaters recharged during previous colder climates (Morgenstern et al. 2017).

### **3.4 Analytical Techniques**

Activities of tritium were determined at GNS using liquid scintillation in Quantulus™ ultra-low-level counters following vacuum distillation and electrolytic enrichment (Morgenstern and Taylor 2009). Tritium activities are expressed in tritium units (TU), in which 1 TU represents a  $^{3}\text{H}/^{1}\text{H}$  ratio of  $1 \times 10^{-18}$ . Tritium enrichment by a factor of 95 at GNS yields a detection limit of 0.02 TU, and deuterium calibration of each sample ensures a 1% reproducibility of tritium enrichment. Relative precision (1 SD) of routine individual analyses are 1.8–2.3%.

Concentrations of CFCs (CFC-11, CFC-12, CFC-113), argon, nitrogen and methane ( $\text{CH}_4$ ) were analysed using an analytical system like that of Busenberg and Plummer (1992); the analytical system for  $\text{SF}_6$  is described in van der Raaij (2003). The CFC and  $\text{SF}_6$  concentrations in Figure 3.1 are for southern hemispheric air (where 1 ppt is one part per trillion by volume of CFC,  $\text{SF}_6$  or Halon-1301 in air, or  $10^{12}$ ).

Detection limits in terms of gas dissolved in water were  $5 \times 10^{-14}$  mol kg<sup>-1</sup> water for CFCs,  $1 \times 10^{-16}$  mol kg<sup>-1</sup> water for SF<sub>6</sub> and  $3 \times 10^{-16}$  mol for H-1301. Dissolved argon and nitrogen concentrations (analytical accuracy 1% and 3%, respectively) were measured to estimate the temperature at the time of recharge and the excess air concentration, as described by Heaton and Vogel (1981), for calculation of the atmospheric partial pressure (ppt) of CFCs and SF<sub>6</sub> at the time of recharge.

Radon-222 samples from groundwater and river water were collected in 20 mL glass vials with metal-lined lids. Due to the short half-life of radon, the samples were measured within a few days after sampling. We used liquid scintillation spectroscopy with 10 mL of sample water transferred into counting vials and mixed with a mineral-oil-based scintillant and radon absorber, followed by decay counting in a Quantulus™. Detection limits were typically <0.1 Bq/L. The Radon-222 analytical technique was validated by an inter-laboratory comparison organised by Flinders University, Adelaide, in 2018.

For the measurement of dissolved oxygen in the field, optical probes were used that produce more robust data than membrane probes.

Groundwater chemistry samples were collected following the 2006 standardised sampling protocol for State of the Environment monitoring, consistent with the current National Environmental Standards (Daughney et al. 2006; Milne et al. 2019). The March samples were analysed at the New Zealand Geothermal Analytical Laboratory, which is the same laboratory used for all NGMP samples since 1993. The March samples were analysed for the NGMP suite which include: sodium (Na), calcium (Ca), magnesium (Mg), potassium (K), carbonate (CO<sub>3</sub>), bicarbonate (HCO<sub>3</sub>), chloride (Cl), sulphate (SO<sub>4</sub>), nitrate-nitrogen (NO<sub>3</sub>-N), ammonia-nitrogen (NH<sub>3</sub>-N), dissolved iron (Fe), manganese (Mn) and dissolved reactive phosphorus (DRP) (Table 3.1). Hydrochemical analyses integrity of the March samples was checked by calculating the charge balance error and/or ionic sum to ensure that the electroneutrality of the sample was verified (Moreau-Fournier and Daughney 2010). A historical reconstruction (starting from 1993) of changes in analytical methods used for each of the selected parameters monitored as part of NGMP is available elsewhere (Moreau and Daughney 2021). A temporal map of analytical methods and laboratories for the SOE network is not currently available.

Table 3.1 Current list of parameters monitored at NGMP sites. APHA stands for American Public Health Association, which is a reference for analytical methods (Baird et al. 2017).

Parameter	Units	NGMP analytical method
HCO <sub>3</sub> , CO <sub>3</sub>	mg/L	Titration APHA 2320B
Ca, Mg, K, Na, Fe, Mn, SiO <sub>2</sub>	mg/L	Induced Coupled Plasma-Optical Emission Spectrometry, APHA 3120B
DRP	mg/L	Flow Injection Analyser APHA 4500-P G (modified)
Cl, NO <sub>3</sub> -N, SO <sub>4</sub> , Br, F	mg/L	Ion Chromatography APHA 4110B
NH <sub>3</sub> -N	mg/L	Flow Injection Analyser APHA 4500-NH <sub>3</sub> -N

## 3.5 Data Processing

### 3.5.1 Datasets

West Coast groundwater chemistry and age datasets were aggregated from the following sources (Figure 3.3, Table 3.2):

- Current monitoring datasets (SOE, NGMP, NTS).
- March 2021 sampling (including NGMP, NTS and SOE sampling) – groundwater samples were collected at 29 locations (two springs and 27 wells), out of which 13 sites had not been previously sampled by GNS or WCRC. Water age sampling was undertaken at all sites, whereas, for cost saving, chemistry samples were only collected at SOE sites where historical records were not available.
- GNS Water Dating Laboratory dataset – this dataset consists of historical data accumulated through the years by the laboratory as part of its operations. To reflect the sensitivity of some of this data, exact coordinates were removed from the provided dataset.

The aggregated datasets consisted of groundwater chemistry collected at 97 bores, two springs, one river and an unknown source with time series ranging from one-off measurements to the 1998–2021 time period (Table 3.2, Figure 3.3). The location of the sites is provided in Appendix 1 (Figures A1.1 and A1.2).

Table 3.2 Dataset summary for hydrochemistry and groundwater age.

Network	Measurement Type	Bore	Spring	River	Unknown
NGMP	Hydrochemistry times series + at least one age measurement	9	0	0	0
SOE	Hydrochemistry times series + single age measurement	4	0	0	0
	Hydrochemistry times series; no age measurement	5	0	0	0
SOE/NTS	Hydrochemistry times series + age measurement	12	0	0	0
NTS	Single hydrochemistry and age measurement	9	2	0	0
No network	Chemistry only	54	0	0	0
	Single chemistry or age or both measurements	2	2	0	0
	Age measurements only	1	0	1	1
<b>Total</b>		<b>97</b>	<b>2</b>	<b>1</b>	<b>1</b>

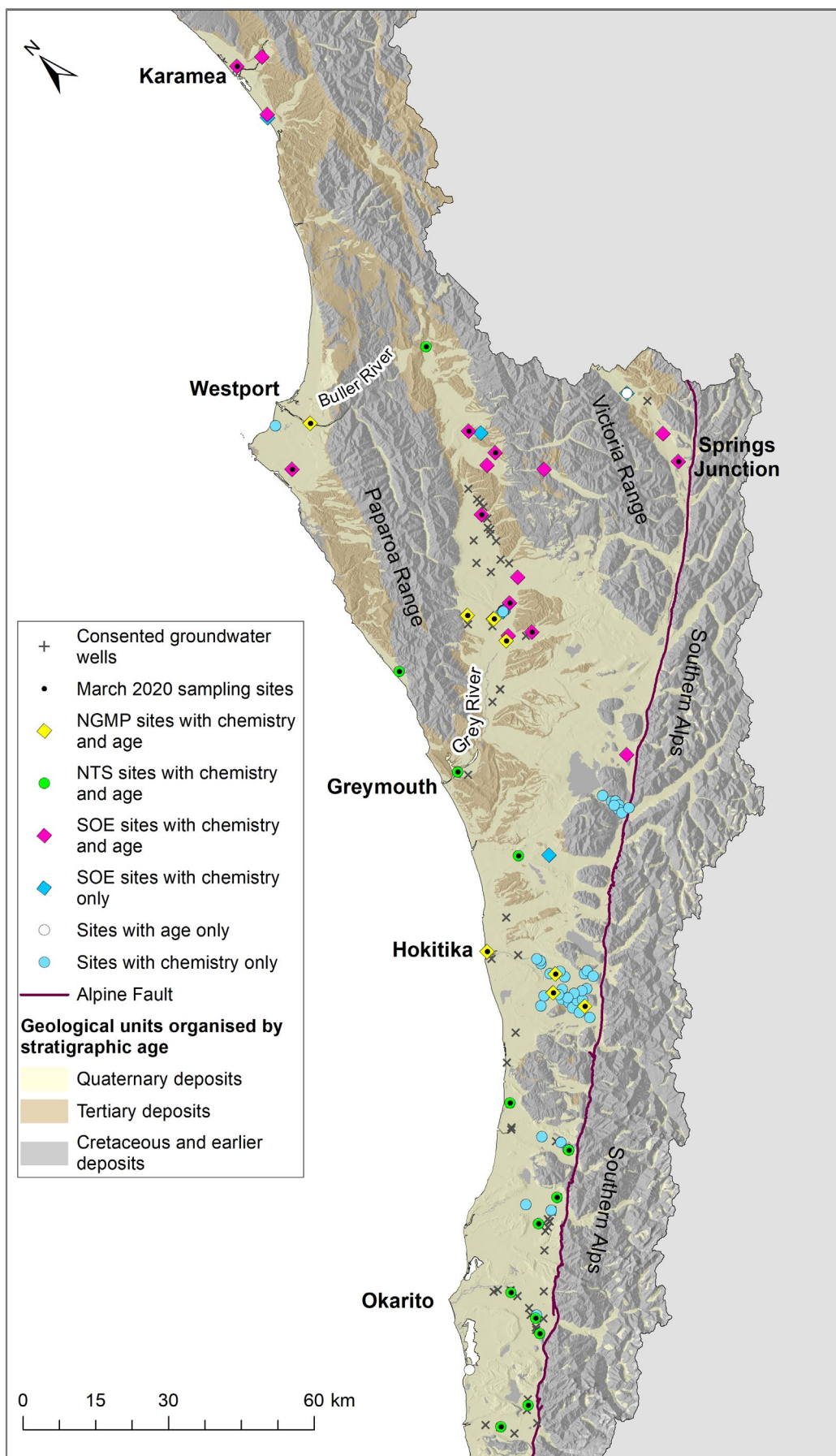


Figure 3.3 Location of sites with groundwater chemistry and age with, where applicable, an indication of the monitoring network in the West Coast region.

### **3.5.2 Age Interpretation**

For age interpretation, we used an average exponential piston flow model with 70% exponential age distribution within the total flow volume. Other models (e.g. binary mixing, alternative percentage for age distribution) were tested using tritium and other tracers and led to inconsistencies between models. Elsewhere in New Zealand, mixing models were constrained by tracing the bomb-tritium through the groundwater systems. However, the first age-tracer samples in this region were collected in 2001, after the bomb-tritium had passed. The lack of bomb-tritium signature, combined with the short memory of the hydrologic system (young water), led to the consistent use of a single, average model for age interpretation.

### **3.5.3 Hydrochemistry Data Processing**

#### **3.5.3.1 State and Trend Analysis**

The hydrochemistry data consisted of a combination of one-off analyses ( $n = 22$ ) and time series ( $n = 74$ ) collected as part of either site investigations (<2 years) or long-term monitoring (>5 years) (Table 3.2). State and trend analysis were performed using the R software (version 3.6.2) using the LWP-Trends (version 2101) and NADA (version 1.6-1.1) libraries. The LWP-Trends library was used to compute the Mann-Kendall trend test (seasonally adjusted or not), Sen's slope estimations and Kruskall-Wallis seasonality tests on censored and uncensored time series that have been processed with Non-Detects and Data Analysis (NADA) methods<sup>1</sup> (Helsel et al. 2020).

To calculate meaningful state and trend metrics, minimum data requirements were set as follows:

- Descriptive statistics (indicative of state over the 2012–2017 time period). Where there is no censoring, median, MAD and percentiles were estimated using statistical formula. For time series affected by less than 25%, median and MAD were estimated using Regression on Order Statistics (ROS) models and percentiles were calculated using statistical formula. Above 25% and below 80% censoring, no percentiles were calculated; median and MAD are computed using ROS models. Above 80% censoring, there is no estimate of median, MAD or percentiles; values are shown as below the highest detection limit.
- Kruskall-Wallis test (includes seasonal, both trend time periods): the number of seasons considered for the analysis is four (autumn, winter, spring and summer). The annual time period commences on 1 March of the first year (start of autumn). To enable seasonality state and trend assessments, all seasons must have at least one observation, and individual seasons require at least two data points.
- Mann-Kendall test and Sen's Slope estimator (includes seasonal and both trend time periods): the time series must contain at least 10 data points, the maximum censored values must be smaller than the maximum observed values, and at least 5 unique observations must be required for each time series.

---

<sup>1</sup> The NADA library implements the statistical methods to handle censored values (i.e. concentrations measured below the detection limit). It is used here to calculate medians and median absolute deviations for time series with left-censored values. For heavily censored datasets (i.e. more than 50% of results are recorded below the detection limit for a given parameter), a Regression on Order Statistics model was used to calculate the median value. Above 80% censoring (i.e. more than 80% of results for a given parameter are below the detection limit), medians were not estimated. Sites that had been sampled only once were still included in the hydrochemical assessment to maximise the number of sites available.

### **3.5.4 Hierarchical Cluster Analysis**

HCA was undertaken using the calculated site-specific median values of nine different parameters: Ca, Mg, Na, K, HCO<sub>3</sub>, Cl, SO<sub>4</sub>, field temperature and field electrical conductivity. In total, 70 groundwater sites had data for the selected parameters and were included in the HCA. Data for other parameters, such as NH<sub>3</sub>-N, Fe, Mn and DRP, were not available for all sites and therefore not included in the analysis. NO<sub>3</sub>-N in groundwater is mainly a reflection of the land use in the recharge area and is considered separately for assessment of the recharge source. Excluding NO<sub>3</sub>-N from the HCA better helps to focus on groundwater evolutionary processes.

Approaches for HCA were based on best practice from previous experience in New Zealand and overseas (e.g. Güler et al. 2002; Daughney and Reeves 2005). HCA was initially conducted on log-transformed and normalised median concentrations, temperatures or conductivity using the nearest-neighbour linkage rule. This approach identifies sites where hydrochemistry is most different from other sites. However, no sites were identified as potential outliers in the dataset. Following this, HCA was then conducted using Ward's linkage rule (Ward 1963). Ward's method is based on an analysis of variance and produces smaller distinct clusters than other linkage rules, in which each site in a cluster is more similar to other sites in the same cluster than to any site assigned to a different cluster. The square of the Euclidean distance was used in HCA as the measure of similarity for both linkage rules.

The appropriateness of the inclusion of single-analysis sites was checked by also performing the HCA on sites with long-term data only. No difference in clustering was observed for wells with long-term data compared to those in which single samples were included. The exclusion of NO<sub>3</sub>-N from the parameter selection did not make a difference in the clustering.

## **4.0 RESULTS AND DISCUSSION – GROUNDWATER PROCESSES AND FLOW DYNAMICS**

In this section, the water tracer results are interpreted with respect to (i) groundwater dynamics from recharge to discharge; (ii) interaction with surface water; (iii) recharge sources; and (iv) understanding of the processes that control groundwater hydrochemistry, including sources and expected loads of nutrients. The techniques are complementary, and the results improve significantly by integrating all techniques.

### **4.1 Data Outputs**

The analytical results from the groundwater samples collected in March 2020 are provided in the digital data file accompanying this report ‘GNS SR2021-16\_March2020\_analyses.xlsx’, with the following worksheets:

- ‘Read\_me’: caveat on the data.
- ‘Site\_information’: contains site details (ID, well depth information, coordinates) for the sample locations.
- ‘Chemistry’: contains the analytical results from the New Zealand Geothermal Analytical Laboratory.
- ‘Age’: contains the age tracer measurements and interpretation from the Water Dating Laboratory.

The chemistry and age-tracer dataset compiled and used in this report is provided in the accompanying digital data files ‘GNS SR2021-16\_Data\_Output.xlsx’, with the following worksheets:

- ‘Read\_me’: caveat on the data.
- ‘Site\_information’: site details (ID, well depth information, coordinates) for the sample locations. The last column indicates whether chemistry and/or age information is available at each site.
- ‘Units’: detailed information (acronym, units, form) for both chemistry and age-tracer parameter.
- ‘Chemistry’: aggregated analytical results from sources detailed in Section 3.5.1.
- ‘Age’: aggregated age-tracer measurements and interpretation from sources detailed in Section 3.5.1.
- ‘State\_Trend’: groundwater chemistry state and trend metrics calculated over the time period available at each site, on a per site per parameter basis. Reported metrics are: median and MAD, percentiles (5<sup>th</sup>, 25<sup>th</sup>, 75<sup>th</sup>, 95<sup>th</sup>), trend magnitudes and categories and p-values for the Mann-Kendall and Kruskal-Wallis tests (Sections 3.2 and 3.5.2).
- ‘HCA’: HCA cluster attribution, where applicable (Sections 3.2 and 3.5.2).

## 4.2 Water Levels

Median water levels west of the Alpine Fault are relatively shallow, i.e. from c. 1 m to 30 m below ground level<sup>2</sup> (m bgl; Figure 4.1). The deepest groundwater levels are observed near the Alpine Fault, in the Grey Valley, and in one well in the Holocene gravel fan of the Buller River near its mouth. Shallower water levels generally occur closer to the coast.

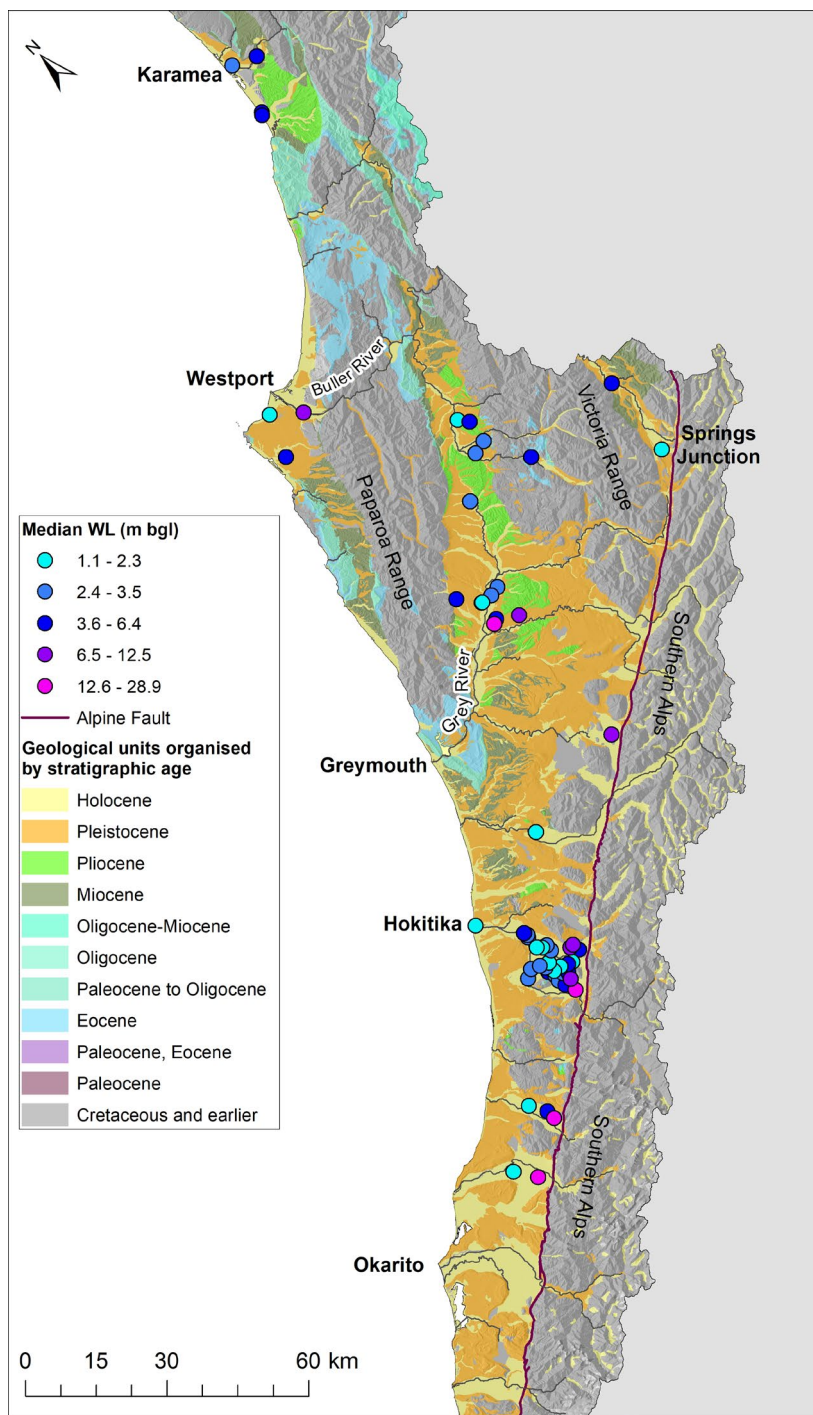


Figure 4.1 Spatial distribution of water levels (WLs) in metres below ground level (m bgl) in the West Coast aquifers, located west of the Alpine Fault.

2 Water levels are routinely monitored as depth below the top of casing. Depths below ground level were calculated by subtracting the height of casing above ground to these measurements where specified or using the default top of casing height value of 0.3 m.

## 4.3 Water Age

### 4.3.1 Long-Term Rainfall Tritium Monitoring

The comparison between tritium in monthly rain samples between the Greymouth and Kaitoke reference rain collector (Figure 2.3, Section 3.1.1) show slightly lower tritium ratios (TR) in Greymouth rain by a factor of 0.91 on average compared to Kaitoke. Consequently, scaling factors of 0.95 were applied for groundwaters recharged near the coast and of up to 1.2 for water recharged in the higher mountains.

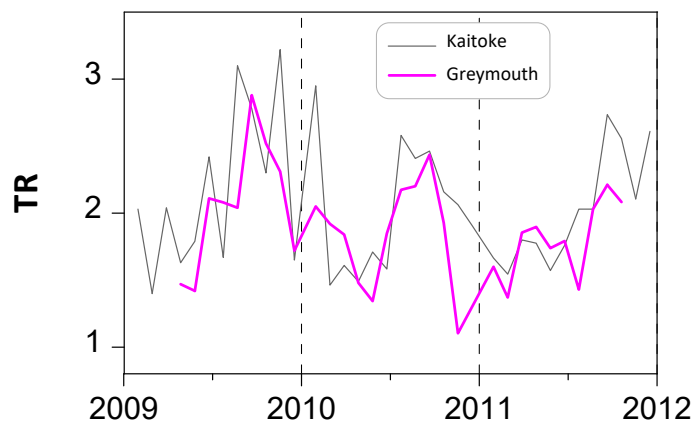


Figure 4.2 Tritium ratios (TR) in rain of Kaitoke and Greymouth (Figure 2.3), measured in monthly samples.

### 4.3.2 Groundwater Residence Time

#### 4.3.2.1 Age-Tracer Results

Most groundwater tritium ratios are similar to those of rainwater (c. 2 TR, Figure 4.3), indicating very young water. Only one sample, located in Okarito, exhibited a very low tritium ratio, indicating old water. Tritium ratio prior age interpretation already showed that groundwater flow dynamics in the West Coast Quaternary deposits are dominated by rapid flow.

For the interpretation of age tracers, it is important to keep in mind that gas tracers in groundwater samples can be contaminated due to air contact during sampling, or in the well head, and in the aquifer due to anthropogenic sources in the recharge area (Section 3.1). About 30% of the sites on the West Coast Quaternary deposits show CFC contamination, indicating the presence of local contamination sources (Figure 4.3). These elevated point source CFC concentrations can be used to identify recharge from local rain, as elevated CFC concentrations do not occur in river water. Contamination for SF6 can be seen in 15% of the sites (Figure 4.3).

MRTs are shown in Figure 4.4 and provided in Appendix 2 and as a digital attachment to this report. Across the region, sites exhibited young groundwater age (0.2–8 years), with the notable exception of a well located in Okarito with a MRT of 140 yr (WCRC141, unknown depth). This age range was observed at the valley scale (e.g. Karamea, Grey, Hokitika, Whataroa). In the Springs Junction area, all three samples (Figure 4.4) indicated groundwater MRT below one year. The dataset did not exhibit a consistent pattern, such as increasing groundwater age towards the coast, suggesting that local conditions, possibly linked to spatial variations in deposits, are controlling groundwater pathways. This would be consistent with observations from the Whataroa Valley east of Hokitika (Cox et al. 2013).

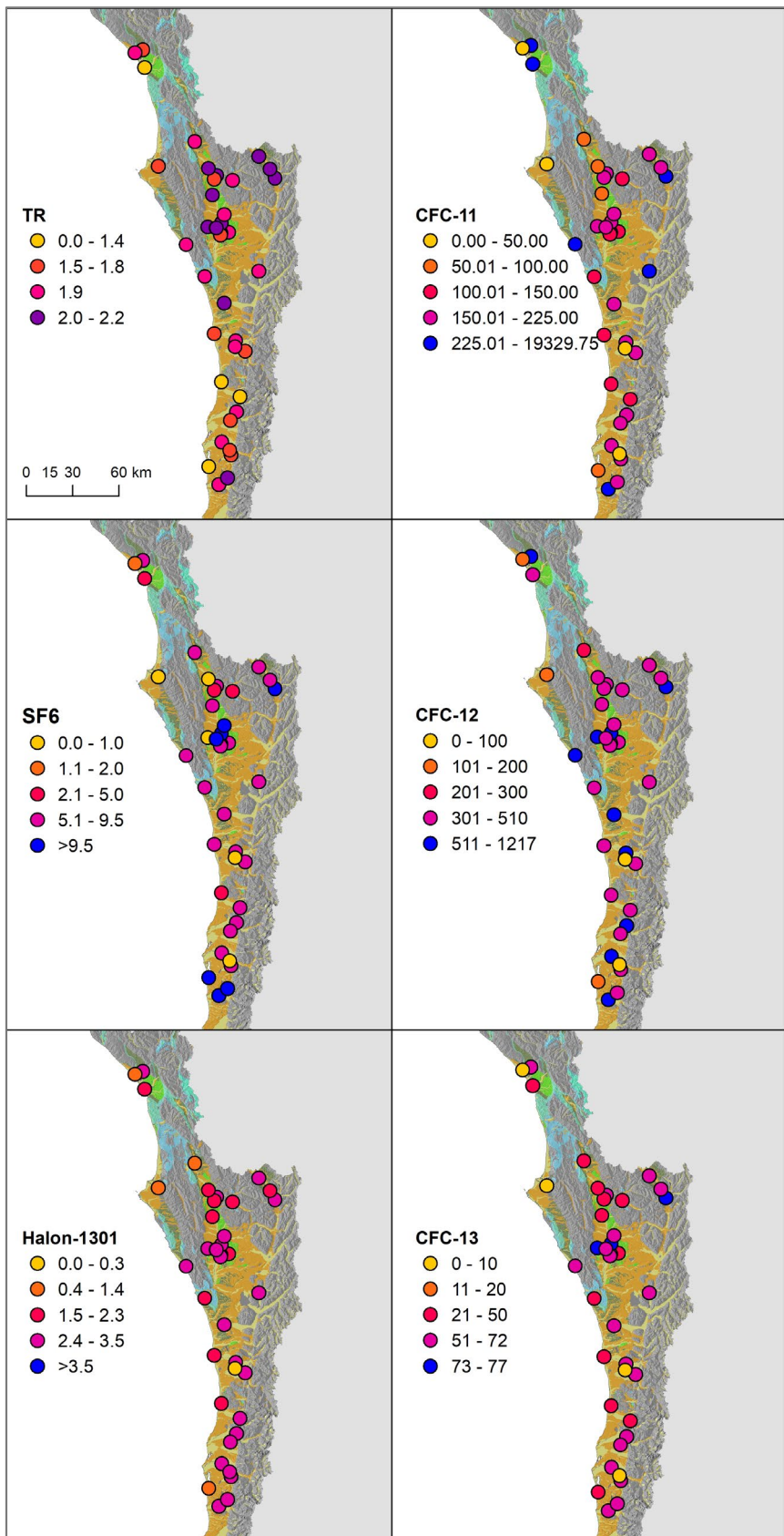


Figure 4.3 Age tracer measurements for groundwaters in the West Coast. Raw tritium ratios (TR) are displayed in tritium units. CFC-11, CFC-12, CFC-13, Halon-1301 and SF<sub>6</sub> partial pressures were calculated from the measured concentrations via Henry's Law using recharge temperatures, after correction for excess air. Modern atmospheric concentrations of these gases are around 225 ppt, 510 ppt, 72 ppt, 3.5 ppt and 9.5 ppt, for CFC-11, CFC-12, CFC-13, Halon-1301 and SF<sub>6</sub>, respectively. Concentrations above these levels are considered to be contaminated with other sources of these tracers, shown in blue.

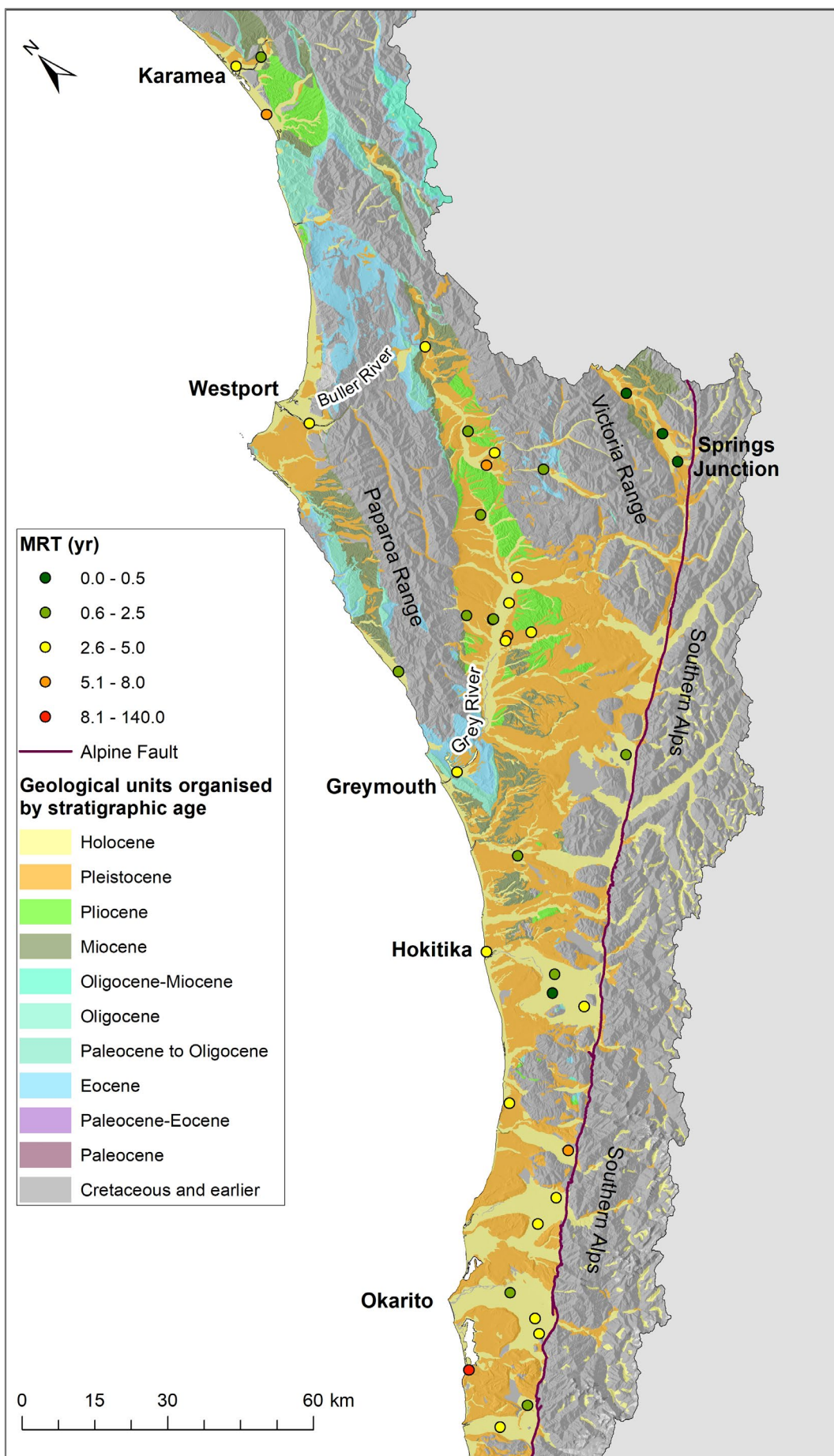


Figure 4.4 Map of groundwater mean residence time (MRT) in years.

#### 4.3.2.2 Radon-222 Results

No measurement of  $^{222}\text{Rn}$  in West Coast groundwater was available prior to this project and data is only available at sites sampled in March 2020. Groundwater  $^{222}\text{Rn}$  concentrations range between 1.6 and 82.6 mBq/L ( $n = 28$ ) and do not exhibit a clear correlation with age (Figure 4.5). The radon transfer from the minerals into the water is not a uniform process. Other conditions, such as the radium concentration of the minerals and the ability to release the  $^{222}\text{Rn}$ , appear to result in a high variability of  $^{222}\text{Rn}$  concentrations. In addition,  $^{222}\text{Rn}$  can also be absorbed by organic matter, which limits the use of  $^{222}\text{Rn}$ -ingrowth as an age tracer. Spatially, most of the low  $^{222}\text{Rn}$  concentrations are located close to the Southern Alps foothills, which is consistent with very young groundwater (Figure 4.6).

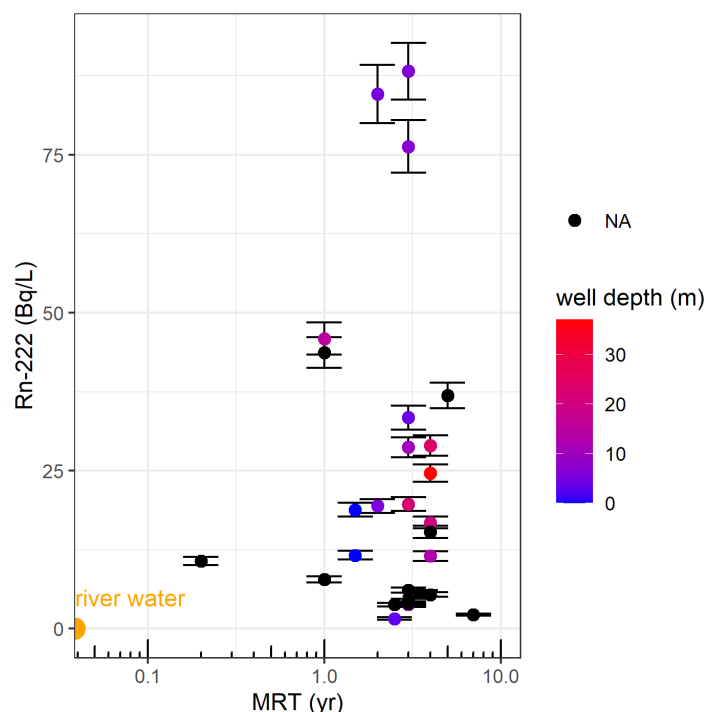


Figure 4.5 Radon-222 concentrations versus mean residence time.

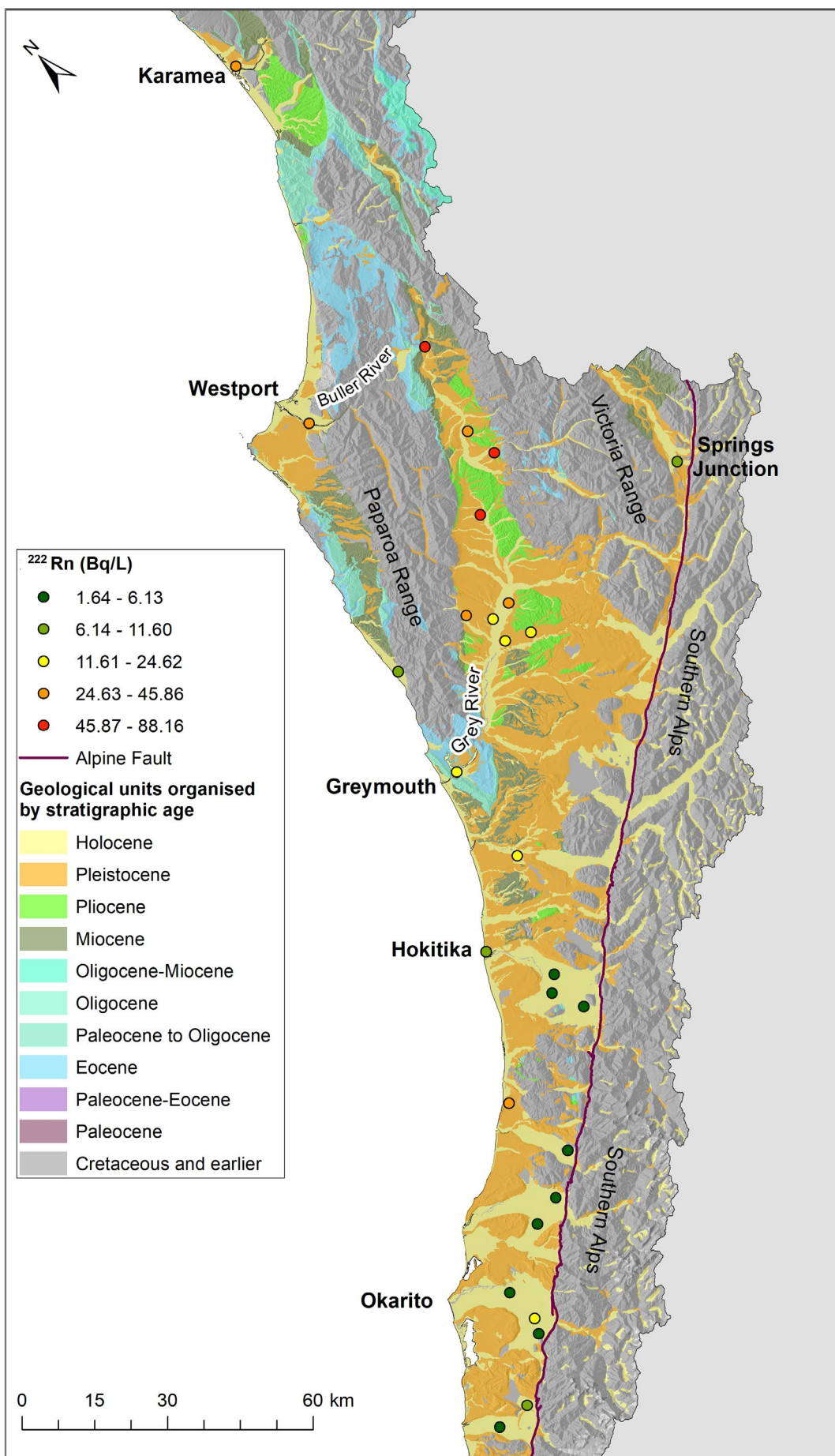


Figure 4.6 Spatial distribution of Radon-222 ( $^{222}\text{Rn}$ ) concentrations in the March 2020 groundwater samples.

## 4.4 Stable Isotopes

Stable isotope ratios measured in groundwater fall close to the local meteoritic line (Kerr et al. 2015) and within the range of ratios measured in river waters, indicating that precipitation mostly occurred under saturated conditions without post-condensation evaporation (Figure 4.7). Groundwater stable isotope ratios are heavier (i.e. less negative) in the low-altitude West Coast region, compared to more negative high-altitude ratios as observed by Kerr et al. (2015) along a transect over Arthur's Pass (Figure 4.8). With increasing altitude, and thereafter distance from the coast,  $\delta^{18}\text{O}$  ratios become more negative. Groundwater isotopic ratios for  $\delta^{18}\text{O}$  range between  $-7.4\text{\textperthousand}$  and  $-5.0\text{\textperthousand}$ , whereas rivers located on the same side of the Southern Alps have been measured as low as  $-10.0\text{\textperthousand}$  and lower with the higher elevations (Kerr et al. 2015).

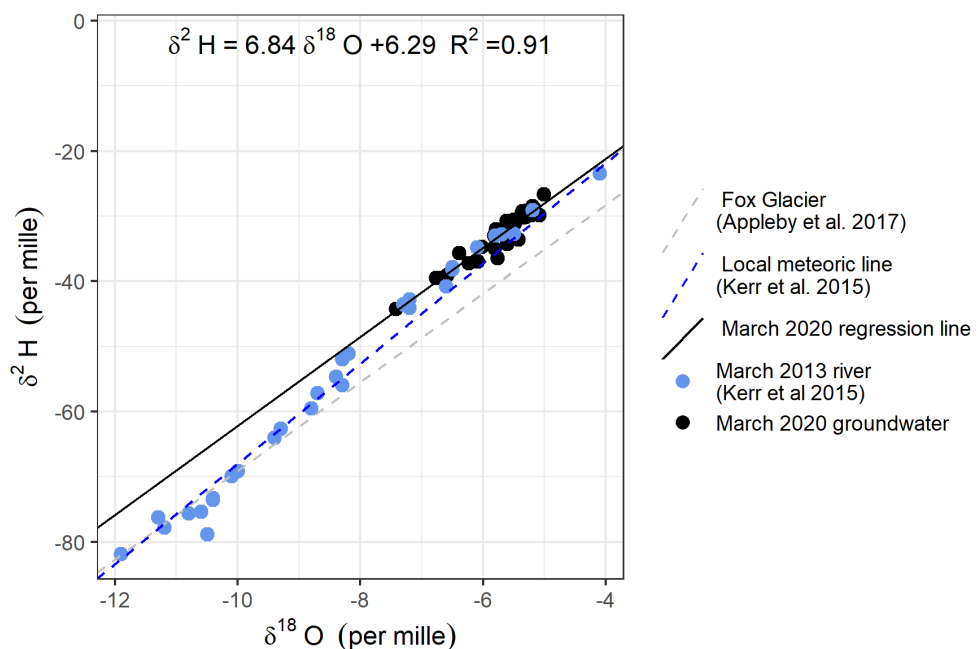


Figure 4.7 Water stable isotope ratios of West Coast groundwaters and river water.

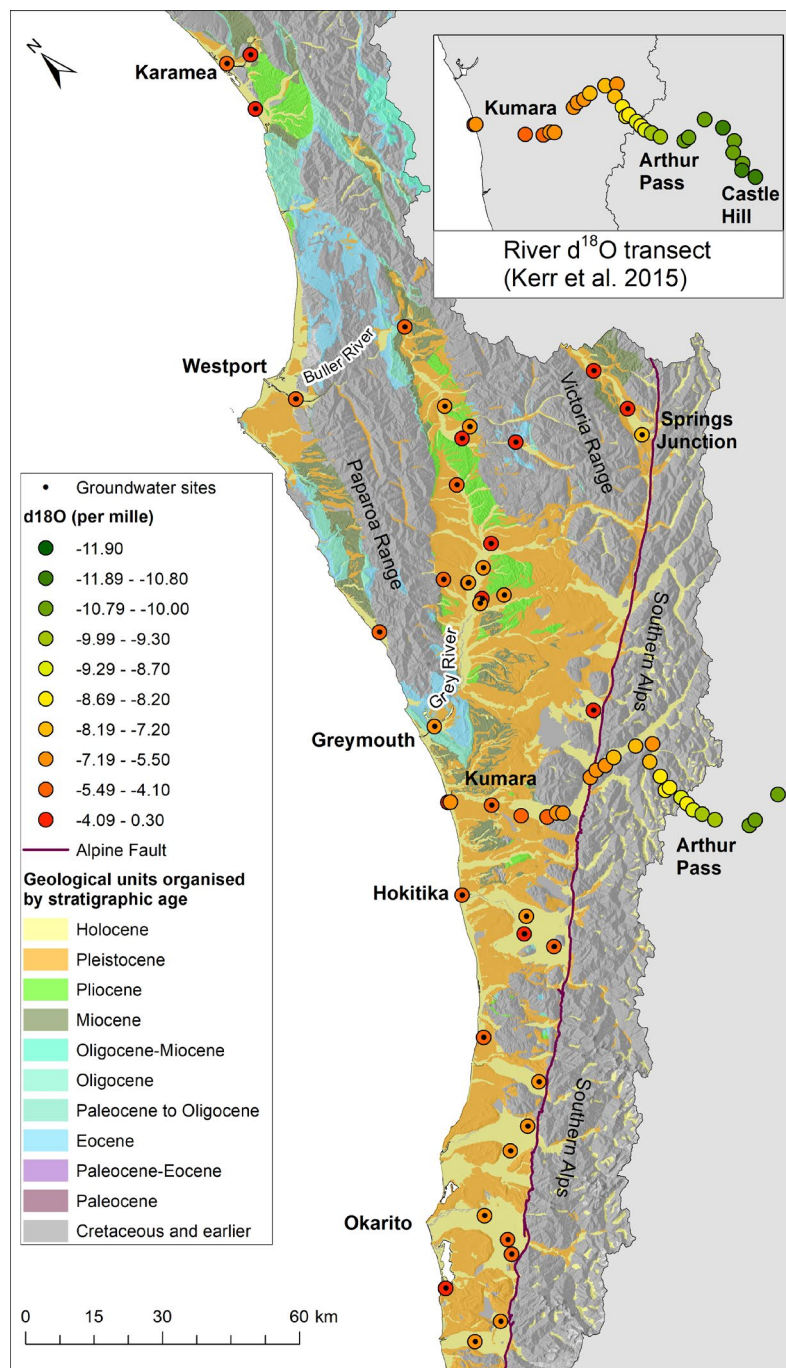


Figure 4.8 Spatial distribution of  $\delta^{18}\text{O}$  ratios measured in groundwater and rivers in the region, compared to a transect along Arthur's Pass as observed by Kerr et al. (2015).

## 4.5 Hydrochemistry

In the following figures, groundwater hydrochemistry parameters are shown versus MRT to identify drivers of hydrochemistry and the impacts of land use versus natural processes on groundwater quality. Note that MRT > 100 years are close to the tritium detection limit, and the MRT may be significantly older (potentially thousands of years). In this situation, the number only indicates the minimum MRT.

During the process of natural groundwater evolution, aquifer matrix minerals are progressively dissolved over time, and ion concentrations increase with groundwater age. In contrast, high concentrations (in particular, those of nutrients) in young groundwater indicate anthropogenic sources from land-use activities.

Unusually high concentrations of  $\text{NO}_3$ , K, Na, Cl and Mg were observed in the sample from Karamea Blackwater, indicating impact from a nearby point-source. Therefore, this sample was not included in the hydrochemistry trends.

An overview of the hydrochemical composition of groundwater from the West Coast in comparison to the average New Zealand groundwater composition is listed in Table 4.1. West Coast groundwaters have low solute concentrations, reflecting short residence times.

Table 4.1 Hydrochemistry statistics, showing number of wells, minimum and maximum concentrations and the 25<sup>th</sup>, 50<sup>th</sup> and 75<sup>th</sup> percentiles for all hydrochemistry data from wells with groundwater age-tracer data. The New Zealand percentiles, shown for comparison, are for groundwater quality data obtained from over 1000 sites, collected as part of 'State of the Environment' (SOE) monitoring programmes run by regional authorities and compiled by the New Zealand Ministry for the Environment (Daughney and Wall 2007).

Parameter	Units	West Coast Data						New Zealand Percentiles		
		No.	Min.	25 <sup>th</sup>	50 <sup>th</sup>	75 <sup>th</sup>	Max.	25 <sup>th</sup>	50 <sup>th</sup>	75 <sup>th</sup>
<b>Ca</b>	mg/L	87	0.89	9.32	12	15.5	47	9.6	15.5	30
<b>Cl</b>	mg/L	86	0.98	2.5	3.3	6.06	120	7.3	15.3	30.1
<b>HCO<sub>3</sub></b>	mg/L	87	1	26	35	45.8	179	40	62.7	145
<b>K</b>	mg/L	86	0.21	1.10	2.06	2.77	46	1	1.6	3.7
<b>Mg</b>	mg/L	86	0.26	0.90	1.355	2.1	14	2.6	4.6	8.5
<b>Na</b>	mg/L	86	1.47	2.55	3.11	4.93	50	9.4	15	29.6
<b>NO<sub>3</sub>-N</b>	mg/L	87	0.001	0.32	0.706	1.54	21	<0.001	1.3	4.4
<b>SiO<sub>2</sub></b>	mg/L	22	0.39	7.84	11.75	13.6	24	13.5	17	29.5
<b>SO<sub>4</sub></b>	mg/L	86	0.11	3.7	5.45	7.55	40	3	6.5	13
<b>DRP</b>	mg/L	53	0.001	0.003	0.004	0.0092	2.2	0.01	0.02	0.07
<b>Fe</b>	mg/L	43	0.002	0.02	0.02	0.0375	21	0.01	0.03	0.23
<b>Mn</b>	mg/L	43	0.0005	0.0018	0.005	0.031	0.79	<0.001	0.01	0.24
<b>NH<sub>3</sub>-N</b>	mg/L	53	0.0005	0.005	0.005	0.01	1.81	<0.001	0.01	0.06
<b>Cond.</b>	$\mu\text{S}/\text{cm}$	86	19.5	76.2	100	138	555	145	210	371
<b>pH</b>	pH unit	84	3.99	5.66	6.02	6.48	9.06	6.4	6.8	7.2
<b>pH</b>	pH unit	84	3.99	5.66	6.02	6.48	9.06	6.4	6.8	7.2

#### 4.5.1 Hierarchical Cluster Analysis

HCA (Section 3.3) was performed on the hydrochemistry data to group sites with similar hydrochemistry. HCA results are displayed as a dendrogram (Figure 4.9). Each vertical line ends at a single sample site. Horizontal lines join hydrochemical groups. The similarity between sites and groups of sites is indicated by the height up the y-axis (distance) of the respective connecting horizontal line. Low horizontal lines join sites with the most similar chemistry. Selection of appropriate threshold lines divides the sites into clusters with similar chemistry.

At the highest threshold, the data is divided into three clusters, A, B and C (Figure 4.9). The main difference between these clusters is that Cluster A has a high conductivity, Cluster B has high concentrations for land-use indicators and Cluster C has very low conductivity, which means low solute concentrations (Figure 4.10). At the second threshold, Cluster B is divided into two sub-clusters, B1 and B2, and Cluster C is divided into C1 and C2.

- Cluster A ( $n = 10$ ) exhibits the highest conductivity (centroid median of 198  $\mu\text{S}/\text{cm}$ ) and solute concentrations (Figure 4.10); Ca and  $\text{HCO}_3$  as dominant species indicate limestone source rock.
- Cluster B ( $n = 21$ ) has intermediate conductivity and highest concentrations of the land-use impact indicators  $\text{NO}_3$ , Ca, Mg, Na, Cl and  $\text{SO}_4$ ; sub-cluster B1 is less dilute (Figure 4.10); Dissolved Oxygen (DO) concentrations for both clusters indicate intermediate to highly oxygenated aquifer conditions;  $\text{NO}_3$  is lower in Cluster B1 than B2.
- Cluster C ( $n = 39$ ) consists of Ca-Mg  $\text{HCO}_3$ -type waters, similar to a diluted version of Cluster A (median conductivity of less than 95  $\mu\text{S}/\text{cm}$ ); sub-cluster C1 is the most pristine cluster and exhibits lower Ca, K,  $\text{HCO}_3$ ,  $\text{NO}_3$  and  $\text{SO}_4$  concentrations; suggesting low-intensity land use or dilution with pristine river water. Where measured, sites from C1 have less negative  $\delta^{18}\text{O}$  values than sites from C2 (not shown).

A description of each cluster is given in Table 4.2 and the geographic distribution of the HCA clusters is shown in Figure 4.12. Groundwater in the Southern Alps foothills is dominated by Cluster A at higher elevation and by clusters C1 and C2 further downgradient towards the coast. Clusters A and C2 also occur in the inland Inangahua catchment (Springs Junction). Clusters B1 and B2 groundwaters occur either side of the Paparoa Range and north of the Victoria Range, downgradient from the Eocene limestones outcrop and within the Paparoa rain shadow.

Table 4.2 Hierarchical Cluster Analysis clusters, showing water type and a general description of notable hydrochemistry and well depths from each cluster.

Cluster	Number of Sites	Water Type	Description, Sample Location
A	10	Ca-Mg $\text{HCO}_3$	Pristine, alpine – high conductivity, highest Ca, $\text{HCO}_3$ , lower $\text{NO}_3$ -N, oxidised. Sites located in Southern Alps foothills.
B1	4	Mixed water types: Ca-Mg- $\text{HCO}_3$ - $\text{SO}_4$ to Na-Ca- $\text{HCO}_3$ -Cl	Impacted, localised – high conductivity, highest concurrent $\text{NO}_3$ -N, $\text{SO}_4$ , K, Na and Cl.
B2	17	Mixed water types: Ca-Mg- $\text{HCO}_3$ - $\text{SO}_4$ to Na-Ca- $\text{HCO}_3$ -Cl	Impacted, widespread – intermediate conductivity, wide range of elevated $\text{NO}_3$ -N, $\text{SO}_4$ , Na. Low K. Widespread, north of Hokitika.
C1	5	Ca-Mg $\text{HCO}_3$	Pristine, valley – lowest conductivity, $\text{SO}_4$ , K, lowest $\text{NO}_3$ -N, distributed across the region.
C2	34	Ca-Mg $\text{HCO}_3$	Signs of impact, valley – lower conductivity, lower $\text{NO}_3$ -N, distributed across the region, outside the Grey Valley.

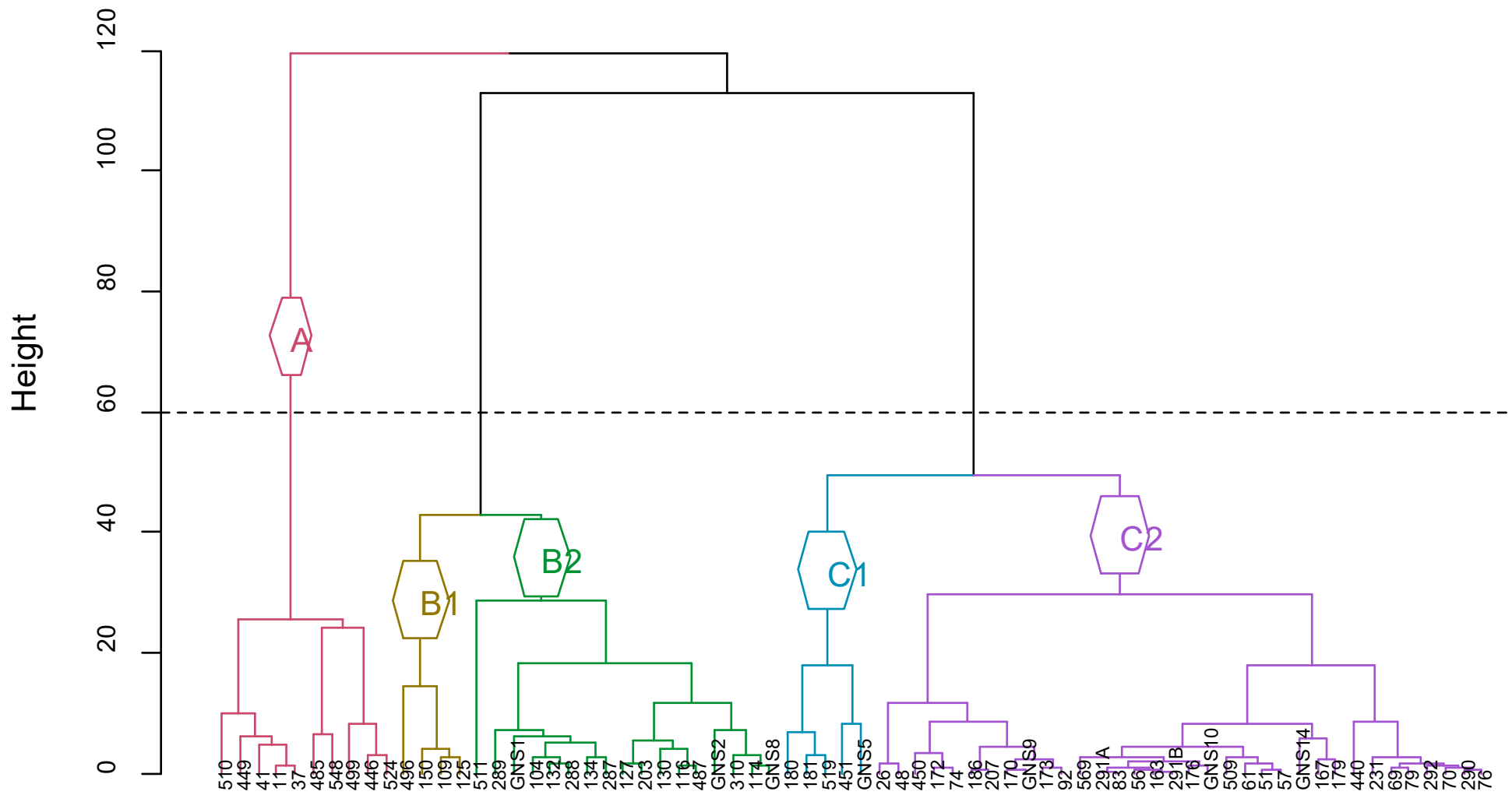


Figure 4.9 Dendrogram produced by Hierarchical Cluster Analysis.

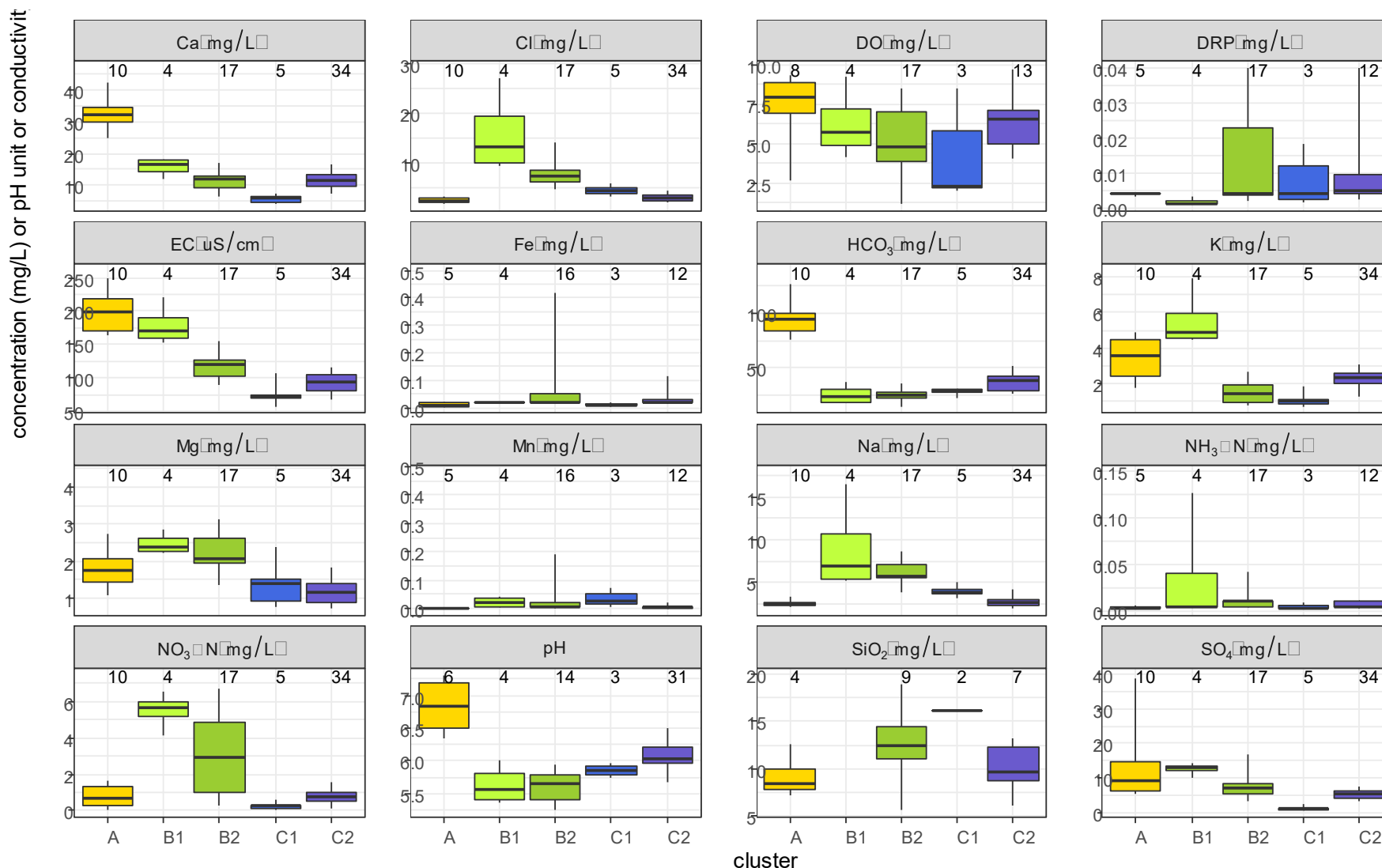


Figure 4.10 Box plots of hydrochemistry parameters organised by second threshold cluster. The number displayed above each box indicates sample size.

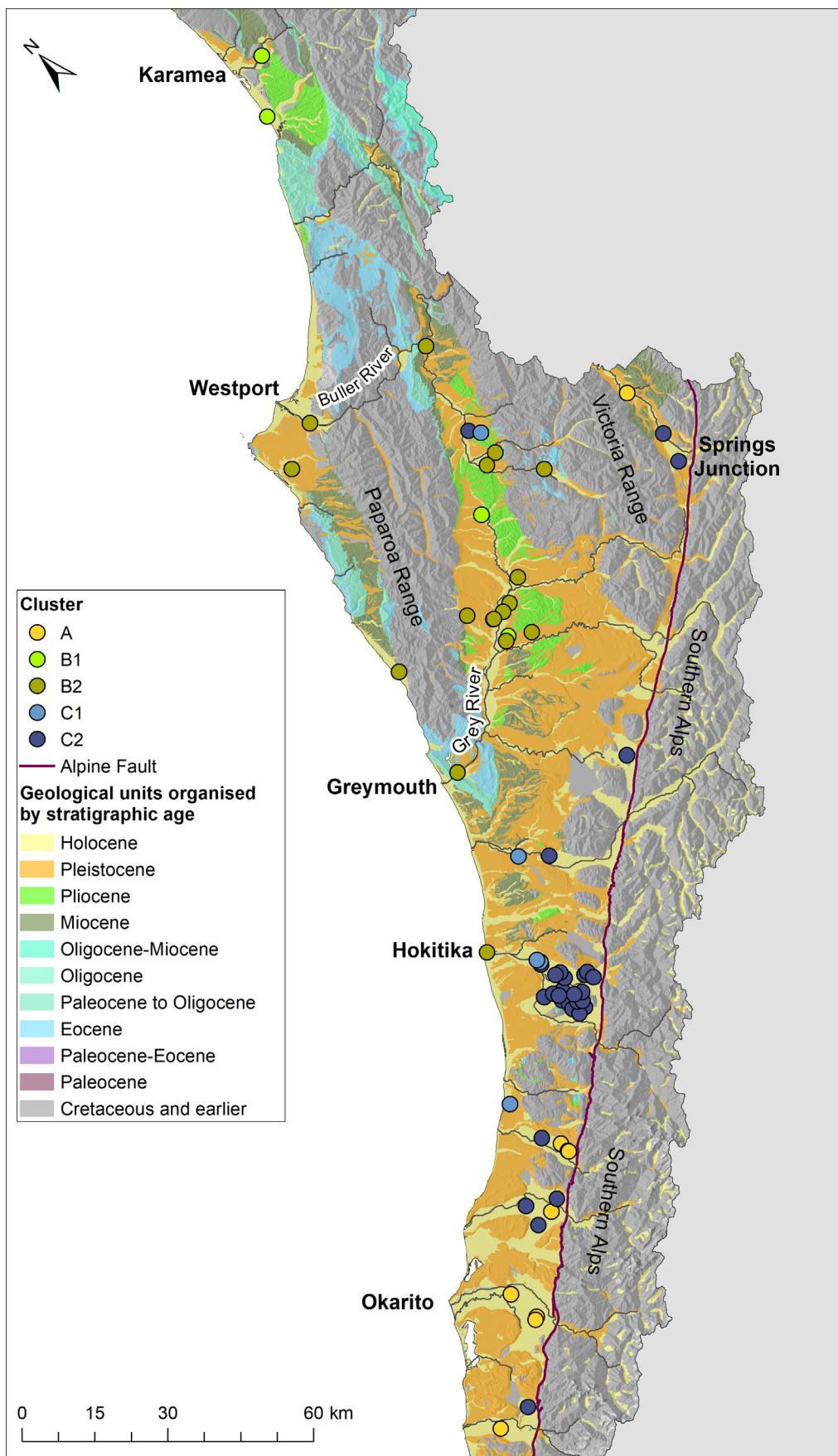


Figure 4.11 Geographic distribution of sites assigned to clusters using Hierarchical Cluster Analysis.

The major ion composition of the five clusters, with corresponding water types based on the relative prevalence of different ions, is depicted by a Piper diagram (Figure 4.12).

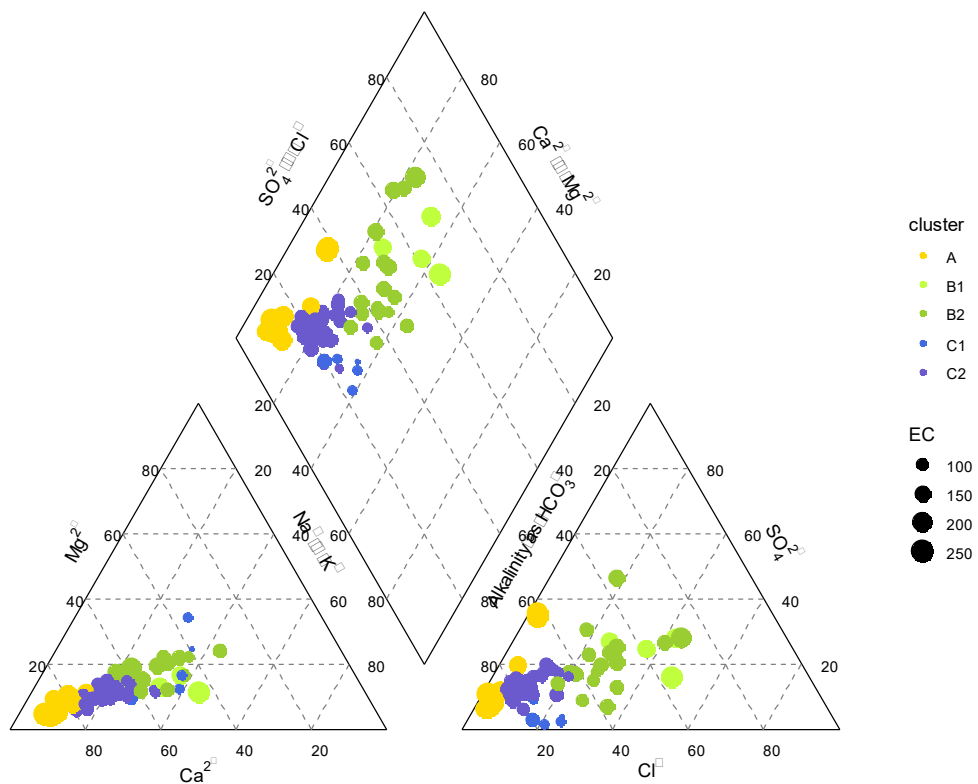


Figure 4.12 Piper diagram showing the variation of major ion chemistry by cluster. The left and right bottom triangles show the major cation and anion ratios on an equivalence basis, respectively; the upper centre diamond plots projections based on the two triangular plots. Sites are grouped into clusters assigned by HCA. The size of the symbols in the centre diamond indicate the relative total dissolved solids (TDS) ( $\mu\text{S}/\text{cm}$ ).

#### 4.5.2 Redox Conditions

Fully oxygenated water in equilibrium with air has a DO concentration of c. 10.5 mg/L. In groundwater systems, the water is separated from the atmosphere, and, in the presence of organic matter or other electron donors (e.g. pyrite), the oxygen is consumed by microbial oxidation reactions. Reduction of oxygen is energetically the most favourable reaction that micro-organisms use, with the result that other reduction reactions (including denitrification) typically do not occur until most of the dissolved oxygen has been consumed. These reactions take time and usually groundwater with long MRT becomes increasingly anoxic (e.g. Böhlke et al. 2002).

The West Coast dataset does not show a clear trend between MRT and DO concentrations, with low (<2.5 mg/L) and high (>6 mg/L) concentrations occurring within the entire MRT range (Figure 4.13). Concentrations of Fe, CH<sub>4</sub> and NH<sub>3</sub>, indicators for highly reducing conditions, are generally low, with a few exceptions, indicating prevailing oxic conditions in the aquifers. However, several sites have elevated Fe, CH<sub>4</sub> and NH<sub>3</sub> concentrations, indicating highly anoxic aquifer conditions up to the stage of methane fermentation (Morgenstern and Daughney 2012). These redox processes up to methane fermentation appear to not require long reaction times, as they also occur in young groundwater of MRT 1 year.

South of Hokitika, groundwater sourced from the Southern Alps foothills exhibit high DO concentrations, contrasting with low concentrations at the coast (Figure 4.14). This is consistent with the occurrence of clean gravel deposits, with limited – up to the absence of – significant

amounts of organic matter that could facilitate microbial reactions at higher elevations, and high hydraulic conductivities suggested by the extremely young groundwater ages in the Holocene gravel fans. Along the Grey River, a range of low to moderate DO concentrations occur, suggesting localised DO depletion that does not reach methane fermentation stage.

There were only three samples with high CH<sub>4</sub> content >1 µmol/L (Figure 4.13b): two coastal samples near Westport and Karamea and one sample near the Alpine Fault east of Okarito (Figure 4.14). This suggests that groundwater conditions there have reached the state of methane fermentation. Deposits with a high content of organic matter, facilitating highly anoxic conditions, are expected in the coastal areas. The Karamea sample had high CH<sub>4</sub> content combined with moderate DO concentration, indicating mixing of oxic and highly anoxic water in the vicinity of the well. This groundwater is very young (MRT of 3 years), indicating that such deposits with high organic matter content may be very hydraulically conductive. While these results indicate that pockets of anoxic conditions with high hydraulic conductivity may exist, the results from the investigated wells indicate that highly anoxic conditions are localised.

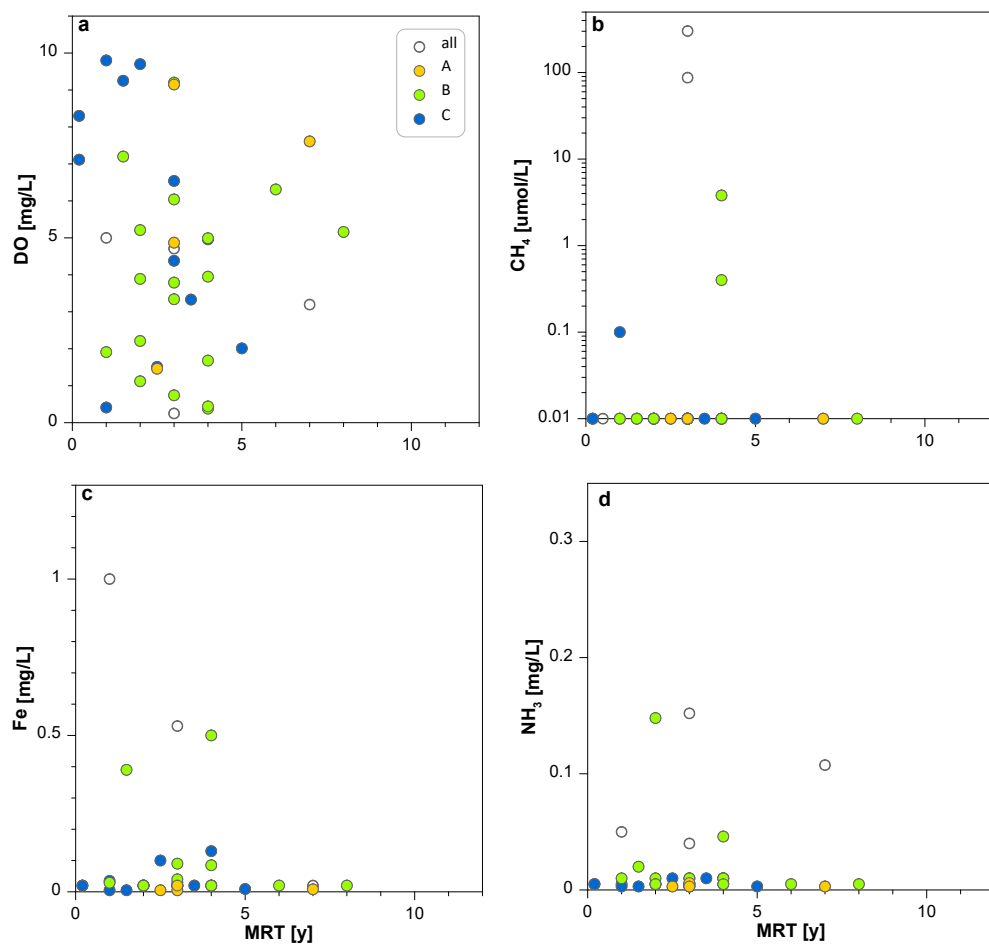


Figure 4.13 Dissolved oxygen, Fe, CH<sub>4</sub> and NH<sub>3</sub>-N concentrations versus mean residence time for West Coast groundwater. This hydrochemistry data originates from various sources over time. Note that this figure only includes sites at which both chemistry and age-tracer data are available, not the entire dataset.

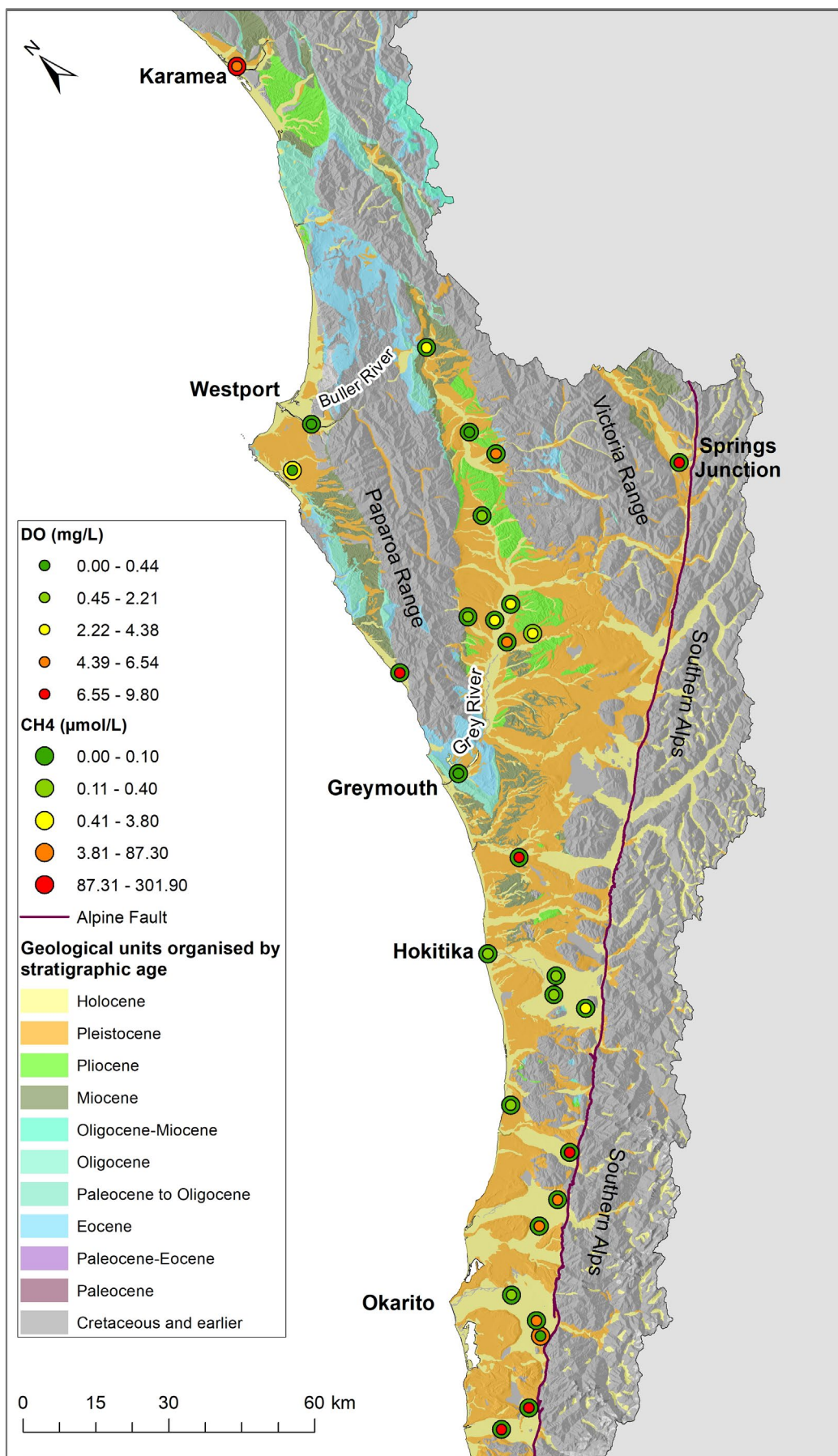


Figure 4.14 Map of dissolved oxygen (inner circle) and CH<sub>4</sub> (outer circle) in groundwater.

### 4.5.3 Nutrients

The main anthropogenic impacts on groundwater quality in New Zealand started with the on-set of industrial agriculture in the 1950s, as deduced from the NGMP dataset of New Zealand. Comparison of ion concentrations of recently recharged groundwater, and groundwater that was recharged before 1950, allowed the identification of the pre-industrial baseline groundwater quality and the impacts of land-use activities on groundwater quality (Morgenstern and Daughney 2012).

The NGMP dataset enabled the identification of agricultural contaminants (mostly nutrients) from high-intensity land use (Table 4.3). Comparison of the West Coast data to the NGMP data allows identification of anthropogenic versus geological sources and determination of the impact from high-intensity land use for most of the hydrochemistry parameters.

Table 4.3 Agricultural indicators for high-intensity land use (Morgenstern and Daughney 2012), showing concentration range prior to high-intensity land use, threshold concentrations that indicate high-intensity agricultural land use and observed maximum concentrations. Threshold concentrations in brackets can be ambiguous.

Agricultural Indicator	Concentration Range Prior to High-Intensity Land Use (mg/L)	Threshold Concentration (mg/L)	New Zealand NGMP Observed Maximum Concentration (mg/L)	WCRC Maximum Concentration (mg/L)
NO <sub>3</sub> -N	0–2.5	2.5	34	21
SO <sub>4</sub>	0–12	12	94	40
Cl	0–60	(60)	100	120
Br	0–0.2	(0.2)	1.3	0.38
Ca	0–50	(50)	110	47
Mg	0–15	(15)	54	14
Cr	0–0.0015	0.0015	0.006	Not available

Of the agricultural indicators listed in Table 4.3 that indicate impact by high-intensity land use in New Zealand, the Mg, NO<sub>3</sub>-N and SO<sub>4</sub> thresholds were exceeded at 7%, 17% and 13% of the West Coast sites, respectively, with some concentrations measuring up to four times the threshold.

Only one sample has sufficient MRT to reflect recharge conditions from the time before low-intensity land use (Okarito, 140 years). However, no hydrochemistry results were associated with this site to provide information on NO<sub>3</sub>-N, SO<sub>4</sub>, DRP and K concentrations. All sampled West Coast groundwaters have an MRT of less than 10 years, and therefore have been recharged after the onset of high-intensity land use.

Most sites (88%) exhibit either NO<sub>3</sub>-N concentrations within the range 0.13–2.5 mg/L (69% of the sites) or concentrations above 2.5 mg/L, indicative of high-intensity land-use effect (Morgenstern and Daughney 2012). All concentrations are below 11.3 mg/L, the maximum permissible level for drinking water supplies (Ministry of Health 2018). While NO<sub>3</sub>-N contamination is not a major problem in West Coast groundwaters regarding the Drinking-water Standards, the observed NO<sub>3</sub>-N concentrations are high enough to cause environmental issues once discharged to the surface (e.g. eutrophication). No major legacy nitrate loads were identified; the rapid groundwater flow in the region makes it unlikely that historic loads reside for long in the aquifers, aside for very local conditions.

$\text{SO}_4$  concentrations of greater than 12 mg/L (indicative of high-intensity land use) and up to about 40 mg/L occur in the entire age range of the sampled groundwaters (Figure 4.15b).  $\text{SO}_4$  and  $\text{NO}_3\text{-N}$  concentrations are strongly correlated. Concentrations of DRP and K in the sampled groundwaters are average by New Zealand standards (Table 4.1). DRP and K do not show a trend with groundwater age (Figure 4.15c, d). This may indicate source from land-use activities, as purely geogenic sources via leaching from the soils and aquifer material would be expected to result in increasing concentrations with increasing MRT.

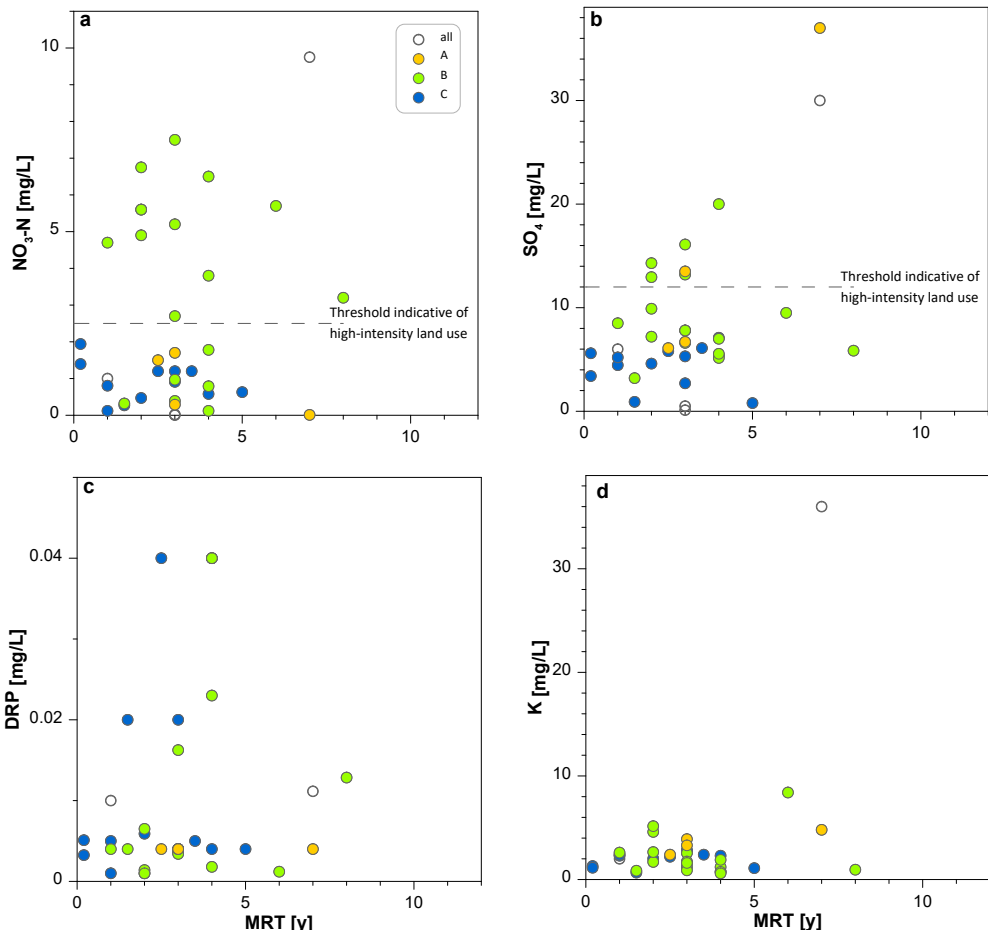


Figure 4.15  $\text{NO}_3\text{-N}$ ,  $\text{SO}_4$ , DRP and K concentrations versus mean residence time for West Coast groundwater. Colour code refers to HCA clusters (Section 4.3.1). Broken lines indicate thresholds for high-intensity land use based on Morgenstern and Daughney (2012). Hydrochemistry data originates from various sources over time. Note that this figure only represents sites at which both chemistry and age-tracer were available.

Overall, nutrient-rich groundwaters are mostly of Cluster B (green symbols) and equally cover the entire age range. For spatial distributions of agricultural contamination, see Section 4.2.4.

#### 4.5.4 Hydrochemistry Evolution

Hydrochemical parameters are part of minerals and usually dissolved from the aquifer material (Figure 4.16). Microbial redox processes can impact on mineral dissolution, resulting in different trends of ion concentrations with MRT in many groundwaters of New Zealand (Morgenstern and Daughney 2012). The West Coast data generally do not follow significantly different trends between oxic and anoxic water. Therefore, the dataset is not separated into oxic and anoxic groundwaters, but rather into HCA clusters (Figure 4.16).

Correlations for Ca, Mg, Na and HCO<sub>3</sub> with groundwater age are weak, probably because: (i) most of these waters are very young, and therefore hydrochemistry reactions have not yet significantly evolved; (ii) higher relative age errors occur within such a narrow young age range; and (iii) the dataset averages over various hydrogeologic units with different mineral compositions and therefore variable hydrochemistry reaction rates.

Linear fits to the entire dataset of the West Coast region, including correlation coefficients, are shown in Figure 4.16 (black dotted lines). The colours of the symbols refer to the HCA clusters (Section 4.3.1), which identify clusters of sites of similar hydrogeologic units with similar hydrochemistry evolutionary processes. Linear fits are shown in the respective colours for the individual HCA clusters for correlations coefficients R<sup>2</sup> > 0.15. Different hydrogeologic units follow different trends of concentrations versus MRT (Figure 4.16), which means that averaging over the entire dataset will lead to poor correlations. The best correlations with MRT are observed for SiO<sub>2</sub> for Cluster B with R<sup>2</sup> = 0.73, and for Mg for Cluster A with R<sup>2</sup> = 0.92 (note that there are only four samples). Also, in other areas of New Zealand, SiO<sub>2</sub> has shown strong correlation with age (ranging to hundreds of years), with potential to use these correlations as indicators of groundwater age (e.g. Morgenstern et al. 2015). Some of the parameters, for example, Mg, Ca and Na, are part of fertilisers and lime and could therefore be indicative of impacts of high-intensity land use on groundwater quality.

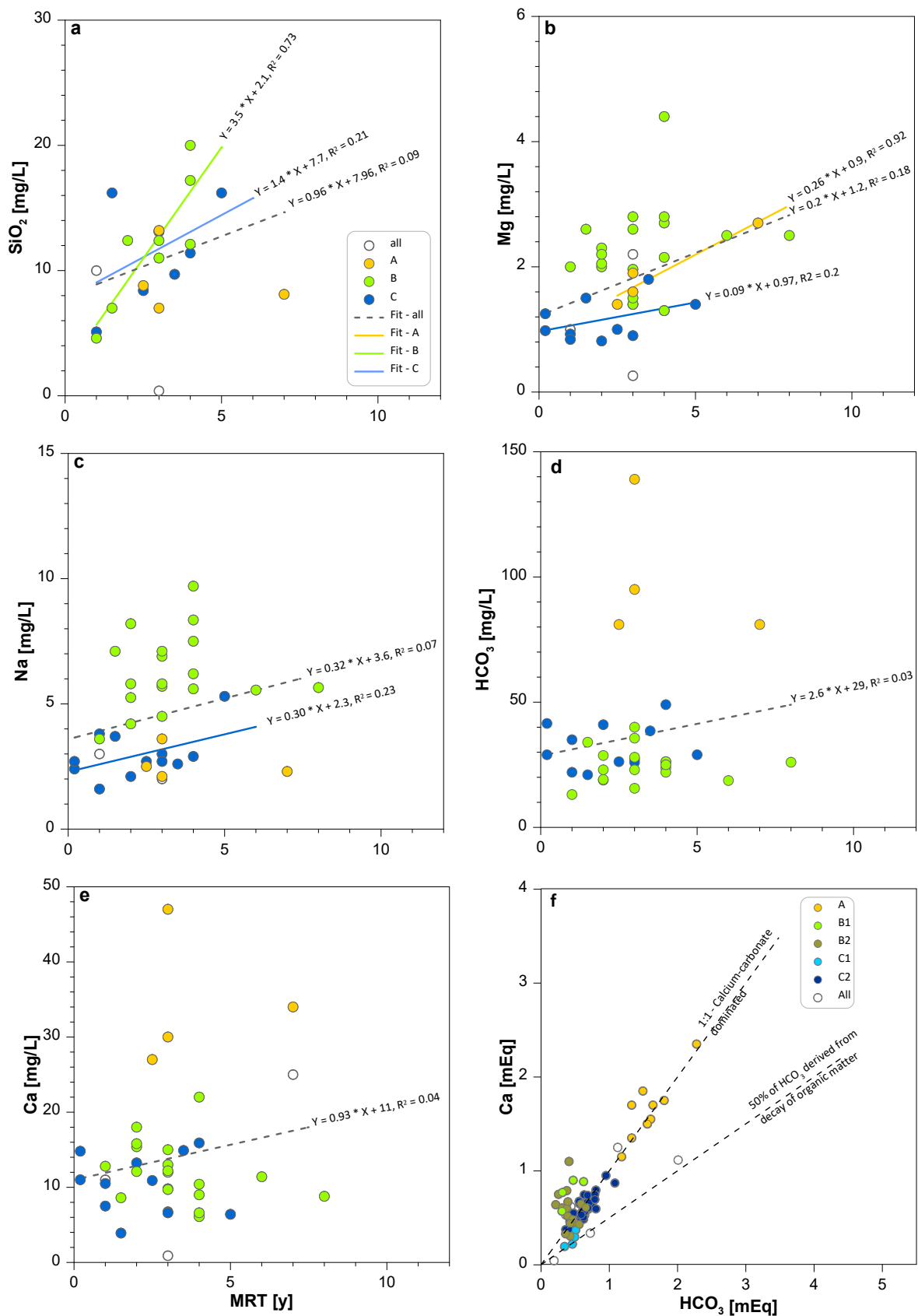


Figure 4.16 SiO<sub>2</sub>, Mg, Ca, Na and HCO<sub>3</sub> concentrations versus mean residence time for West Coast groundwater. This hydrochemistry data originates from various sources over time. Colour code refers to the HCA clusters. (f) shows Ca versus HCO<sub>3</sub> on a milli-equivalent basis.

## 4.5.5 Spatial Distribution of Selected Chemistry Parameters

In this section, examples of spatial distributions of chemistry parameters are shown that can inform recharge sources and flow patterns for the West Coast groundwater system.

### 4.5.5.1 Chloride and $\delta^{18}\text{O}$

Cl and the stable isotope oxygen-18 ( $\delta^{18}\text{O}$ ) are conservative tracers, without significant sources and sinks in the aquifer, and can be used to identify groundwater recharge sources. Inland rain is characterised by significantly lower Cl concentrations and  $\delta^{18}\text{O}$  ratios compared to coastal rain. Low Cl and  $\delta^{18}\text{O}$  in groundwater near the coast therefore indicates recharge contribution from inland rivers.

Cl concentrations measured in West Coast groundwaters are lower than New Zealand medians, with a median of 3.3 mg/L (Table 4.1). Groundwaters with the lowest Cl concentrations are located at the foothills of the Southern Alps (Figure 4.17a – green symbols) and in the narrow valley west of the Victoria Range, which is sheltered from direct oceanic rain by two mountain ranges. These low concentrations are consistent with historical Cl in rain measurements (Lauder, Otago, ranging from 0.2 to 1.1 mg/L over the 1983–1994 time period; Nichol et al. 1997). Near the coast, Cl concentrations are higher, indicating coastal rain recharge.

Cl concentrations in the Grey Valley are slightly higher but still low compared to coastal areas, consistent with concentrations of local rain sheltered by the Paparoa Range from direct oceanic sources. Concentrations are variable between closely located sites (Figure 4.17a), consistent with less connected groundwater systems (longer residence time) and more complex flow paths.

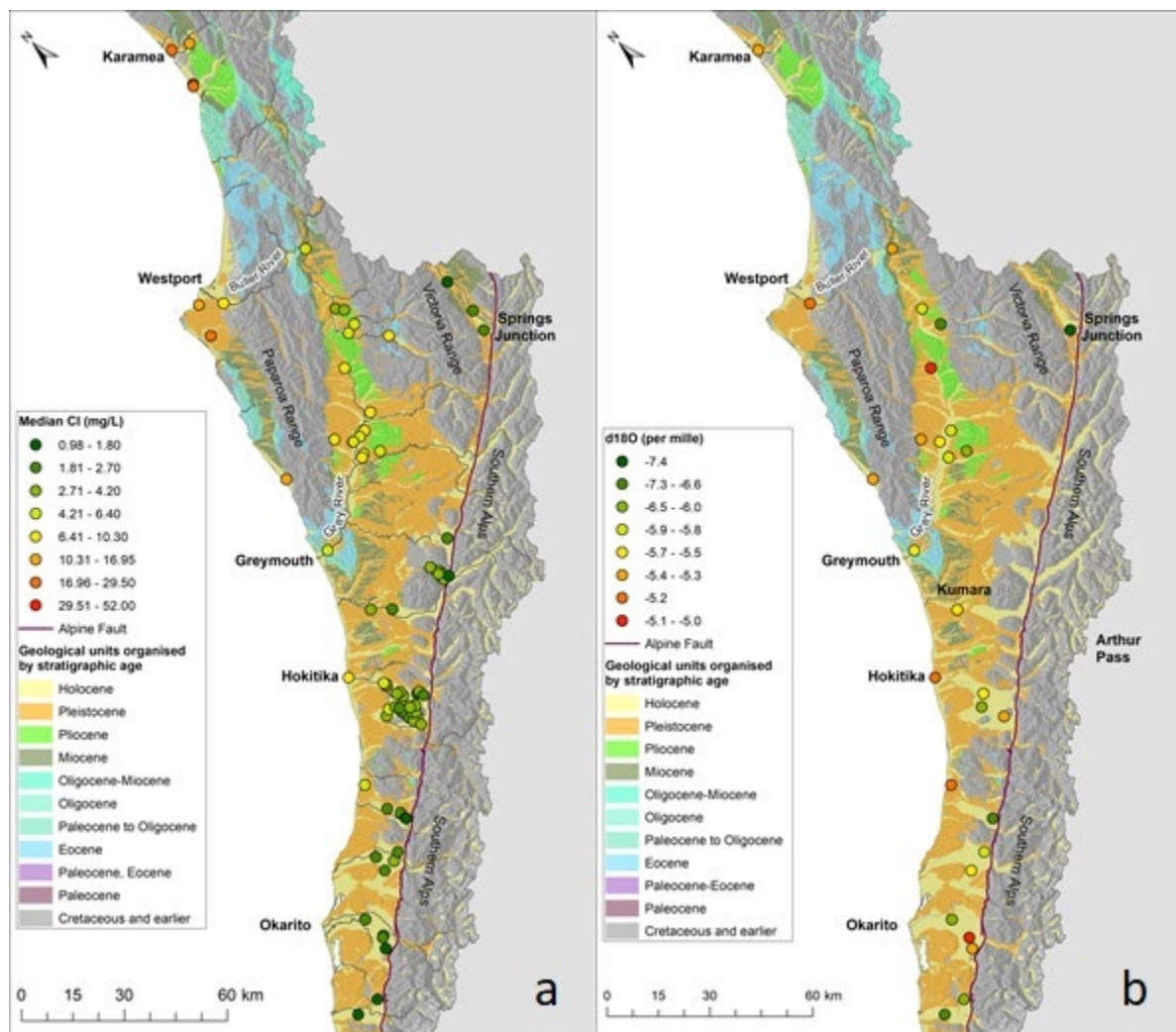


Figure 4.17 Spatial distribution of chloride (Cl) (a) and  $\delta^{18}\text{O}$  (b) in West Coast groundwaters. The figure shows that low Cl concentrations and  $\delta^{18}\text{O}$  ratios occur at the Southern Alps foothills in the south and west of the Victoria Range in the north.

The Cl distribution patterns are in general mirrored by  $\delta^{18}\text{O}$  (Figure 4.17b). In addition to the recharge pattern indicated by Cl, medium  $\delta^{18}\text{O}$  ratios at the two groundwater wells near the Alpine Fault west of Okarito indicate that, despite Cl attesting of Alpine water recharge, these two wells contain water that is recharged from local foothill streams. This contrasts with the water in the downgradient well, which is characterised by a higher-altitude river  $\delta^{18}\text{O}$  ratio. The situation is similar at the well near the Alpine Fault upgradient of Hokitika (Whataroa groundwater system).

#### 4.5.5.2 Nitrate

$\text{NO}_3$  is the most pervasive agricultural contaminant in New Zealand's groundwaters.  $\text{NO}_3\text{-N}$  concentrations in West Coast groundwater range from low (<1 mg/L) to high (9.75 mg/L) and are unevenly distributed in the region (Figure 4.18a). Hotspots occur around Kārāmea and Westport, away from the gravel fans, and in the Grey Valley and are related to arable or dairy farming; all samples with high  $\text{NO}_3\text{-N}$  concentrations >1.5 mg/L occur in areas of high-producing grassland (Figure 4.18b).

Not all dairy farming areas are associated with high  $\text{NO}_3$  groundwater concentrations. South of Hokitika, where all collected samples originate from high-producing grassland, with similar moderate dairy farming and beef and sheep land use,  $\text{NO}_3$  concentrations are low. Only one

of these groundwater samples had an  $\text{NO}_3\text{-N}$  concentration of 1.7 mg/L, with the others generally well below 1.2 mg/L. However, all of these samples are associated with Holocene gravel fans. They have a dilute hydrochemistry signature (Section 4.3.1) and are very young, which indicates high flow rates. These low  $\text{NO}_3$  concentrations, despite moderate dairy farming and beef and sheep land use in these areas, are a result of large dilution of locally recharged rainwater, containing nitrate, by pristine low- $\text{NO}_3$  river water. These Holocene gravel fans are hydraulically connected to and receive large recharge from their rivers. The same applies to the very young groundwaters with MRT <0.5 years near Springs Junction and to the groundwater in the Buller River fan near the river mouth.

In contrast, in the Grey Valley,  $\text{NO}_3\text{-N}$  contamination is more prominent, with concentrations ranging between 2 and 7.5 mg/L. Land-use activities that cause  $\text{NO}_3\text{-N}$  leaching are relatively uniform and consistent since 1996. The elevated  $\text{NO}_3\text{-N}$  concentrations support the conclusions of recharge from local rain, which leaches the  $\text{NO}_3$  from the land surface into the groundwater. The Grey River, in contrast, contains less than 1 mg/L  $\text{NO}_3\text{-N}$  (i.e. A-band on the National Objective Framework; Beaumont et al. 2018). The sampled wells in this area are generally not associated with the Holocene gravel fan of the river, therefore the observed  $\text{NO}_3\text{-N}$  concentrations in groundwater are likely to represent the undiluted  $\text{NO}_3\text{-N}$  concentration of the locally recharged water.

Denitrification in anoxic groundwater systems can also decrease  $\text{NO}_3\text{-N}$  concentrations (Section 4.3.2), despite initially high concentrations in the recharge water due to land use. Low  $\text{NO}_3\text{-N}$  (< 0.01 mg/L) at the site near Karamea is likely to be a result of denitrification; the site is within high-producing grassland, with moderate dairy farming and beef and sheep land use, but the water is highly anoxic (Figure 4.11).

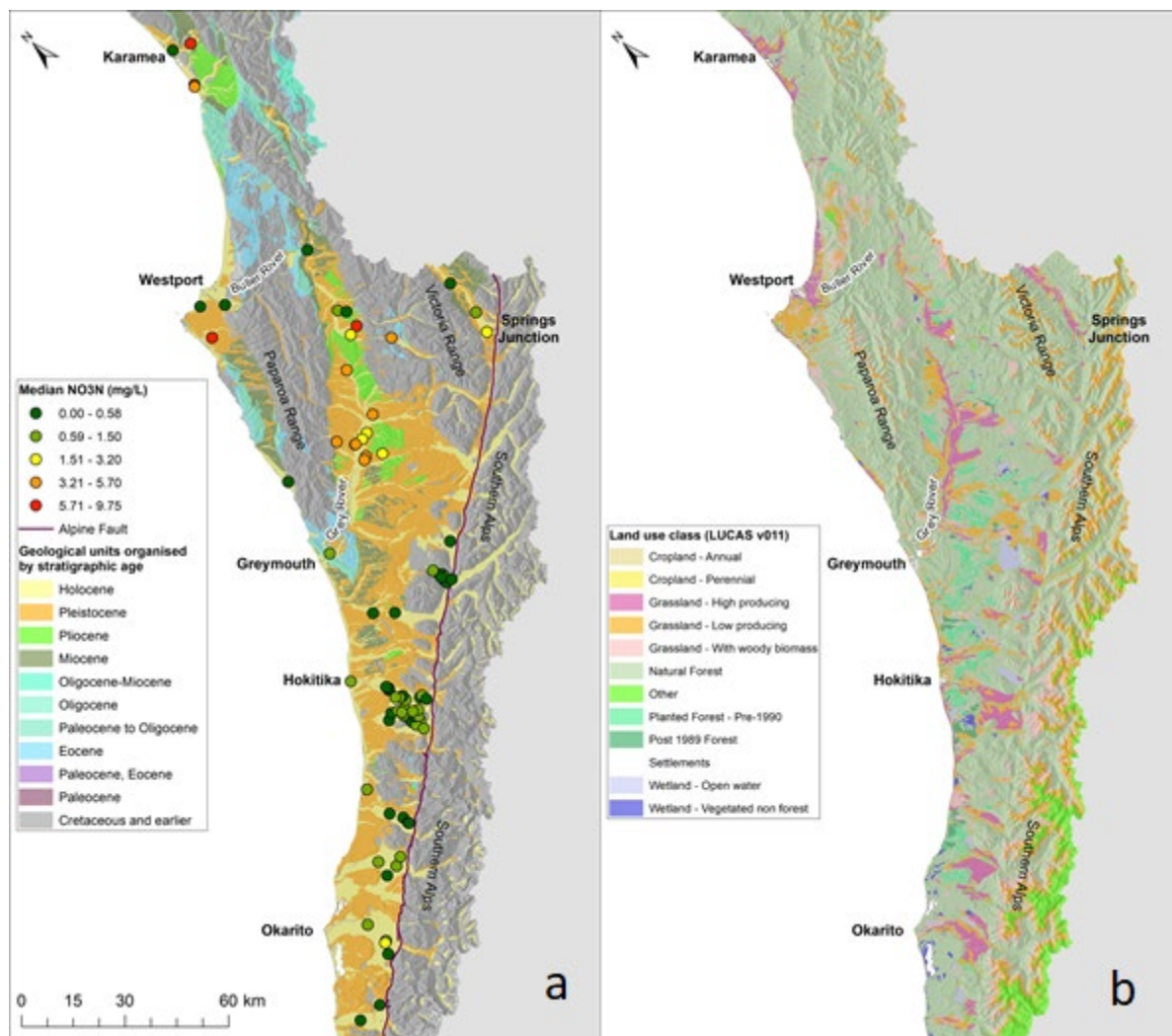


Figure 4.18 Spatial distribution of nitrate ( $\text{NO}_3\text{-N}$ ) in West Coast groundwater.

#### 4.5.5.3 Bicarbonate

The main sources of bicarbonate ( $\text{HCO}_3$ ) in groundwater are uptake of  $\text{CO}_2$  from the atmosphere, uptake of  $\text{CO}_2$  in the soil zone from microbial and plant root respiration, reduction reactions of organic matter and sulphate in the groundwater system, and dissolution of carbonate rocks. Absence of a correlation between  $\text{HCO}_3$  and sulphate in West Coast groundwater indicates that the main sources of elevated  $\text{HCO}_3$  in groundwater are reduction reactions of organic matter and dissolution of carbonate rocks in the groundwater system.

In the Grey Valley,  $\text{HCO}_3$  concentrations are very low (dark green symbols), reflective of the local geology in absence of carbonate rocks (Figure 4.19). However, in Westland and around Springs Junction,  $\text{HCO}_3$  concentrations are higher (yellow to red symbols), likely due to the proximity of outcropping hard rock from the hydrogeological basement, contrasting with gravel downstream. Moderate  $\text{HCO}_3$  concentrations are also found close to the Eocene limestone outcrops (Figure 4.19).

Dissolution of carbonate rocks in the groundwater system is the main reason for these higher  $\text{HCO}_3$  concentrations. Figure 4.9f shows the molar ratios between Ca and  $\text{HCO}_3$ . Most Ca and  $\text{HCO}_3$  data with high concentrations plot along the 1:1 line, indicating calcium carbonate dissolution source. Note that the molar ratios could be biased due to land-use activities. A large fraction of the data plots sits above the calcium carbonate 1:1 dissolution

line. All samples with the largest excess Ca are from high-producing exotic grass areas, indicating that lime application is the likely source of this excess Ca. The sites with highest Ca and  $\text{HCO}_3$  concentrations that plot along the 50% line contain anoxic water, indicating that, for those groundwaters, 50% of the  $\text{HCO}_3$  is derived from decaying organic matter.

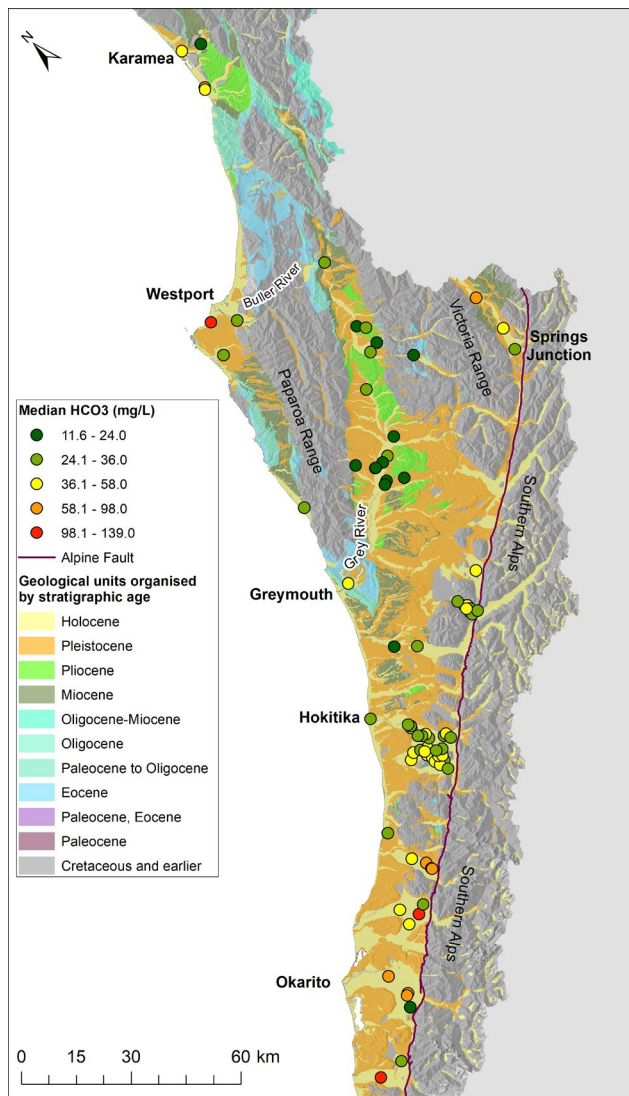


Figure 4.19 Spatial distribution of bicarbonate ( $\text{HCO}_3$ ) in West Coast groundwater.

#### 4.5.5.4 Sodium and Magnesium

The spatial distribution of Na and Mg in West Coast groundwater indicates a strong NE–SW gradient (Figure 4.20). Groundwaters associated with Southern Alps discharges have very low Na concentrations, with the lowest concentrations generally furthest south. The spatial distribution of Mg concentrations exhibits a similar spatial distribution than Na, likely to reflect differences in geology.

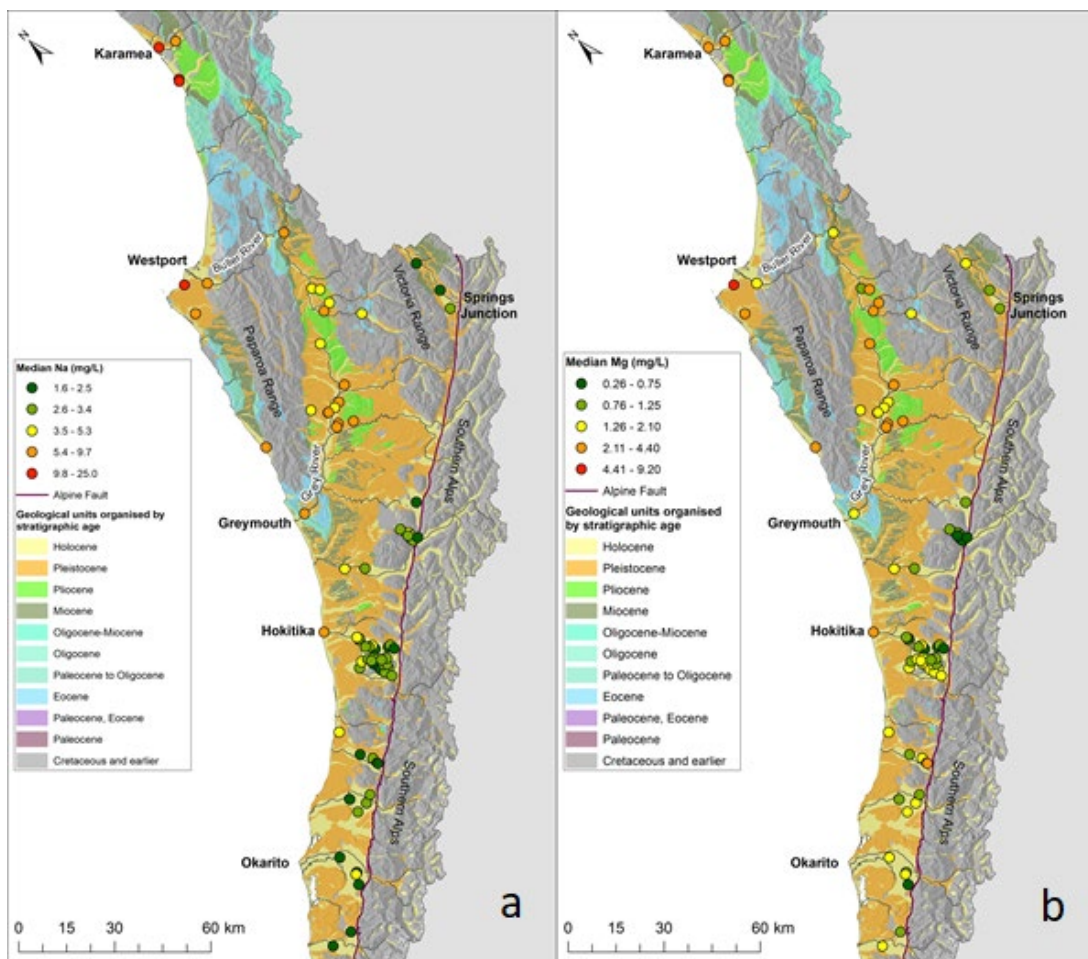


Figure 4.20 Spatial distribution of sodium (Na) (a) and magnesium (Mg) in West Coast groundwater.

#### 4.5.6 Temporal Variability

Most of the temporal trends calculated were uncertain and imperceptible. Perceptible trends were observed at 30 sites for 1–12 parameters, in most cases with concurrent increases and decreases for different parameters. The maximum number of concurrent trends occurred at well 291A, with as many increases (Fe, field conductivity, HCO<sub>3</sub>, K, Mn, SiO<sub>2</sub>) as decreases (Br, Cl, field turbidity, NH<sub>3</sub>-N, NO<sub>3</sub>-N, SO<sub>4</sub>).

The most frequent increases were Ca concentrations (nine sites), often accompanied by Mg, K, SiO<sub>2</sub> and SO<sub>4</sub>, which is consistent with previously reported trends (Moreau 2019). The most likely reason is increasing application of agrochemicals (e.g. lime). The most frequent decreases were DO concentrations (nine sites), which was not correlated with trends in Fe and Mn concentrations due to the limited number of measurements. Decreases in DO indicated depleting shallow oxic groundwater, likely due to increased pumping or less recharge from oxic water. Field conductivity increased at seven sites and decreased at five, with rates ranging from -8.6 to 5.8 µS/cm (Figure 4.21).

Four sites exhibit perceptible NO<sub>3</sub>-N increases at rates ranging from 0.11 to 0.35 mg/L per year, accompanied by Ca, Mg, SO<sub>4</sub> and/or K increases (Figure 4.22), reflecting increasing land-use activities such as dairy and sheep and beef farming. These fast NO<sub>3</sub>-N increase rates exceed the threshold for naturally increasing trends, defined using an aggregated NGMP and SOE dataset (0.1 mg/L; Moreau and Daughney 2021). Perceptible decrease in NO<sub>3</sub>-N concentrations occur at five sites at rates of 0.04–0.1 mg/L per year. There were no perceptible trends detected for the other nutrient, DRP.

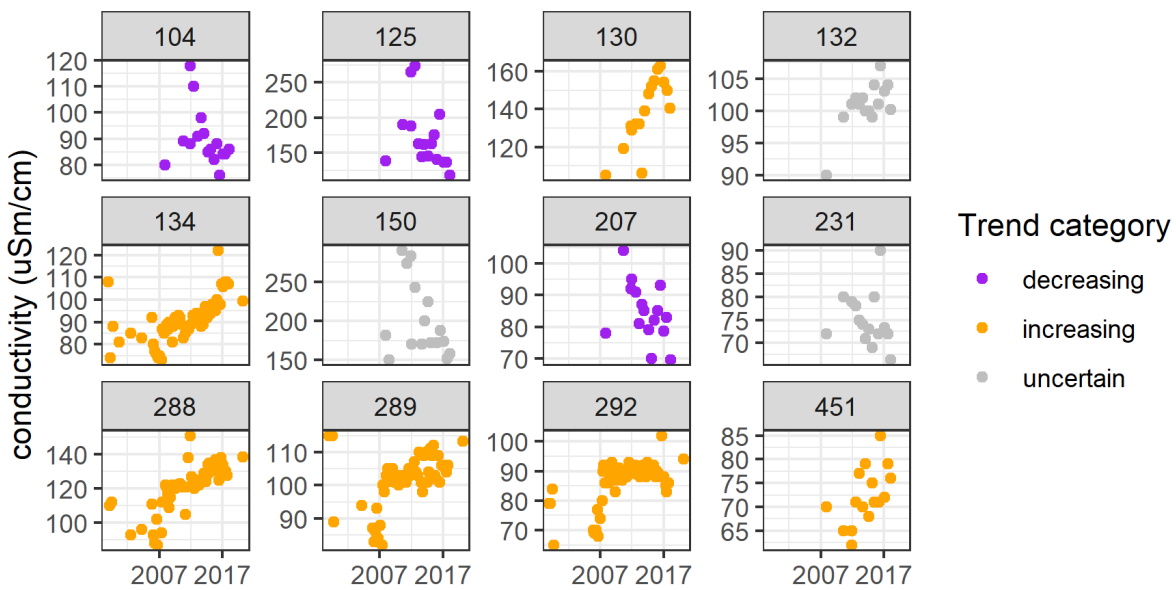


Figure 4.21 Field conductivity time series at sites with more than 10 data points with a perceptible trend.

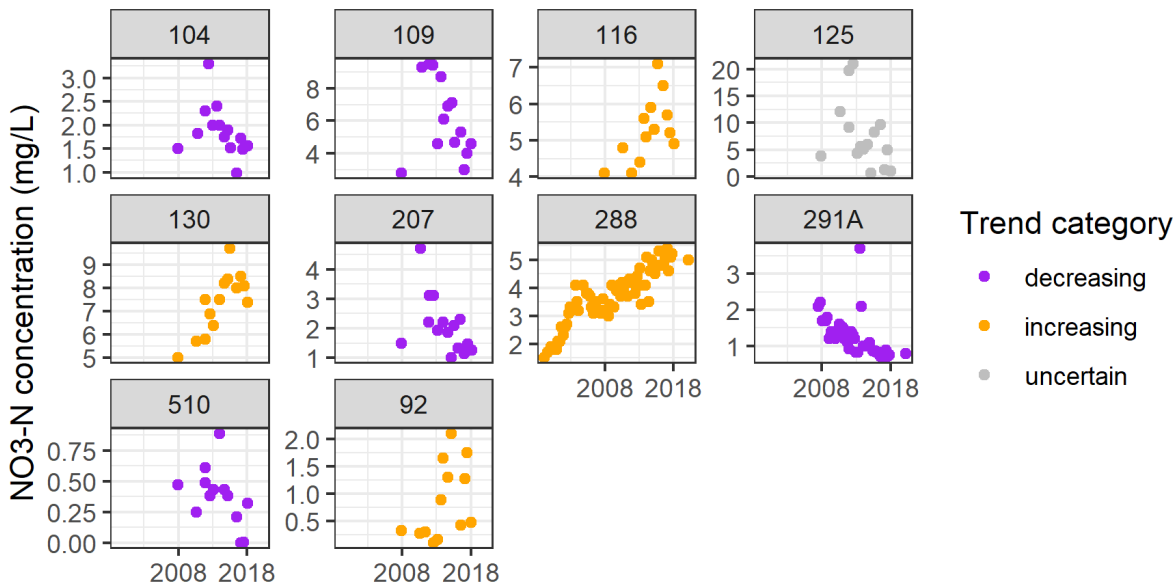


Figure 4.22  $\text{NO}_3\text{-N}$  concentration time series at sites with more than 10 data points exhibiting a perceptible trend.

## 4.6 Groundwater Flow Dynamics

This section provides a summary of the indications that can be derived from the previously discussed tracer concentrations regarding recharge source, recharge rates and flow connections.

### 4.6.1 Recharge Source of Groundwater and Connection to Surface Water

For the West Coast, the argon and dissolved nitrogen concentrations did not provide a means to assess recharge source. Concentrations between the various gas tracers were very inconsistent. Recharge information for the West Coast groundwater systems mainly stems from  $^{18}\text{O}$  and Cl data (Section 4.5.5.1), which are both conservative tracers in groundwater systems that provide complementary information about recharge sources. The data indicate a clear pattern of recharge source for the West Coast groundwater system: low concentrations and lighter (i.e. more negative) ratios indicate recharge from high-altitude rivers and streams.

In the groundwater of the Holocene gravel fans of the Southern Alps rivers, the  $^{18}\text{O}$  and Cl tracer signatures are consistent with those of their higher-altitude Alpine rivers and foothill streams, confirmed by HCA results (Section 4.5.1) and  $\text{NO}_3\text{-N}$  data (Section 4.5.5.2). This indicates that those gravel fans are well connected to local rivers and streams.

In contrast, in the Grey Valley, HCA and  $\text{NO}_3\text{-N}$  data show undiluted signatures of locally recharged groundwater – not diluted by their rivers and streams, which have more pristine tracer signatures. Concentrations are variable between closely located sites, consistent with less connection between groundwater systems. These groundwater systems are not connected to the river and streams.

Near the coast, despite only few data available, groundwater tracer signatures are generally consistent with those of locally recharged coastal rain, indicating that river-recharged groundwater may be limited to the Holocene gravel fans, which is supported by  $^{18}\text{O}$  and Cl groundwater signatures.

#### 4.6.2 Vertical Flow and Recharge

Unconfined recharge situations result in stratified groundwater ages, and the related vertical recharge rates can be estimated from the age-depth relationship of the groundwater (Cartwright and Morgenstern 2012; Morgenstern et al. 2019). Figure 4.23a shows groundwater age versus depth for West Coast groundwater, separated into the different clusters (hydrogeologic units, Section 4.3.1). Black lines show estimated minimum and maximum recharge rates as indicated by the entire dataset. Note that these recharge rates are associated with relatively high uncertainty because very little information is available as to the depth at which active groundwater flow into the wells occurs.

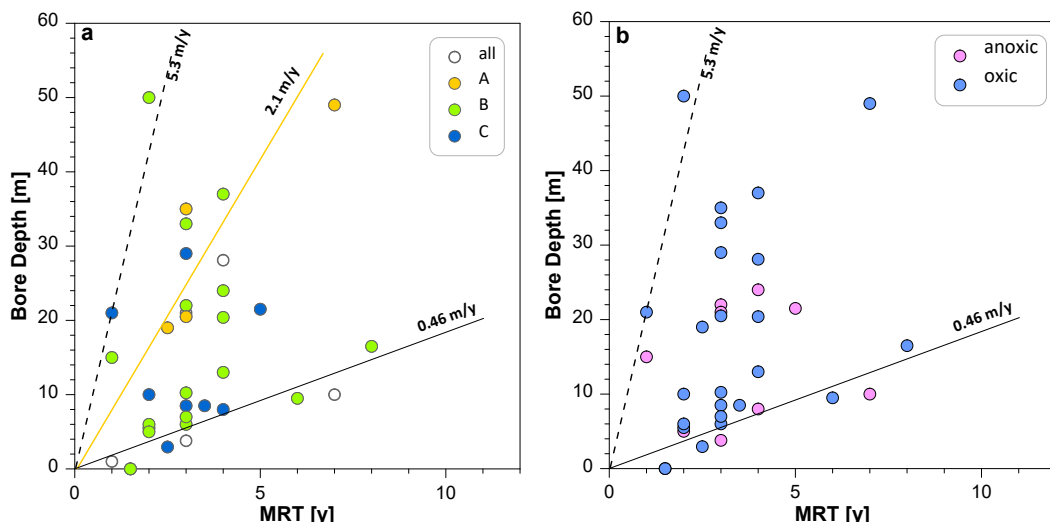


Figure 4.23 (a) Groundwater mean residence time (MRT) versus depth for all wells, separated into the different clusters (Section 4.3.1). Age versus depth trends are indicated by lines (assuming a porosity of 0.25). The yellow line is indicative of a vertical recharge rate of 2.1 m/y for Cluster A (pristine Southern Alps foothills associated with Holocene gravel fans). (b) Same groundwater MRT versus depth data, separated into oxic and anoxic groundwater.

There is no unique overall trend between groundwater age and depth, indicating confined or disconnected groundwater system conditions throughout large parts of the West Coast aquifers. Anoxic conditions are generally associated with slightly lower recharge rates, indicating less conductive groundwater systems (Figure 4.23b).

Cluster A (Figure 4.23a), indicative of pristine, river-recharged Holocene gravels (Section 4.4.1), shows a relatively uniform relationship with depth, indicative of recharge of about 2100 mm/y. This is a relatively high recharge rate, indicating recharge contribution from the rivers into their Holocene gravel fans, as also indicated by low NO<sub>3</sub>-N concentrations, despite land-use activities in these areas that are generally related to high N-leaching.

The data of Clusters B and C cover a large range of recharge rates. The data near the recharge rate line of 5300 mm/y may not be realistic; these wells have relatively high depth uncertainty. The data close to the recharge rate line of 460 mm/y may indicate low hydraulic conductivity in Pleistocene and coastal deposits.

#### 4.6.3 Conceptual Groundwater Flow as Indicated by Tracer Concentrations

Prevailing oxic groundwater conditions in the West Coast region indicate well-flushed groundwater systems (Section 4.5.2), confirmed by very young groundwater throughout most of the region (Section 4.3.2.1). Low mineral concentrations also indicate rapid groundwater flows and therefore limited opportunity for groundwater to dissolve minerals (Section 4.5). There are localised anoxic groundwater systems, but even deposits with high organic matter content that produce highly anoxic aquifer conditions up to the stage of methane fermentation appear to be highly hydraulically conductive, as indicated by the young water in these (<3 years).

Figure 4.24 provides a schematic summary of the conceptual flow of the West Coast groundwater systems that builds on the age, chemistry and stable-isotope data, as well as their interpretations presented in the previous sections.

The Holocene river fans appear to be well connected to their Alpine rivers and streams, as their groundwaters are dominated by tracer signatures that are indicative of recharge from these sources (Section 4.6.1). The shallowest groundwater levels occur consistently in the Holocene gravels in the south, just downgradient of the Alpine Fault (Section 4.2), likely because, after transition of the rivers from the high-gradient mountains to the low-gradient lowlands at the Alpine Fault, thick, clean gravel infills have high hydraulic conductivity. These are the areas expected to have the largest loss of water from the rivers into their adjacent Holocene gravel fans. Groundwater ages do not consistently increase downgradient, indicating that flow is dominated by localised connections to the rivers rather than overall downgradient flow.

Groundwater in the Grey Valley has tracer signatures indicative of recharge from local rain and are not connected to the rivers (Section 4.6.1). Again, groundwater ages do not consistently increase downgradient, indicating a less-connected groundwater–surface water system in Grey Valley. Similarly, the remainder of the region's groundwater systems appear to be dominated by recharge from local rain (Section 4.5.5.1).

There is insufficient groundwater age data near the coast to allow assessment of groundwater connection to the sea, e.g. groundwater outflow to the sea. Old groundwater was found near Okarito, but this is expected in a swampy lagoon area. Aquifers with such hydrogeological settings are unlikely to have connection with the sea.

The large range of recharge rates (Section 4.6.2) indicates variable groundwater recharge conditions. The groundwater systems with the lowest recharge rates may indicate low hydraulic conductivity in localised less-connected groundwater systems in the Pleistocene and coastal deposits.

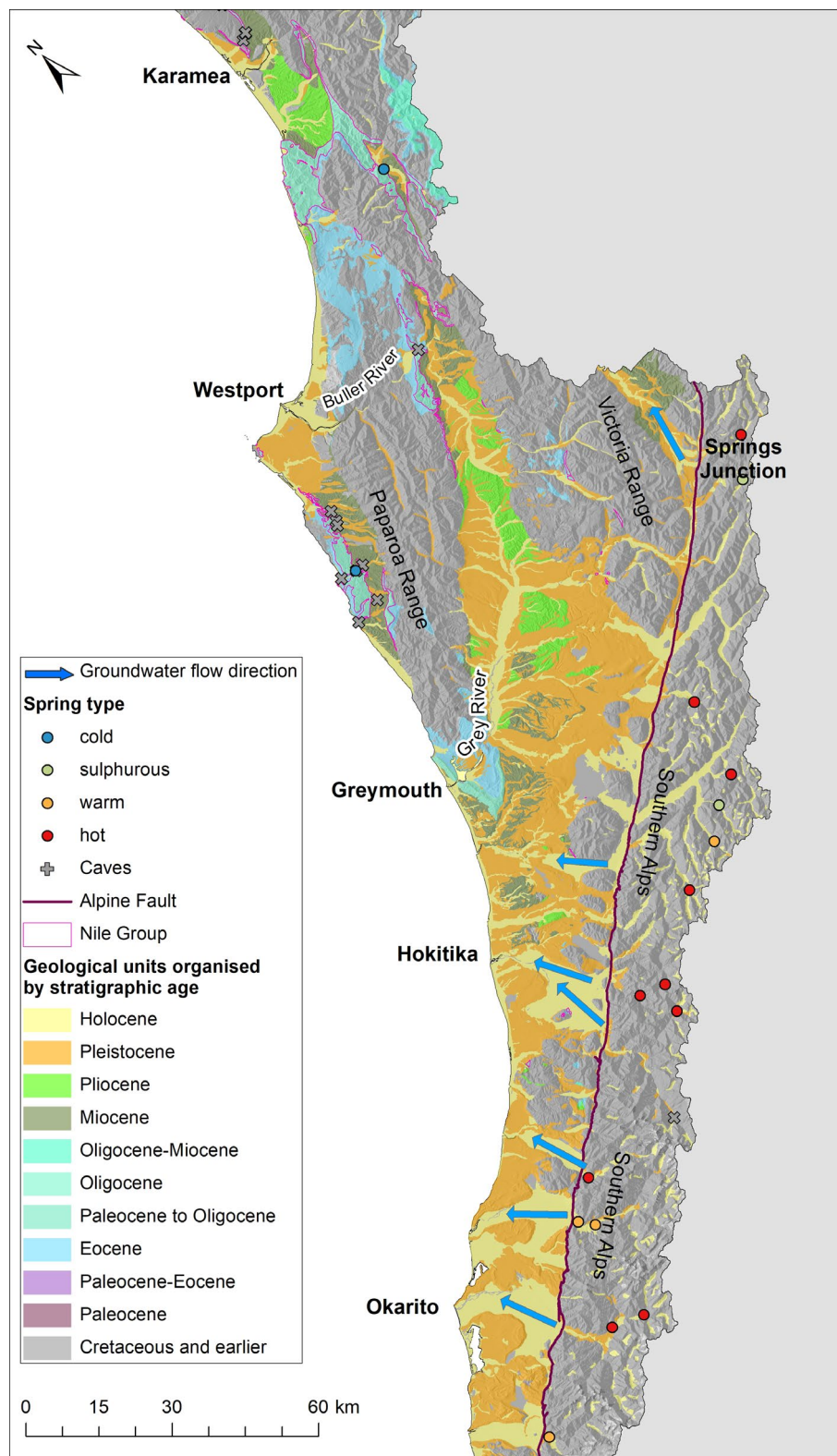


Figure 4.24 Conceptual groundwater flow in the West Coast region inferred from groundwater recharge source and age data. Blue arrows indicate groundwater flow in the Quaternary gravel fans recharged from their Alpine rivers and foothill streams. Groundwater ages (circles) do not show consistent trends downgradient.

## **5.0 CONCLUSION**

This collaborative project between WCRC and GNS aimed to improve understanding of the water dynamics through the West Coast aquifers to inform management and policy development. Specifically, this report addressed the following questions and problems:

### **1. Groundwater Recharge, Flow and Discharge Questions**

- How are groundwaters and surface waters connected in the Holocene gravel fans?
  - Groundwaters and surface waters are well connected only in the Holocene gravel fans.
- Where does the river-recharged groundwater flow within the aquifer?
  - River recharge to groundwater occurs in the Holocene gravel fans.
- Where is groundwater recharged from local rain?
  - Rainfall is actively contributing to groundwater recharge throughout the region.
- What are the time scales of the water flow through the aquifer?
  - Groundwater flow in the region is fast flowing, with residence time of less than 10 years. Groundwater at one well located at the coast has a significantly longer residence time (greater than 100 years); however, this is expected to be due to very localised conditions where groundwater flow is possibly negligible.

### **2. Groundwater Chemistry Questions**

- What are the drivers of nitrate and phosphorus levels in the groundwater?
  - The driver for nitrate levels in groundwater is high-intensity land use, masked by dilution with pristine river water. The young groundwater ages imply that this is not a legacy effect. The driver for phosphorus levels are not obviously related to land use and is likely to be geogenic.
- Why do some monitoring wells show a high variability in hydrochemistry parameters, including nitrate? Is the source of the water at a well changing over time due to abstraction?
  - Most monitoring sites are located within the Grey River Catchment, which is consistent with higher water use in this area. Hydrochemistry data exhibits high spatial variability, which for some parameters is strongly linked to geology and for others to land use. Groundwater chemistry indicates signs of impact ranging from low to high. The most impacted area is the Grey Valley, which is consistent with less rainfall recharge due to the Paparoa Range rain shadow effect, combined with higher land and water use. Temporal variability indicates some local deteriorating trends. The young groundwater ages imply that this is not a legacy effect. The fast water transit time suggests that changes in freshwater management practices may result in improvements in a relatively short time frame.

- What characteristics of the water system are being monitored by the existing groundwater monitoring wells? Is the groundwater of sufficient age to be sensitive to current land-use changes, or is it diluted by river water?
  - A comprehensive overview of historical and current groundwater monitoring was provided in this report. This study also included additional sampling to extend the network. The assembled dataset indicates that groundwater in this region is young and expected to be sensitive to land-use changes.
- What are the flow pathways of surface contaminants, such as agricultural nutrients?
  - Groundwater chemistry and age data clearly indicate some impact from anthropological activities, with pathways likely to be a combination of rainfall infiltration and surface water interaction. The current dataset is not suited to inform the interaction between groundwater and lakes in the region.

### **3. Groundwater Management Questions**

- Does groundwater age (residence time) vary due to abstraction?
  - Although there is evidence of increased abstraction in the Grey Valley, there was no indication of residence time varying with abstraction.

## **6.0 RECOMMENDATIONS**

To cover existing data and knowledge gaps, we recommend the following investigations be undertaken:

- A targeted survey in the Grey Valley to record land use and associated nitrate application; continue monitoring pumping rates and actual metered data. This will provide better understanding of hydrochemical variability and its drivers at monitored sites.
- A water-level survey around selected lakes to better understand their potential interaction with groundwater.
- A targeted groundwater-age survey near the coast to allow assessment of groundwater connection to the sea, e.g. groundwater outflow to the sea, potential saline seawater intrusion.
- Continue quarterly monitoring for the same extended suite of chemical parameters to monitor multi-parameter concentration increases. This has contributed to the understanding of temporal variation in hydrochemistry and will inform on the efficiency of freshwater management measures. Considerations may be given to extend the network to include some sites south of Hokitika to establish new hydrochemistry times series. For practical reasons, these sites may be sampled less frequently, as they are not currently indicating strong groundwater quality deterioration.
- Establish a refined surveying of bores and groundwater levels with common datum (e.g. mean sea level). This would include measuring: (i) the top of the casing of the bores or ground elevation (e.g. with a RTK GPS or hand-held GPS, recording accuracy), (ii) the relative distance between the top of the casing and the ground level and (iii) the water table depth. The use of a consistent water table depth sign convention and its record in metadata (e.g. above ground is negative) is also recommended (some existing time series would then have to be converted). Bore depth should also be measured where not recorded (e.g. using a manual dip meter if no submersible pump is installed). Groundwater elevation data in reference to a common datum will allow comparison of values between sites and may provide information on groundwater connectivity to surface water bodies.

## 7.0 ACKNOWLEDGMENTS

The authors thanks Emma Perrin-Smith (WCRC), Millie Taylor (WCRC) and Chris Busson (WCRC) for providing data and facilitating fieldwork during this study, Patrick Knerlich (Buller District Council), Shruti Thapa (Grey District Council), Mike Sharp (Department of Conservation) and all of the well owners for enabling site access for the March 2020 sampling round. We are also grateful to Frederika Mourot (GNS) and Stew Cameron (GNS) for their constructive comments throughout the internal review process. This work was co-funded by the New Zealand Ministry of Business, Innovation & Employment via the Endeavour Te Whakaheke O Te Wai programme (CO5X1803) and the Envirolink Grant (2127-WCRC196).

## 8.0 REFERENCES

- Ameli AA, Gabrielli C, Morgenstern U, McDonnell JJ. 2018. Groundwater subsidy from headwaters to their parent water watershed: a combined field-modeling approach. *Water Resources Research*. 54(7):5110–5125. doi:10.1029/2017WR022356.
- Baird R, Eaton AD, Rice EW, Bridgewater L, editors. 2017. Standard methods for the examination of water and wastewater. 23<sup>rd</sup> ed. Washington (DC): American Public Health Association, American Water Works Association, Water Environment Federation. 1 vol.
- Beaumont S, Busson C, Horrox J, Langdon J, Mills H, Perrin-Smith E. 2018. State of the Environment: West Coast region – summary 2018. Greymouth (NZ): West Coast Regional Council. 31 p.
- Beyer M, Morgenstern U, Jackson B. 2014. Review of techniques for dating young groundwater (<100 years) in New Zealand. *Journal of Hydrology (New Zealand)*. 53(2):93–111.
- Beyer M, Morgenstern U, van der Raaij R, Martindale H. 2017. Halon-1301 – further evidence of its performance as an age tracer in New Zealand groundwater. *Hydrology and Earth System Sciences*. 21(8):4213–4231. doi:10.5194/hess-21-4213-2017.
- Böhlke JK, Wanty R, Tuttle M, Delin G, Landon M. 2002. Denitrification in the recharge area and discharge area of a transient agricultural nitrate plume in a glacial outwash sand aquifer, Minnesota. *Water Resources Research*. 38(7):10-11–10-26. doi:10.1029/2001wr000663.
- Busenberg E, Plummer LN. 1992. Use of chlorofluorocarbons ( $\text{CCl}_3\text{F}$  and  $\text{CCl}_2\text{F}_2$ ) as hydrologic tracers and age-dating tools: the alluvium and terrace system of central Oklahoma. *Water Resources Research*. 28(9):2257–2283. doi:10.1029/92wr01263.
- Busenberg E, Plummer LN. 2000. Dating young groundwater with sulfur hexafluoride: natural and anthropogenic sources of sulfur hexafluoride. *Water Resources Research*. 36(10):3011–3030. doi:10.1029/2000wr900151.
- Cartwright I, Morgenstern U. 2012. Constraining groundwater recharge and the rate of geochemical processes using tritium and major ion geochemistry: Ovens catchment, southeast Australia. *Journal of Hydrology*. 475:137–149. doi:10.1016/j.jhydrol.2012.09.037.
- Cook PG, Herczeg AL, editors. 2000. Environmental tracers in subsurface hydrology. Boston (MA): Kluwer Academic Publishers. 529 p.
- Cox SC, Barrell DJA, compilers. 2007. Geology of the Aoraki area. Lower Hutt (NZ): GNS Science. 1 map + 71 p., scale 1:250,000. (Institute of Geological & Nuclear Sciences 1:250,000 geological map; 15).
- Cox SC, Sims A, Sutherland R. 2013. Whataroa groundwater surveys, Westland, New Zealand. Lower Hutt (NZ): GNS Science. 15 p. (GNS Science report; 2013/21).

- Daughney CJ, Jones A, Baker T, Hanson C, Davidson P, Zemansky GM, Reeves RR, Thompson M. 2006. A national protocol for state of the environment groundwater sampling in New Zealand. Wellington (NZ): Ministry for the Environment. 54 p. (GNS Science miscellaneous series; 5).
- Daughney CJ, Reeves RR. 2005. Definition of hydrochemical facies in the New Zealand National Groundwater Monitoring Programme. *Journal of Hydrology (New Zealand)*. 44(2):105–130.
- Daughney CJ, Wall M. 2007. Groundwater quality in New Zealand: state and trends 1995–2006. Lower Hutt (NZ): GNS Science. 65 p. Consultancy Report 2007/23. Prepared for the Ministry for the Environment.
- Gabrielli CP, Morgenstern U, Stewart MK, McDonnell JJ. 2018. Contrasting groundwater and streamflow ages at the Maimai watershed. *Water Resources Research*. 54(6):3937–3957. doi:10.1029/2017WR021825.
- Güler C, Thyne GD, McCray JE, Turner KA. 2002. Evaluation of graphical and multivariate statistical methods for classification of water chemistry data. *Hydrogeology Journal*. 10(4):455–474. doi:10.1007/s10040-002-0196-6.
- Heaton THE, Vogel JC. 1981. “Excess air” in groundwater. *Journal of Hydrology*. 50:201–216. doi:10.1016/0022-1694(81)90070-6.
- Helsel DR, Hirsch RM, Ryberg KR, Archfield SA, Gilroy EJ. 2020. Statistical methods in water resources. In. *Hydrologic analysis and interpretation*. Reston (VA): U.S. Geological Survey. 458 p. (Techniques and methods; 4-A3).
- Heron DW, custodian. 2020. Geological map of New Zealand [map]. 3<sup>rd</sup> ed. Lower Hutt (NZ): GNS Science. 1 USB, scale 1:250,000. (GNS Science geological map; 1). doi:10.21420/03PC-H178.
- Horrox J, Chaney E, Eaves A. 2015. West Coast surface water quality. Greymouth (NZ): West Coast Regional Council. 115 p. State of the Environment Technical Report 14001.
- Ingram RGS, Hiscock KM, Dennis PF. 2007. Noble gas excess air applied to distinguish groundwater recharge conditions. *Environmental Science & Technology*. 41(6):1949–1955. doi:10.1021/es061115r.
- Kerr T, Srinivasan MS, Rutherford J. 2015. Stable water isotopes across a transect of the Southern Alps, New Zealand. *Journal of Hydrometeorology*. 16(2):702–715. doi:10.1175/jhm-d-13-0141.1.
- Larned ST, Snelder T, Unwin MJ, McBride GB. 2016. Water quality in New Zealand rivers: current state and trends. *New Zealand Journal of Marine and Freshwater Research*. 50(3):389–417. doi:10.1080/00288330.2016.1150309.
- LINZ Data Service. 2021. Wellington (NZ): Land Information New Zealand. NZ building outlines; [updated 2021 Jun 14; accessed 2021 Sep 1]; [dataset]. <https://data.linz.govt.nz/layer/101290-nz-building-outlines/>
- Macara GR. 2016. The climate and weather of West Coast. 2<sup>nd</sup> ed. [Place unknown] (NZ): National Institute of Water & Atmospheric Research. 38 p. (NIWA science and technology series; 72).
- Maiss M, Brenninkmeijer CAM. 1998. Atmospheric SF<sub>6</sub>: trends, sources, and prospects. *Environmental Science & Technology*. 32(20):3077–3086. doi:10.1021/es9802807.
- Małoszewski P, Zuber A. 1982. Determining the turnover time of groundwater systems with the aid of environmental tracers: 1. Models and their applicability. *Journal of Hydrology*. 57(3–4):207–231. doi:10.1016/0022-1694(82)90147-0.

- Maloszewski P, Zuber A. 1991. Influence of matrix diffusion and exchange reactions on radiocarbon ages in fissured carbonate aquifers. *Water Resources Research*. 27(8):1937–1945. doi:10.1029/91wr01110.
- Martindale H, van der Raaij RW, Knowling MJ, Morgenstern U. 2018. Quantifying groundwater discharge into New Zealand rivers using radon and concurrent flow gauging. Lower Hutt (NZ): GNS Science. 39 p. (GNS Science report; 2018/25).
- McBride GB. 2019. Has water quality improved or been maintained? A quantitative assessment procedure. *Journal of Environmental Quality*. 48(2):412–420. doi:10.2134/jeq2018.03.0101.
- McDonnell JJ, Gabrielli C, Ameli A, Ekanayake J, Fenicia F, Freer J, Graham C, McGlynn B, Morgenstern U, Pietroniro A, et al. 2021. The Maimai M8 experimental catchment database: forty years of process-based research on steep, wet hillslopes. *Hydrological Processes*. 35(5):e14112. doi:10.1002/hyp.14112.
- McGlynn BL, McDonnel JJ, Brammer DD. 2002. A review of the evolving perceptual model of hillslope flowpaths at the Maimai catchments, New Zealand. *Journal of Hydrology*. 257(1–4):1–26. doi:10.1016/S0022-1694(01)00559-5.
- Milne J. 2019. Water quality. Part 1 of 4: sampling, measuring, processing and archiving of discrete groundwater quality data. [Place unknown]: National Environmental Monitoring Standards; [accessed 2021 Aug]. <https://www.nems.org.nz/documents/water-quality-part-1-groundwater/>
- Ministry for the Environment. 2020. National Policy Statement for Freshwater Management 2020. Wellington (NZ): Ministry for the Environment. 70 p.
- Ministry of Health. 2018. Drinking-water Standards for New Zealand 2005 (Revised 2018). Wellington (NZ): Ministry of Health; [accessed 2021 Sep]. <https://www.health.govt.nz/publication/drinking-water-standards-new-zealand-2005-revised-2018>
- Mongillo MA, Clelland L. 1984. Concise listing of information on the thermal areas and thermal springs of New Zealand. Wellington (NZ): Department of Scientific and Industrial Research. 228 p. (DSIR geothermal report; 9).
- Moreau M. 2019. West Coast Regional Council State of the Environment groundwater monitoring report 2018. Wairakei (NZ): GNS Science. 25 p. Consultancy Report 2018/109. Prepared for West Coast Regional Council. Revised May 2019.
- Moreau M, Daughney CJ. 2015. Update of national groundwater quality indicators: state and trends, December 2004–2013. Wairakei (NZ): GNS Science 32 p. Consultancy Report 2015/16. Prepared for Ministry for the Environment.
- Moreau M, Daughney C. 2021. Defining natural baselines for rates of change in New Zealand's groundwater quality: dealing with incomplete or disparate datasets, accounting for impacted sites, and merging into state of the-environment reporting. *Science of The Total Environment*. 755(2):143292. doi:10.1016/j.scitotenv.2020.143292.
- Moreau-Fournier M, Daughney CJ. 2010. Procedure for checking laboratory water chemistry results prior upload to the Geothermal-Groundwater database. Wairakei (NZ): GNS Science. 62 p. Internal Report 2010/06.
- Morgenstern U, Daughney CJ. 2012. Groundwater age for identification of baseline groundwater quality and impacts of land-use intensification – The National Groundwater Monitoring Programme of New Zealand. *Journal of Hydrology*. 456–457:79–93. doi:10.1016/j.jhydrol.2012.06.010.

- Morgenstern U, Daughney CJ, Leonard G, Gordon D, Donath FM, Reeves R. 2015. Using groundwater age and hydrochemistry to understand sources and dynamics of nutrient contamination through the catchment into Lake Rotorua, New Zealand. *Hydrology and Earth System Sciences*. 19(2):803–822. doi:10.5194/hess-19-803-2015.
- Morgenstern U, Davidson P, Townsend DB, White PA, van der Raaij RW, Stewart MK, Moreau M, Daughney CJ. 2019. From rain through river catchment to aquifer: the flow of water through the Wairau hydraulic system. Lower Hutt (NZ): GNS Science. 83 p. (GNS Science report; 2019/63).
- Morgenstern U, Taylor CB. 2009. Ultra low-level tritium measurement using electrolytic enrichment and LSC. *Isotopes in Environmental and Health Studies*. 45(2):96–117. doi:10.1080/10256010902931194.
- Morgenstern U, van der Raaij RW, Martindale H, Toews MW, Stewart MK, Matthews A, Trompetter V, Townsend DB. 2017. Groundwater dynamics, source and hydrochemical processes as inferred from Horizon's regional age tracer data. Lower Hutt (NZ): GNS Science. 63 p. (GNS Science report; 2017/15).
- Mourot F, White PA. 2020. Groundwater quantity allocation limits for the West Coast region: case study in the Upper Grey River Freshwater Management Unit. Wairakei (NZ): GNS Science. 32 p. Consultancy Report 2020/125. Prepared for Ministry of Business, Innovation & Employment.
- Nathan S, Rattenbury MS, Suggate RP, compilers. 2002. Geology of the Greymouth area [map]. Lower Hutt (NZ): Institute of Geological & Nuclear Sciences. 1 map + 58 p., scale 1:250,000. (Institute of Geological & Nuclear Sciences 1:250,000 geological map; 12).
- Nichol SE, Harvey MJ, Boyd IS. 1997. Ten years of rainfall chemistry in New Zealand. *Clean Air*. 31(1):30–37.
- [NIWA] National Institute of Water & Atmospheric Research. [2021]. Auckland (NZ): NIWA. National and regional climate maps: West Coast; [accessed 2021 Aug 23]. <https://niwa.co.nz/climate/national-and-regional-climate-maps/west-coast>
- [NZSS] New Zealand Speleological Society. c2020. Waitomo Caves (NZ): Cave statistics; [accessed 2021 Aug]. <http://caves.org.nz/cave-statistics/>
- Plummer LN, Busenberg E. 2000. Chlorofluorocarbons. In: Cook PG, Herczeg AL, editors. *Environmental tracers in subsurface hydrology*. Boston (MA): Kluwer Academic. p. 441–478.
- Raiber M, Daughney CJ. 2009. Assessment of groundwater quality in the West Coast Regional Council State of the Environment Monitoring Programme to December 2008. Lower Hutt (NZ): GNS Science. 38 p. + 1 CD. Consultancy Report 2009/35. Prepared for West Coast Regional Council.
- Rattenbury MS, Cooper RA, Johnston MR. 1998. Geology of the Nelson area [map]. Lower Hutt (NZ): Institute of Geological & Nuclear Sciences. 1 map + 67 p., scale 1:250,000. (Institute of Geological & Nuclear Sciences 1:250,000 geological map; 9).
- Rattenbury MS, Jongens R, Cox SC, compilers. 2010. Geology of the Haast area [map]. Lower Hutt (NZ): GNS Science. 1 map + 58 p., scale 1:250,000. (Institute of Geological & Nuclear Sciences 1:250,000 geological map; 14).
- Stewart MK, Morgenstern U, Gusyev MA, Małoszewski P. 2017. Aggregation effects on tritium-based mean transit times and young water fractions in spatially heterogeneous catchments and groundwater systems. *Hydrology and Earth System Sciences*. 21(9):4615–4627. doi:10.5194/hess-21-4615-2017.

- Taylor CB. 1968. A comparison of tritium and strontium-90 fallout in the Southern Hemisphere. *Tellus*. 20(4):559–576. doi:10.3402/tellusa.v20i4.10038.
- van der Raaij RW. 2003. Age-dating of New Zealand groundwaters using sulphur hexafluoride [MSc thesis]. Wellington (NZ): Victoria University of Wellington. 122 p.
- Ward JH. 1963. Hierarchical grouping to optimize an objective function. *Journal of the American Statistical Association*. 58(301):236–244. doi:10.1080/01621459.1963.10500845.
- [WCRC] West Coast Regional Council. 2014. Regional Land and Water Plan. Greymouth (NZ): West Coast Regional Council. 282 p.
- [WCRC] West Coast Regional Council. [2021]. Greymouth (NZ): West Coast Regional Council. [Flood monitoring of Karamea, Mokihinui, Buller, Grey, Hokitika and Waiho rivers]; [updated 2021 Sep 29; accessed 2021 Sep 29]. <https://data.wcrc.govt.nz/cgi-bin/HydWebServer.cgi>
- White PA, Moreau M, Mourot F, Rawlinson ZJ. 2019. New Zealand Groundwater Atlas: hydrogeological-unit map of New Zealand. Wairakei (NZ): GNS Science. 89 p. Consultancy Report 2019/144. Prepared for Ministry for the Environment.
- Zemansky GM, Horrox J. 2007a. Groundwater nutrient movement: Inchbonnie catchment. Lower Hutt (NZ): GNS Science. 70 p. (GNS Science report; 2007/35).
- Zemansky GM, Horrox J. 2007b. Kowhitirangi and Kokatahi Plains groundwater assessment. Lower Hutt (NZ): GNS Science. 57 p. (GNS Science report; 2007/34).
- Zuber A, Witczak S, Różański K, Śliwka I, Opoka M, Mochalski P, Kuc T, Karlikowska J, Kania J, Jackowicz-Korczyński M, et al. 2005. Groundwater dating with  $^3\text{H}$  and  $\text{SF}_6$  in relation to mixing patterns, transport modelling and hydrochemistry. *Hydrological Processes*. 19(11):2247–2275. doi:10.1002/hyp.5669.

## **APPENDICES**

This page left intentionally blank.

## APPENDIX 1 MAP OF THE WEST COAST REGION SHOWING THE LOCATIONS OF CHEMISTRY AND AGE SITES

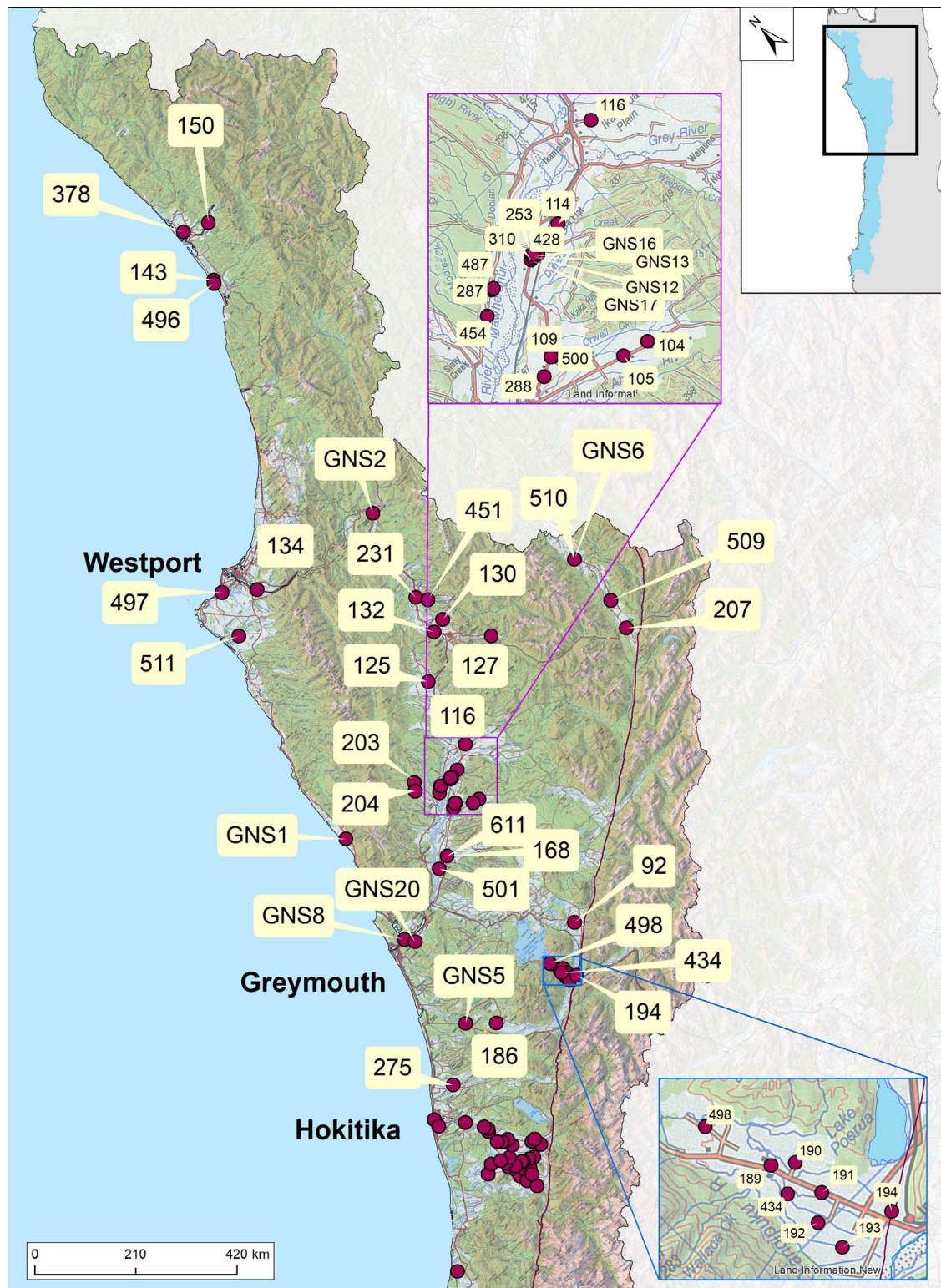


Figure A1.1 Map of the West Coast region showing the locations of chemistry and age-tracer sites, north of Hokitika.

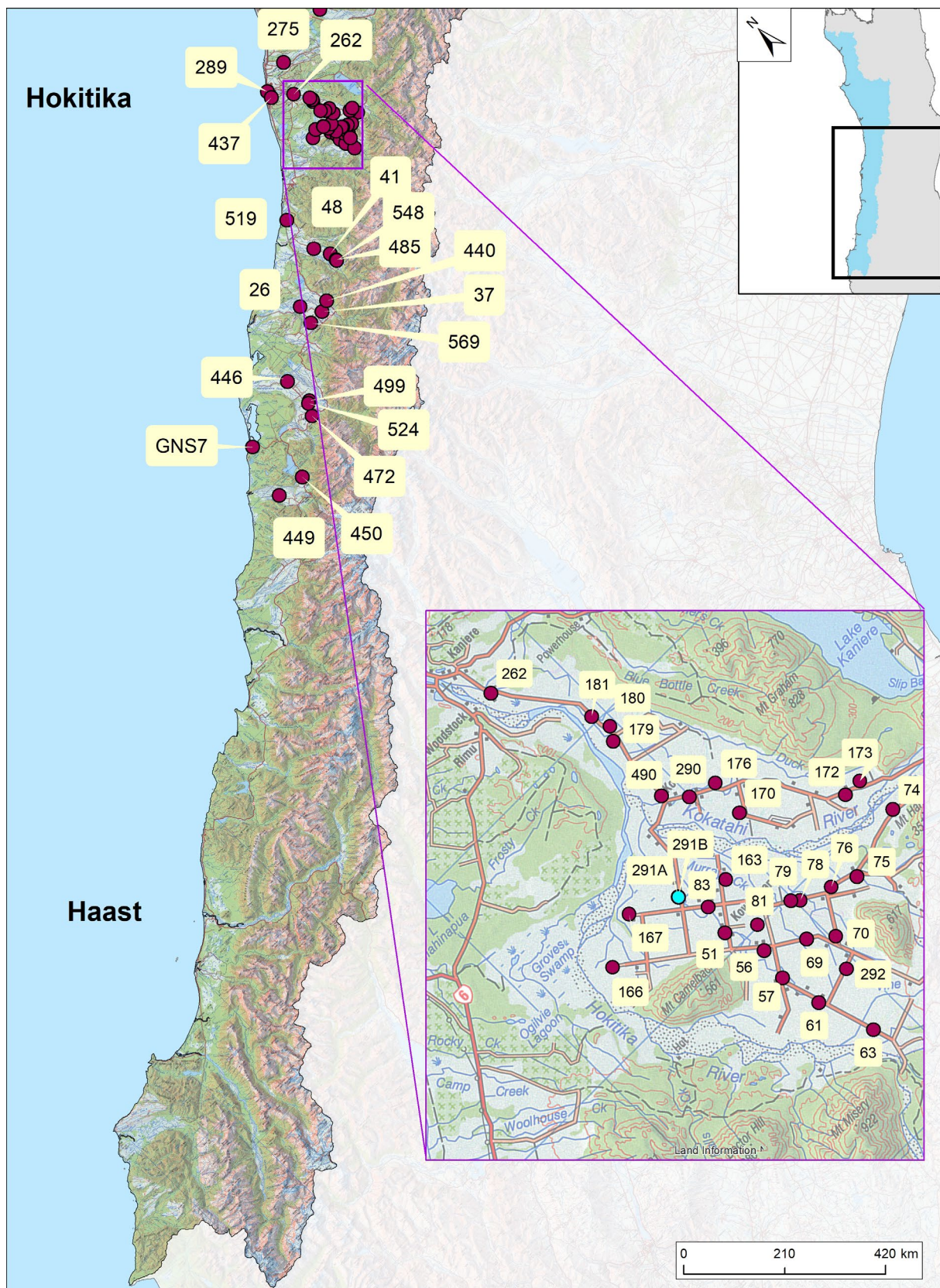


Figure A1.2 Map of the West Coast region showing the locations of chemistry and age-tracer sites, south of Hokitika.

## APPENDIX 2 GROUNDWATER MEAN RESIDENCE TIME

Table A2.1 West Coast Regional Council groundwater ages.

<b>Well ID</b>	<b>Easting (NZTM)</b>	<b>Northing (NZTM)</b>	<b>Bore Depth (m)</b>	<b>Mean Residence Time (MRT)</b>
92	1482344	5276933	~10	2
104	1486424	5308665	20.4	4
109	1482457	5311527	9.5	6
114	1487439	5316136	10.24	3
116	1492352	5318672	33	3
125	1496138	5333101	5	2
127	1511904	5330588	~50	2
130	1507211	5340114	6	3
132	1504177	5339516	15	8
134	1484550	5371338	24	4
143	1523333	5422642	10	7
150	1530909	5431788	6	2
203	1479420	5320505	15	1
207	1532622	5312168	-	0.2
231	1506512	5347160	-	1
288	1481417	5311122	37	4
289	1433302	5268616	13	4
290	1439978	5255423	2.95	2.5
292	1439560	5246443	7 to 10	3
378	1525893	5434050	3.79	3
440	1407606	5222610	-	3
446	1387065	5215440	-	2.5
449	1366081	5197353	-	3
450	1373203	5196523	-	1
472	1385319	5205291	-	3
487	1482786	5316122	~5.5	2
509	1534429	5318461	-	0.2
519	1414583	5243193	-	5
524	1386914	5208109	-	4
548	1416260	5227793	-	7
569	1401112	5221478	-	4
291A	1436947	5253002	-	3.5
GNS1	1461297	5322253	0	1.5
GNS2	1512545	5365671	-	3
GNS3	-	-	-	4
GNS5	1451866	5278037	0	1.5
GNS6	1535085.181	5329623.861	-	0.5
GNS7	-	-	-	140
GNS8	1455200	5299084	26	3



[www.gns.cri.nz](http://www.gns.cri.nz)

#### Principal Location

1 Fairway Drive, Avalon  
Lower Hutt 5010  
PO Box 30368  
Lower Hutt 5040  
New Zealand  
T +64-4-570 1444  
F +64-4-570 4600

#### Other Locations

Dunedin Research Centre	Wairakei Research Centre	National Isotope Centre
764 Cumberland Street	114 Karetoto Road	30 Gracefield Road
Private Bag 1930	Private Bag 2000	PO Box 30368
Dunedin 9054	Taupo 3352	Lower Hutt 5040
New Zealand	New Zealand	New Zealand
T +64-3-477 4050	T +64-7-374 8211	T +64-4-570 1444
F +64-3-477 5232	F +64-7-374 8199	F +64-4-570 4657